UNCLASSIFIED

AD NUMBER

AD-913 816

NEW LIMITATION CHANGE

TO

DISTRIBUTION STATEMENT - A

Approved for public release;
distribution is unlimited.

LIMITATION CODE: 1

FROM

DISTRIBUTION STATEMENT - B

LIMITATION CODE: 3

AUTHORITY

Cmdr, AFWAL via ltr; dtd Dec 15, 1980

19990226164

THIS PAGE IS UNCLASSIFIED

AD913816

AFAL-TR-73-303

Technical Report

BIDIRECTIONAL REFLECTANCE MODEL VALIDATION AND UTILIZATION

1 November 1969 Through 31 December 1972

J. R. MAXWELL, J. BEARD, S. WEINER, D. LADD, and S. LADD

Infrared and Optics Division
Environmental Research Institute of Michigan
Ann Arbor, Michigan 48107

TECHNICAL REPORT AFAL-TR-73-303

October 1973

Distribution limited to U.S. Government agencies only; Test and Evaluation: 4 October 1972. Other requests for this document must be submitted to AFAL/[illegible], Wright-Patterson Air Force Base, Ohio 45433

Prepared for
Air Force Avionics Laboratory
Air Force Systems Command
Wright-Patterson Air Force Base, Ohio 45433

NOTICES

Note. When Government drawings, specifications, or other data are used for any purpose other than in connection with a definitely related Government procurement operation, the United States Government thereby incurs no responsibility nor any obligation whatsoever; and the fact that the Government may have formulated, furnished, or in any way supplied the said drawings, specifications, or other data is not to be regarded by implication or otherwise as in any manner licensing the holder or any other person or corporation or conveying any rights or permission to manufacture, use, or sell any patented invention that may in any way be related thereto.

Copies of this report should not be returned unless return is required by security considerations, contractual obligations, or notice on a specific document.

BIDIRECTIONAL REFLECTANCE MODEL VALIDATION AND UTILIZATION
1 November 1969 Through 31 December 1972

J. R. MAXWELL, J. BEARD, S. WEINER,
D. LADD, and S. LADD

FOREWORD

The work reported herein, covering the period from 1 November 1969 through 31 December 1972, was carried out by the Infrared and Optics Division of the Willow Run Laboratories, then a unit of The University of Michigan's Institute of Science and Technology. (On 1 January 1973, the Willow Run Laboratories separated from the University and became independent as the Environmental Research Institute of Michigan (ERIM), P.O. Box 618, Ann Arbor, MI 48107.) The Air Force Avionics Laboratory (AFAL) of the Air Force Systems Command, Wright-Patterson Air Force Base, Ohio, commissioned this work under Contract F33615-70-C-1123, Project 6239, Task 10. Mr. Bruno Wernicke AFAL/RSP is Technical Monitor for the Air Force.

Our interest in the development of a bidirectional reflectance model is an outgrowth of on-going research in target signatures which has thus far produced eleven Data Compilations listing reflectance characteristics for materials of interest to the Target Signature Analysis Center (TSAC) and its patrons.

Some work toward extending the model to account for a non-Lambertian, nonspecular reflectance component assumed to result from scattering within the target material was performed under Contract DAAD05-72-C-0246 with the Army Ballistic Research Laboratories (BRL). Under the same BRL contract, the model was also coded in Fortran IV and an extensive measurement program implemented and used in a validation of the complete model. Because the present unified model has been realized as a result of work performed at WRL/ERIM under the present Air Force Avionics Laboratory contract as well as from work done under the BRL contract, the BRL-sponsored portion of the model is also described in this report.

This research effort is continuing at ERIM's Willow Run facilities under the direction of Dr. Robert Maxwell as Principal Investigator, with guidance provided by Mr. R. R. Legault, Director of the Infrared and Optics Division. The ERIM number for this report is 196400-1-T.

This report was submitted by the authors on 11 July 1973.

This technical report has been reviewed and is approved.

Albert W. Berg

Albert W. Berg, Chief
Reconnaissance Sensor Development Branch
Reconnaissance Division
Air Force Avionics Laboratory

ABSTRACT

This report describes a method for using bidirectional reflectance information previously reported in the Eleventh Supplement to the Target Signature Analysis Center: Data Compilation [1, 2] and further validates the bidirectional reflectance model originated and extended under recent contracts. It includes bidirectional reflectance model parameters for a variety of paints. Parameters were extracted from measurement data reported in the Eleventh Supplement. Reduced reflectance data are also provided; these data may be used with the computer model or optionally, in an interpolation procedure for estimating reflectances without the aid of a computer.

The computer model makes it possible to calculate bidirectional reflectance data from a very small amount of measured data. Accuracy demonstrated in the Model Validation section indicates that the model is very effective, although improvement can still be obtained at large receiver zenith angles. The interpolation procedure also shows excellent agreement with measurement.

CONTENTS

1. Introduction 1

2. Bidirectional Reflectance 3

3. Background Information 6

4. Surface Model 8
   - 4.1. Available Area 8
   - 4.2. Fresnel Coefficients 8
   - 4.3. Shadowing and Obscuration 10

5. Volume Models 12
   - 5.1. Lambertian 12
   - 5.2. Non-Lambertian 12

6. Model Validation 17
   - 6.1. Reflectance for Sample Material A02018-001 17
   - 6.2. Reflectance for Sample Material A02018-002 28
   - 6.3. Polarization Angle for Sample Materials A02018-001 and A02018-002 28
   - 6.4. Percent Polarization for Sample Materials A02018-001 and A02018-002 48

7. Model Parameters 55
   - 7.1. Source Polarization Parameters 55
   - 7.2. Surface Model Parameters 56
   - 7.3. Lambertian Volume Model Parameters 57
   - 7.4. Non-Lambertian Volume Model Parameters 57
   - 7.5. Parameters Used to Generate Typical Data for Comparison Purposes 57

8. Reflectance Estimation Method 58
   - 8.1. Procedure for Estimating Reflectance Values by Interpolation 58
   - 8.2. Application of Procedure 59

Appendix I: Fixed Bistatic Data for Paints from Data Compilation 63

Appendix II: Bidirectional Reflectance Data for Four Typical Types of Paint 71

Appendix III: Documentation of Bidirectional Reflectance Program (Rhoprime) 81

Appendix IV: Instructions for Use of Program with Sample Computer Output 96

Appendix V: Rhoprime Program Listing 102

References 124

FIGURES

1. Bidirectional Reflectance Geometry and Parameters 1
2. Example of Reflectance ρ' for A02018-001. θ_r Scanned in Plane 7
3. Volume Scattering Geometry and Parameters 13
4. Fixed Bistatic ρ' for A02018-001. Polarizations $\perp\perp, \perp 45, \perp\parallel$ 19
5. Measured ρ' for A02018-001. ϕ_r = 0, 180°; Polarizations $\perp\perp, \perp{-45}, \perp\parallel$ 21
6. Calculated ρ' for A02018-001 Using Lambertian Volume Model and Non-Lambertian Volume Model With and Without Shadowing and Obscuration Factor, $\theta_i = 40°$; $\phi_r = 0°, 180°$; Polarizations $\perp\perp, \perp\parallel$ 22
7. Measured ρ' for A02018-001. $\phi_r = 90°, 270°$; Polarizations $\perp\perp, \perp{-45}, \perp\parallel$ 24
8. Calculated ρ' for A02018-001 Using Lambertian Volume Model and Non-Lambertian Volume Model With and Without Shadowing and Obscuration Factor, $\theta_i = 40°$, $\phi_i = 180°$; $\phi_r = 90°, 270°$; Polarizations $\perp\perp, \perp\parallel$ 25
9. Measured ρ' for A02018-001. $\phi_r = 30°, 210°$; Polarizations $\perp\perp, \perp{-45}, \perp\parallel$ 27
10. Calculated ρ' for A02018-001 Using Non-Lambertian Volume Model With Shadowing and Obscuration Factor. $\phi_r = 30°, 210°$; Polarizations $\perp\perp, \perp\parallel$ 28
11. Measured ρ' for A02018-001. $\phi_r = 60°, 240°$; Polarizations $\perp\perp, \perp{-45}, \perp\parallel$ 29
12. Calculated ρ' for A02018-001 Using Non-Lambertian Volume Model With Shadowing and Obscuration Factor. $\phi_r = 60°, 240°$; Polarizations $\perp\perp, \perp\parallel$ 30
13. Measured ρ' for A02018-001. $\phi_r = 0°, 180°$; Polarizations $-45\perp, -45{-45}, -45\parallel$ 31
14. Calculated ρ' for A02018-001 Using Non-Lambertian Volume Model With Shadowing and Obscuration Factor. $\phi_r = 0°, 180°$; Polarizations $-45\perp, -45\parallel$ 32
15. Measured ρ' for A02018-001. $\phi_r = 90°, 270°$; Polarization $\parallel\perp, \parallel{-45}, \parallel\parallel$ 33
16. Calculated ρ' for A02018-001 Using Non-Lambertian Volume Model With Shadowing and Obscuration Factor. $\phi_r = 90°, 270°$; Polarizations $\parallel\perp, \parallel\parallel$ 34
17. Measured ρ' for A02018-001. $\phi_r = 30°, 210°$; Polarizations $\parallel\perp, \parallel{-45}, \parallel\parallel$ 35
18. Calculated ρ' for A02018-001 Using Non-Lambertian Volume Model With Shadowing and Obscuration Factor. $\phi_r = 30°, 210°$; Polarizations $\parallel\perp, \parallel\parallel$ 36

19. Measured ρ' for A02018-001. $\phi_r = 60^o, 240^o$; Polarizations ∥⊥,∥-45,∥∥ 37

20. Calculated ρ' for A02018-001 Using Non-Lambertian Volume Model With Shadowing and Obscuration Factor. $\phi_r = 60^o, 240^o$; Polarizations ∥⊥,∥∥ 38

21. Fixed Bistatic ρ' for A02018-002. Polarizations ⊥⊥,⊥45,⊥∥ 39

22. Measured ρ' for A02018-002. $\phi_r = 0^o, 180^o$; Polarizations ⊥⊥,⊥-45,⊥∥ 40

23. Calculated ρ' for A02018-002 Using Lambertian Volume Model. $\phi_r = 0^o, 180^o$; Polarizations ⊥⊥, ⊥∥. 41

24. Measured ρ' for A02018-002. $\phi_r = 90^o, 270^o$; Polarizations ⊥⊥,⊥-45,⊥∥ 42

25. Calculated ρ' for A02018-002 Using Lambertian Volume Model. $\phi_r = 90^o, 270^o$; Polarizations ⊥⊥, ⊥∥ 43

26. Measured ρ' for A02018-002. $\phi_r = 0^o, 180^o$; Polarizations ∥⊥,∥-45,∥∥ 44

27. Calculated ρ' for A02018-002 Using Lambertian Volume Model. $\phi_r = 0^o, 180^o$; Polarizations ∥⊥,∥∥ 45

28. Measured ρ' for A02018-002. $\phi_r = 90^o, 270^o$; Polarizations ∥⊥,∥-45,∥∥ 46

29. Calculated ρ' for A02018-002 Using Lambertian Volume Model. $\phi_r = 90^o, 270^o$; Polarizations ∥⊥,∥∥. 47

30. Variation of Polarization Angle of Reflected Radiance as Function of Source-Receiver Position. $\phi_r = 0^o, 180^o$ 49

31. Variation of Polarization Angle of Reflected Radiance as Function of Source-Receiver Position. $\phi_r = 30^o, 210^o$ 50

32. Variation of Polarization Angle of Reflected Radiance as Function of Source-Receiver Position. $\phi_r = 60^o, 240^o$ 51

33. Variation of Polarization Angle of Reflected Radiance as Function of Source-Receiver Position. $\phi_r = 90^o, 270^o$ 52

34. Percent Polarization Variation for A02018-002 as Function of Source-Receiver Position. $\phi_r = 0^o, 180^o$; Perpendicular Source 53

35. Percent Polarization Variation for A02018-002 as Function of Source-Receiver Position. $\phi_r = 0^o, 180^o$; Parallel Source 53

36. Percent Polarization Variation for A02018-001 as Function of Source-Receiver Position. $\phi_r = 0^o, 180^o$; Perpendicular Source 53

37. Percent Polarization Variation for A02018-001 as Function of Source-Receiver Position. $\phi_r = 90^o, 270^o$; Perpendicular Source 54

38. Percent Polarization Variation for A02018-001 as Function of Source-Receiver Position. $\phi_r = 0^o, 180^o$; Parallel Source 54

39. Fixed Bistatic ρ' for A01027; $\lambda = 0.63\ \mu m$ 64

40. Fixed Bistatic ρ' for A01044; $\lambda = 0.63\ \mu m$ 64

41. Fixed Bistatic ρ' for A01047; $\lambda = 0.63\ \mu m$ 64

42. Fixed Bistatic ρ' for A01224; $\lambda = 0.63\ \mu m$ 64
43. Fixed Bistatic ρ' for A01295; $\lambda = 0.63\ \mu m$ 65
44. Fixed Bistatic ρ' for A01341; $\lambda = 0.63\ \mu m$ 65
45. Fixed Bistatic ρ' for A01342; $\lambda = 0.63\ \mu m$ 65
46. Fixed Bistatic ρ' for A01343; $\lambda = 0.63\ \mu m$ 65
47. Fixed Bistatic ρ' for A01444; $\lambda = 0.63\ \mu m$ 66
48. Fixed Bistatic ρ' for A01444; $\lambda = 1.06\ \mu m$ 66
49. Fixed Bistatic ρ' for A01453; $\lambda = 0.63\ \mu m$ 67
50. Fixed Bistatic ρ' for A01453; $\lambda = 1.06\ \mu m$ 67
51. Fixed Bistatic ρ' for A01454; $\lambda = 0.63\ \mu m$ 67
52. Fixed Bistatic ρ' for A01454; $\lambda = 1.06\ \mu m$ 67
53. Fixed Bistatic ρ' for A01455; $\lambda = 0.63\ \mu m$ 68
54. Fixed Bistatic ρ' for A01456; $\lambda = 0.63\ \mu m$ 68
55. Fixed Bistatic ρ' for A01456; $\lambda = 1.06\ \mu m$ 68
56. Fixed Bistatic ρ' for A01608; $\lambda = 0.63\ \mu m$ 68
57. Fixed Bistatic ρ' for A01629; $\lambda = 0.63\ \mu m$ 69
58. Fixed Bistatic ρ' for A01638; $\lambda = 0.63\ \mu m$ 69
59. Fixed Bistatic ρ' for A01640; $\lambda = 0.63\ \mu m$ 69
60. Fixed Bistatic ρ' for A01701; $\lambda = 0.63\ \mu m$ 69
61. Fixed Bistatic ρ' for A02001; $\lambda = 1.06\ \mu m$ 70
62. Fixed Bistatic ρ' for A02004; $\lambda = 1.06\ \mu m$ 70
63. Fixed Bistatic ρ' for Typical Material No. 1 72
64. Fixed Bistatic ρ' for Typical Material No. 2 72
65. Fixed Bistatic ρ' for Typical Material No. 3 72
66. Fixed Bistatic ρ' for Typical Material No. 4 72
67. ρ' for Material No. 1. $\theta_i = 2^\circ$; $\phi_r = 0^\circ, 180^\circ$ 73
68. ρ' for Material No. 1. $\theta_i = 2^\circ$; $\phi_r = 90^\circ, 270^\circ$ 73
69. ρ' for Material No. 1. $\theta_i = 20^\circ$; $\phi_r = 0^\circ, 180^\circ$ 73
70. ρ' for Material No. 1. $\theta_i = 20^\circ$; $\phi_r = 90^\circ, 270^\circ$ 73
71. ρ' for Material No. 1. $\theta_i = 40^\circ$; $\phi_r = 0^\circ, 180^\circ$ 74
72. ρ' for Material No. 1. $\theta_i = 40^\circ$; $\phi_r = 90^\circ, 270^\circ$ 74
73. ρ' for Material No. 1. $\theta_i = 60^\circ$; $\phi_r = 0^\circ, 180^\circ$ 74
74. ρ' for Material No. 1. $\theta_i = 60^\circ$; $\phi_r = 90^\circ, 270^\circ$ 74
75. ρ' for Material No. 2. $\theta_i = 2^\circ$; $\phi_r = 0^\circ, 180^\circ$ 75
76. ρ' for Material No. 2. $\theta_i = 2^\circ$; $\phi_r = 90^\circ, 270^\circ$ 75
77. ρ' for Material No. 2. $\theta_i = 20^\circ$; $\phi_r = 0^\circ, 180^\circ$ 75
78. ρ' for Material No. 2. $\theta_i = 20^\circ$; $\phi_r = 90^\circ, 270^\circ$ 75
79. ρ' for Material No. 2. $\theta_i = 40^\circ$; $\phi_r = 0^\circ, 180^\circ$ 76
80. ρ' for Material No. 2. $\theta_i = 40^\circ$; $\phi_r = 90^\circ, 270^\circ$ 76
81. ρ' for Material No. 2. $\theta_i = 60^\circ$; $\phi_r = 0^\circ, 180^\circ$ 76

82. ρ' for Material No. 2. $\theta_i = 60^o$; $\phi_r = 90^o, 270^o$ 76

83. ρ' for Material No. 3. $\theta_i = 2^o$; $\phi_r = 0^o, 180^o$ 77

84. ρ' for Material No. 3. $\theta_i = 2^o$; $\phi_r = 90^o, 270^o$ 77

85. ρ' for Material No. 3. $\theta_i = 20^o$; $\phi_r = 0^o, 180^o$. 77

86. ρ' for Material No. 3. $\theta_i = 20^o$; $\phi_r = 90^o, 270^o$ 77

87. ρ' for Material No. 3. $\theta_i = 40^o$; $\phi_r = 0^o, 180^o$. 78

88. ρ' for Material No. 3. $\theta_i = 40^o$; $\phi_r = 90^o, 270^o$ 78

89. ρ' for Material No. 3. $\theta_i = 60$; $\phi_r = 0^o, 180^o$ 78

90. ρ' for Material No. 3. $\theta_i = 60^o$; $\phi_r = 90^o, 270^o$ 78

91. ρ' for Material No. 4. $\theta_i = 2^o$; $\phi_r = 0^o, 180^o$ 79

92. ρ' for Material No. 4. $\theta_i = 2^o$; $\phi_r = 90^o, 270^o$ 79

93. ρ' for Material No. 4. $\theta_i = 20^o$; $\phi_r = 0^o, 180^o$ 79

94. ρ' for Material No. 4. $\theta_i = 20^o$; $\phi_r = 90^o, 270^o$ 79

95. ρ' for Material No. 4. $\theta_i = 40^o$; $\phi_r = 0^o, 180^o$ 80

96. ρ' for Material No. 4. $\theta_i = 40^o$; $\phi_r = 90^o, 270^o$ 80

97. ρ' for Material No. 4. $\theta_i = 60^o$; $\phi_r = 0^o, 180^o$ 80

98. ρ' for Material No. 4. $\theta_i = 60^o$; $\phi_r = 90^o, 270^o$ 80

99. Bidirectional Reflectance Geometry 83

TABLES

I. Model Parameters for Sample Paints 18

II. True Source Polarization Angles 18

III. RHOPRIME Input Listing 99

IV. Long Form Output 100

V. Short Form Output 101

BIDIRECTIONAL REFLECTANCE MODEL
VALIDATION AND UTILIZATION

1
INTRODUCTION

A model for predicting the radiance at a remote sensor must include the spatial, spectral, and polarization characteristics of the bidirectional reflectance and directional emittance with respect to target and background surfaces. In principle, the directional reflectance and directional emittance properties of materials must be known for all source and receiver angles, polarizations, and wavelengths. A Lambertian assumption may be valid for some types of backgrounds, but for most man-made targets is scarcely adequate. Measurement of all spatial, polarization, and spectral characteristics of the bidirectional reflectance and directional emittance for a large number of material samples is impractical. Even if such measurement were performed, the data could not all be stored efficiently enough to make it accessible for digital computations. Clearly, an empirical model is required to approximate the bidirectional reflectance and directional emittance properties from a limited number of measurements.

The bidirectional reflectance model developed by the Environmental Research Institute of Michigan (ERIM) is described in this report. The model accounts for effects that produce both specular and diffuse components. In particular, a surface model relates bidirectional reflectance for all source-receiver angles and polarizations to fixed bistatic measurements and a Brewster angle measurement. In addition, the model enables calculation of either a Lambertian diffuse component or a non-Lambertian diffuse component. The latter component accounts for angular and depolarization properties arising from internal scattering effects. Our extension of the bidirectional reflectance model has considerably improved the fit between model predictions and measured data, as will be shown in Section 6.

In addition, we calculated fixed bistatic data from reflectance data for 20 materials included in the Data Compilation of the Eleventh Supplement [2]. Results of these calculations are graphed and tabulated in Appendix I.

A useful method for deriving reflectance data when no computer is available is also presented. For this purpose, simulated data representing typical sets of parameters are provided as well as a method whereby typical fixed bistatic data may be used to bracket measured zero bistatic data for a particular material so that the bidirectional reflectance for that material may be estimated by an interpolation method as described in Section 8.

As it now stands, the model permits generation of an enormous amount of bidirectional reflectance data from a very small amount of measured data. The accuracy shown in Section 6 on Model Validation indicates that the model is very effective, although it can still be improved, particularly at large receiver zenith angles. With the ability to account for elliptical (particularly circular) polarization now built in, the model is available for use with circularly polarized sources, if these sources prove useful in the future.

In this report, we compare measured data with results computed from both the initial model and from the extended model, and then evaluate the relative performance of the two. We establish a domain of validity for each, based on material properties. Since the modeling is empirical, only a limited amount of measured data are required as input parameters. In this case, the parameters are the fixed bistatic data. Therefore, data from the Data Compilation [1, 2] are used to derive fixed bistatic curves contained in Appendix I.

All modeling described in this report was performed with respect to one wavelength, $\lambda = 1.06$ μm.

BIDIRECTIONAL REFLECTANCE

One physical property which can be measured directly from a sample of material is bidirectional reflectance. The physical definition is

$$\rho'(\theta_i, \phi_i; \theta_r, \phi_r) = \frac{\delta L_r(\theta_r, \phi_r)}{\delta E_i(\theta_i, \phi_i)} \tag{1a}$$

where $\delta E_i(\theta_i, \phi_i)$ is the incremental irradiance (power per unit area) impingent on the surface of a material from the direction (θ_i, ϕ_i), and $L_r(\theta_r, \phi_r)$ is the resulting increment of radiance (power per unit projected area per unit solid angle) scattered from that surface in the direction (θ_r, ϕ_r). Figure 1 illustrates the situation. The bistatic angle, 2β, is that angle between the vectors which point to the source and the receiver respectively.

Equation (1a) can be rewritten in terms of directly-accessible experimental parameters as

$$\rho'(\theta_i, \phi_i; \theta_r, \phi_r) = \frac{\dfrac{\delta P_r}{\delta A \cos\theta_r \delta\Omega_r}}{\dfrac{\delta P_i}{\delta A}} \tag{1b}$$

where δP_i is the power, in watts, incident from the direction (θ_i, ϕ_i) on the small area δA, and δP_r is the resulting power scattered into the small solid angle $\delta\Omega_r$ in the direction (θ_r, ϕ_r).

When polarization dependence is to be shown, subscripts are appended to the ρ' term. Thus when we write $\rho'_{\alpha_i \alpha_r}$, the leading subscript, α_i, describes the source polarization while the trailing subscript, α_r, describes the receiver polarization. The source polarization, always referred to the plane of incidence, describes the polarization state of the electric field vector. The appended subscript symbols $\parallel$ and $\perp$ indicate whether the source electric vector polarization is parallel to or perpendicular to the incidence plane. The reflected electric field polarization state is specified by the same symbols, but here the reference plane is that reflectance plane defined by the sample normal and the direction to the receiver. (For example, $\rho'_{\perp\parallel}$ represents reflectance measured when source polarization is perpendicular to the incidence plane and receiver polarization is parallel to the reflectance plane.) Notice that when either the source or the receiver, or both, are scanned in angle over the sample, the incidence and reflectance planes change orientation with relation both to the sample and to each other.

Bidirectional reflectance depends on the physical properties of the material as well as on the geometric state of its surface. Different surface states result in different reflectances. Hence, a complete collection of bidirectional reflectance data for any single material would require measurements of a large number of samples of the material, each with a different surface state. Each sample would have to be measured with several source-receiver polarization combinations. Consequently a very large number of source and receiver positions would be

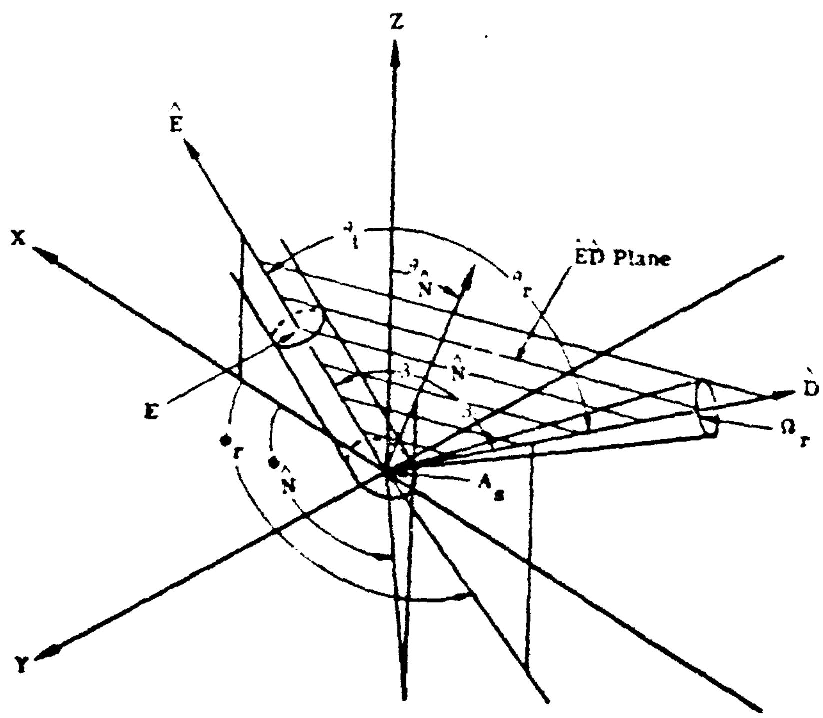

FIGURE 1. BIDIRECTIONAL REFLECTANCE GEOMETRY AND PARAMETERS

required for each set of polarization states. Finally, the entire procedure would have to be repeated at many different wavelengths. The purpose of modeling is to predict reflectance data from only a limited number of measurements and hence eliminate the need for an otherwise unwieldy measurement program.

3
BACKGROUND INFORMATION

The bidirectional reflectance model is based on observations of polarized bidirectional data from rough, painted surfaces which exhibit a Brewster angle (Fresnel-like behavior in relation to the specular geometry). The degree of depolarization appears slight, and on that basis for the initial modeling work in this program single specular reflection from the rough front surface was assumed to be the dominant reflection mechanism. Multiple front-surface reflections and internal scatterings were observed to be smaller and were initially incorporated into a Lambertian "volume" model to account for the diffuse component.

The assumption that the diffuse component is Lambertian, however, makes it difficult to account for certain anomalies that occur when measured data are compared with the model's output. For example, Fig. 2 is a bidirectional reflectance curve showing the reflectances at the receiver as the receiver scans over zenith angles from 0^{o} to 90^{o} in the $\phi_r = 0^{o}$ and $\phi_r = 180^{o}$ half planes. The source remains fixed at $\theta_i = 40^{o}$ and $\phi_i = 180^{o}$. The upper curve shows reflectances when source and receiver are both linearly polarized at the same polarization angle with respect to the target-incidence and target-receiver planes. (In this case, both are perpendicular-polarized.) The lower curve shows reflectances when source and receiver are cross-polarized with respect to one another. (Source is perpendicular-polarized; receiver is parallel-polarized.) Note the marked angular dependence in the lower curve. If the nonspecular component were truly Lambertian, no such angular dependence would be present.

Also, although radiation sources in this work are all linearly polarized, future work may well involve more general cases. Therefore, the model should account for the most general type of polarization—namely, elliptical.

For the above reasons, and in order to obtain a closer overall correspondence between model prediction and measured data, the model has been extended to account for the following:

(1) possible non-Lambertian angular dependence of depolarized component
(2) shadowing and obscuration produced by the roughness of the surface
(3) elliptical polarization

The model—a phenomenological one in that its use requires a limited number of measurements—is described in the next two sections. Section 4 includes a discussion of specular reflectance from the surface, effects caused by shadowing and obscuration resulting from surface roughness, and polarization effects. Section 5 describes the volume model.

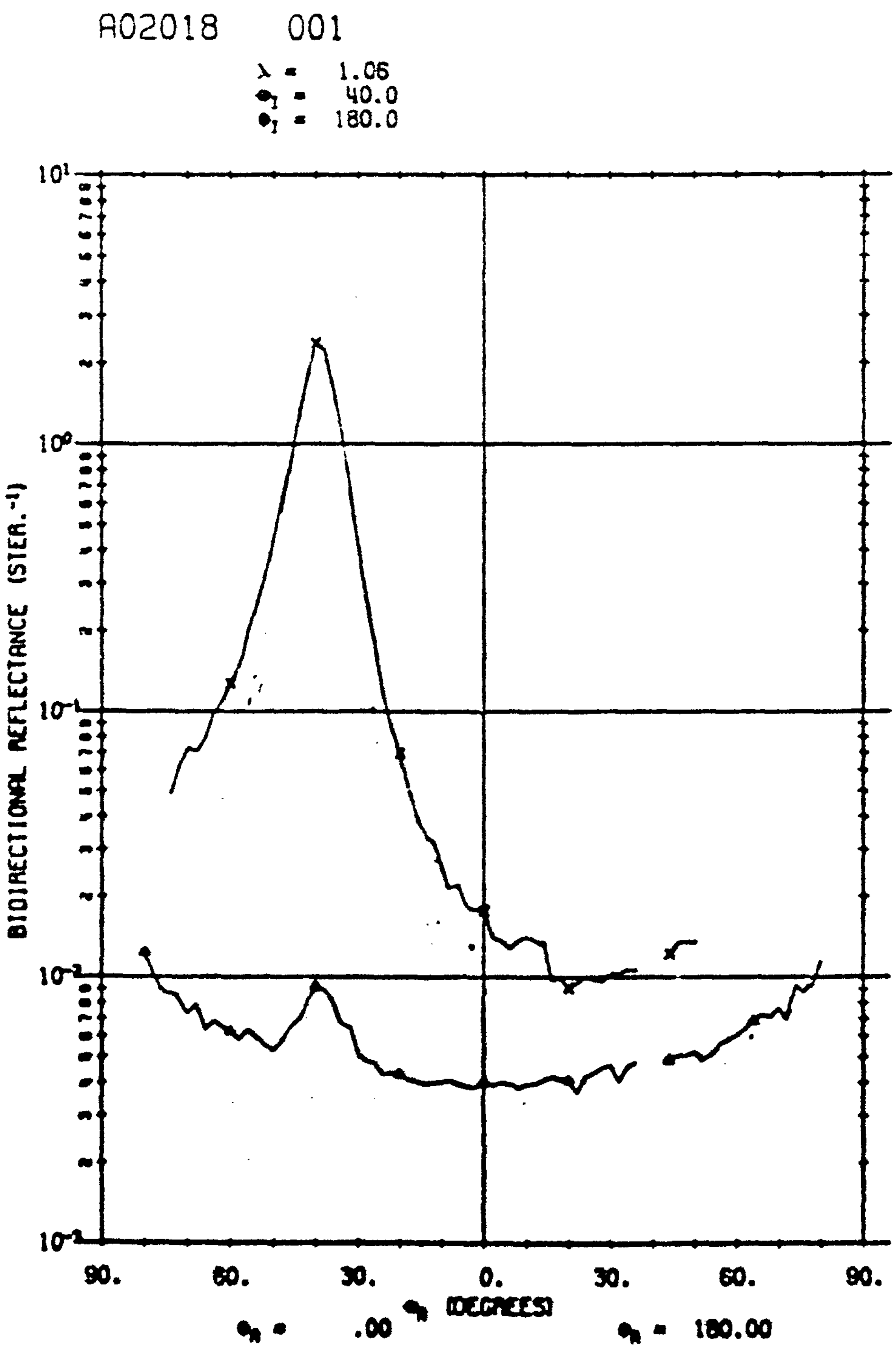

FIGURE 2. EXAMPLE OF ρ' FOR A02018-001. θ_i = 40°, θ_r scanned in plane.

4
SURFACE MODEL

In this section, we review the surface model and also discuss the interference effects that necessitated model modification.

4.1. AVAILABLE AREA

If the rough surface is considered to be made up of small sequins having a distribution of orientations, there will be some specular reflectance at any receiver angle and the extent of that reflectance will be determined in part by the amount of surface oriented for specular reflection at that receiver angle. (The area available for such reflection will also depend on how some sequins shadow or obscure others.) Since measurements do, in fact, show a reflectance distribution over the hemisphere, we assume that the above description is valid and that there is, indeed, a distribution of surface areas which have normals pointing in different directions. Therefore, to establish the distribution of available surface area, we define a density function $\Xi(\theta, \phi)$ which describes the relative density of local surface normals (per steradian) pointing in the direction (θ, ϕ).

The effect of the distribution of surface normals is measured by a zero bistatic measurement in which $\theta_i = \theta_r$ and $\phi_i = \phi_r$. (Note that we really use a fixed bistatic scan with a small bistatic angle. A true zero bistatic scan would be very difficult to obtain since source and receiver obviously cannot occupy the same position.)

4.2. FRESNEL COEFFICIENTS

Fresnel reflectance coefficients describe the reflectance and polarization of specularly reflected radiation as functions of source and detector positions and of the complex index of refraction. However, since we are trying to find reflectance as a function of source and detector positions only, we must know—or be able to determine—the index of refraction. (As discussed later in this section, we can determine the index by measuring the Brewster angle.) Since, in the surface model, we consider only single, local specular reflections, the Fresnel equations automatically account for polarization.

If the receiver subtends the solid angle $\delta\Omega_r$ from the sample (see Fig. 1) the solid angle $\delta\Omega_{\hat{n}}$ in which local surface normals must lie to permit collection of the local specularly reflected radiation by the receiver is given by:

$$\delta\Omega_{\hat{n}} = \frac{\delta\Omega_r}{4} \cos\beta \qquad (2)$$

This solid angle is centered about the direction $\left(\theta_{\hat{n}}, \phi_{\hat{n}}\right)$.

Let δP_i be power incident on area δA. The fraction of surface area, $\delta A\left(\theta_{\hat{n}}, \phi_{\hat{n}}\right)$, which reflects radiation into the receiver is given by

$$\delta A\left(\theta_{\hat{n}}, \phi_{\hat{n}}\right) = \Xi\left(\theta_{\hat{n}}, \phi_{\hat{n}}\right)\delta A\, \delta\Omega_{\hat{n}} \tag{3}$$

The power incident on $\delta A\left(\theta_{\hat{n}}, \phi_{\hat{n}}\right)$ is

$$\delta P_i \frac{\delta A\left(\theta_{\hat{n}}, \phi_{\hat{n}}\right)}{\delta A} \frac{\cos\beta}{\cos\theta_i} \,. \tag{4}$$

Since the Fresnel reflectance, $R(\beta)$, is just the ratio of reflected power to incident power, then

$$\delta P_r = R(\beta)\delta P_i \frac{\delta A\left(\theta_{\hat{n}}, \phi_{\hat{n}}\right)}{\delta A} \frac{\cos\beta}{\cos\theta_i} \tag{5}$$

Recall that in Eq. (1b): $\rho'(\theta_i,\phi_i;\ \theta_r,\phi_r) = \dfrac{\dfrac{\delta P_r}{\delta A \cos\theta_r \delta\Omega_r}}{\dfrac{\delta P_i}{\delta A}}$. Substituting Eqs. (5), (3) and (2):

$$\rho'(\theta_i,\phi_i;\ \theta_r,\phi_r) = \frac{R(\beta)\Xi\left(\theta_{\hat{n}}, \phi_{\hat{n}}\right)}{4\cos\theta_i \cos\theta_r} \tag{6}$$

By considering the case when source and receiver are in the same position, i.e., a zero bistatic ($\beta = 0$) case, $\Xi\left(\theta_{\hat{n}}, \phi_{\hat{n}}\right)$ can be determined. In this situation

$$\rho'\left(\theta_{\hat{n}},\phi_{\hat{n}};\ \theta_{\hat{n}},\phi_{\hat{n}}\right) = \frac{R(0)\,\Xi\left(\theta_{\hat{n}}, \phi_{\hat{n}}\right)}{4\cos^2\theta_{\hat{n}}} \tag{7}$$

and

$$\Xi(\theta, \phi) = \frac{4\rho'\left(\theta_{\hat{n}},\phi_{\hat{n}};\ \theta_{\hat{n}},\phi_{\hat{n}}\right)\cos^2\theta_{\hat{n}}}{R(0)} \tag{8}$$

Now substitute back into Eq. (6) and

$$\rho'(\theta_i,\phi_i;\ \theta_r,\phi_r) = \frac{R(\beta)}{R(0)} \frac{\rho'\left(\theta_{\hat{n}},\phi_{\hat{n}};\ \theta_{\hat{n}},\phi_{\hat{n}}\right)\cos^2\theta_{\hat{n}}}{\cos\theta_i \cos\theta_r} \tag{9}$$

Equation (9) is an expression for the bidirectional reflectance given in terms of measured data and Fresnel reflectance coefficients. However, to evaluate the Fresnel coefficients so they can be used in Eq. (9) takes a little work. For example, $R(\beta)$ is a function of the real and imaginary parts of the complex index of refraction, $n' = n - ik$ (see Ref. 3 or Appendix III). Therefore, n and k must be found before $R(\beta)$ can be determined.

Moreover, k is taken to be very small* so that n can be determined experimentally by measuring the Brewster angle, θ_B, and then using $n = \tan \theta_B$ to solve for n.

4.3. SHADOWING AND OBSCURATION

Referring to Eq. (9), we can derive a zero bistatic curve, $\rho'\left(\theta_{\hat{n}},\phi_{\hat{n}};\theta_{\hat{n}},\phi_{\hat{n}}\right)$, from a $\rho'(\theta_i\phi_i,\theta_r\phi_r)$ curve with θ_i, ϕ_i fixed and θ_r variable by inverting the equation so that

$$\rho'\left(\theta_{\hat{n}}\phi_{\hat{n}},\theta_{\hat{n}}\phi_{\hat{n}}\right) = \frac{R(0)}{R(\beta)}\frac{\rho'(\theta_i\phi_i\theta_r\phi_r)\cos\theta_i\cos\theta_r}{\cos^2\theta_{\hat{n}}} \tag{10}$$

after doing this for a variety of θ_i's, we found that the curves obtained differed systematically from those obtained from a fixed bistatic measurement. Apparently, because of surface roughness, some sequins shadow or obscure others; this reduces reflectance everywhere except at a purely back-scattered position. The model must therefore be modified to correct for such interference.

Torrance and Sparrow [4] have developed an analytical function that helps correct the situation; however, we have constructed our own function using empirical considerations only. Our function results in better agreement between measured and derived fixed bistatic curves than does the analytical function of Torrance and Sparrow. The empirical function (SO) is defined as:

$$SO = \frac{1+\frac{\phi_{\hat{n}}}{\Omega}e^{-2\beta/\tau}}{1+\frac{\phi_{\hat{n}}}{\Omega}}\left(\frac{1}{1+\frac{\phi_n}{\Omega}\frac{\theta_i}{\Omega}}\right) \tag{11}$$

where Ω and τ are parameters, and ϕ_n is a factor calculated from the geometry, which adjusts the fall-off rate of the shadowing and obscuration function in the forward-scattered direction.

*For the calculations in this study, results of past measurement programs [1] were used to establish the refractive indices. In those programs, it was determined that the magnitude of the total index of refraction was close to 1.65; that the imaginary part of the index of refraction could be neglected, compared to the real part; and that the index of refraction, for the wavelengths of incident radiation under consideration (1 to 4 μm), did not vary appreciably.

We now modify Eq. (9):

$$\rho'(\theta_i,\phi_i;\ \theta_r,\phi_r) = \frac{R(\beta)}{R(0)} \frac{\rho'\left(\theta_{\hat{n}},\phi_{\hat{n}};\ \theta_{\hat{n}},\phi_{\hat{n}}\right)\cos^2\theta_{\hat{n}}}{\cos\theta_i \cos\theta_r}\ (SO) \tag{12}$$

Equation (10) becomes

$$\rho'\left(\theta_{\hat{n}},\phi_{\hat{n}};\ \theta_{\hat{n}},\phi_{\hat{n}}\right) = \frac{R(0)}{R(\beta)} \frac{\rho'(\theta_i,\phi_i;\ \theta_r,\phi_r)\cos\theta_i\cos\theta_r}{\left(\cos^2\theta_{\hat{n}}\right)(SO)} \tag{13}$$

5
VOLUME MODELS

The following discussion outlines the reasoning behind the extended portion of the bidirectional reflectance model. (The extended portion is referred to as the "volume" model.)

Different materials with varying degrees of surface roughness and different optical properties show differences in nonspecular reflectance behavior. These differences show up in the extent to which the nonspecular reflectance is dependent upon angular position of the receiver.

To make provision for materials that do exhibit such angular dependence and for those that do not, two volume models are used. The following discussion describes, first, a Lambertian volume model which has no angular dependence, and then a non-Lambertian volume model in which angular dependence is important.

5.1. LAMBERTIAN

In addition to Fresnel reflection from a surface, other effects such as might take place beneath the surface can produce a nonspecular reflectance component everywhere in the hemisphere. If the surface roughness as well as the absorption properties of the surface are right, this volume reflectance may be completely diffuse and uniform over the hemisphere. Moreover, the reflected radiation will be totally depolarized, regardless of the polarization of the source. Thus, if the receiver is polarized in the orthogonal direction to the source polarization, an in-plane measurement will represent the volume component only. However, only half the volume component is actually represented, since there should be an equal diffuse contribution polarized in the same direction as the source.

The Lambertian volume component is one of the input parameters for the model when a target material with Lambertian reflectance properties is considered. A method whereby values for this parameter may be extracted is described in Section 6.

5.2. NON-LAMBERTIAN

On the basis of the Lambertian diffuse model described above, no angular dependence would be expected for the diffuse component. However, for some materials, actual measurements show that there is an angular dependence. To provide for the angular dependence of the diffuse component, the model has been extended by including scattering that takes place beneath the surface.

Assuming an exponential scattering function as the radiation first enters and then leaves the surface, and making reference to Fig. 3, we construct an expression for the volume scattering component of the bidirectional reflectance as follows:

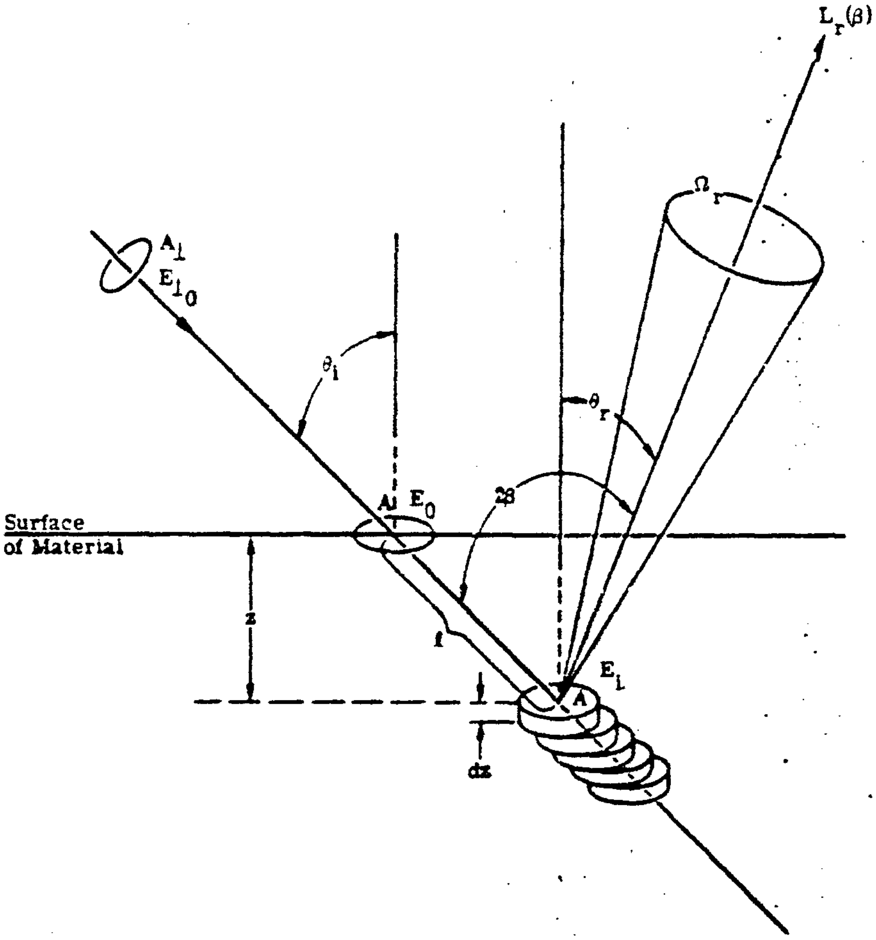

FIGURE 3. VOLUME SCATTERING GEOMETRY AND PARAMETERS

$E_{\perp 0}$ = irradiance at surface of area $A_\perp$, where $A_\perp$ is the area of cross section of the collimated beam and is normal to the beam

E_0 = irradiance on surface element of area A

E_i = irradiance on surface of slab or area A at distance z beneath surface

$L_r(\beta)$ = radiance scattered from primary beam through 2β in direction of receiver

β = half of angle between target-to-source and target-to-receiver vectors

σ = total scattering cross section (ignoring absorption)

$\sigma(\beta)$ = differential scattering cross section with respect to β, i.e., $\int \sigma(\beta)\, d\Omega = \int d\sigma/d\Omega\, d\Omega = \sigma$

Ω = solid angle subtended at target by receiver, assuming a point target

θ_i = angle of incident beam relative to fixed z axis

θ_r = angle of reflected beam relative to fixed z axis

The objective of the following calculation is to determine that portion of the primary beam scattered from distance z beneath the surface through an angle 2β toward a receiver which subtends solid angle Ω.

First, the bidirectional reflectance defined in Eq. (1) is now $\rho' = L_r/E_0$ with respect to the slab (see Fig. 3). To determine E_0:

$$A_\perp = A \cos \theta_i \tag{14}$$

$$E_0 = \frac{P}{A} = \frac{P/A_\perp}{\cos \theta_i} = \frac{P \cos \theta_i}{A_\perp} = E_{\perp 0} \cos \theta_i \tag{15}$$

where P is the power at surface of area A.

The irradiance incident on the slab at distance z beneath its surface is:

$$E_i = E_0 e^{-\sigma \ell} = E_0 e^{-\sigma z/\cos \theta_i} \tag{16}$$

where $\ell = z/\cos \theta_i$. Hence

$$E_i = E_{\perp 0} \cos \theta_i e^{-\sigma z/\cos \theta_i} \tag{17}$$

and

$$dE_i = -E_{\perp 0} \sigma e^{-\sigma z/\cos \theta_i} dz \tag{18}$$

where dE_i is the amount by which irradiance decreases in going from distance z to distance z + dz beneath surface. Note also that $e^{-\sigma z/\cos \theta_i}$ and $e^{-\sigma z/\cos \theta_r}$ represent the scattering loss from the beam on the way in and on the way out of the material, respectively. To determine L_r.

$P_r = L_r A\Omega_r \cos\theta_r$ = power at the receiver (19)

dL_r = radiance scattered, in direction of receiver, from one small slab of thickness dz (20)

Radiance from slab in direction θ_r (or β) can be written:

$$dL_r = -dE_i\sigma(\beta) \tag{21}$$

since $\sigma(\beta)$ is, by definition the fraction of beam scattered into 2β. Note that (since we are ignoring absorption) irradiance lost from the incident beam is the radiance of the scattered beam; therefore a minus sign precedes dE_i. Hence, if there is no further power loss

$$dP_r = -A\Omega_r dE_i\sigma(\beta) \tag{22}$$

However, power loss caused by beam scattering occurs on the way out as well as the way in; the loss is represented by $\left(e^{-\sigma z/\cos\theta_r}\right)$ on the way out.

Therefore

$$dP_r = \left(-A\Omega_r\,\sigma(\beta)e^{-\sigma z/\cos\theta_r}dE_i\right) = -\frac{A_i}{\cos\theta_i}\Omega_r\sigma(\beta)e^{-\sigma z/\cos\theta_r}dE_i \tag{23}$$

Substituting the expression for dE_i, Eq. (18), into Eq. (23), we obtain:

$$dP_r = E_{i0}\sigma e^{-\sigma z/\cos\theta_i}\left(\frac{A_i\sigma(\beta)e^{-\sigma z/\cos\theta_r}}{\cos\theta_i}\right)\Omega_r\,dz \tag{24}$$

$$P_r = \int_0^\infty dP_r = \frac{E_{i0}A_i\Omega_r}{\cos\theta_i}\cdot\frac{\sigma(\beta)}{\left(\frac{1}{\cos\theta_i}+\frac{1}{\cos\theta_i}\right)} \tag{25}$$

where the integration from 0 to ∞ assumes no transmission of power through the material, i.e., the material has effectively an infinite thickness with respect to transmission. Therefore

$$L_r = \frac{P_r}{A\cos\theta_r\Omega_r} = \frac{E_{i0}\sigma(\beta)}{\cos\theta_r\left(\frac{1}{\cos\theta_i}+\frac{1}{\cos\theta_r}\right)} \tag{26}$$

and

$$\rho' = \frac{L_r}{E_0} = \frac{\sigma(\beta)}{\cos\theta_i\cos\theta_r\left(\frac{1}{\cos\theta_i}+\frac{1}{\cos\theta_r}\right)} = \frac{\sigma(\beta)}{(\cos\theta_i+\cos\theta_r)} \tag{27}$$

In ignoring the finite thickness of the layer of material, we have also ignored the possible specular reflectance of the bottom surface. To account for the possibility of specular reflection from the bottom layer, it may be useful to provide a parameter function peaked near $\theta_{\hat{n}} = 0$. Therefore, we include all β dependence in a function $f(\beta)$, and all $\theta_{\hat{n}}$ dependence in a function $g\left(\theta_{\hat{n}}\right)$, and write

$$\rho' = 2\,\frac{\rho_V f(\beta) g\left(\theta_{\hat{n}}\right)}{\cos\theta_i + \cos\theta_r} \tag{28}$$

where $f(\beta)$ and $g\left(\theta_{\hat{n}}\right)$ provide freedom for empirical adjustment. The constant, ρ_V, represents the value of ρ' when $\theta_i = \theta_r = 0$ and $f(\beta) = g\left(\theta_{\hat{n}}\right) = 1$.

6
MODEL VALIDATION

Use of the bidirectional reflectance model requires a limited amount of measured data (namely the zero bistatic measurement) from which complete sets of reflectances can be calculated. The results of these model-calculated bidirectional reflectances can then be compared to corresponding results of actual measurements. This was the procedure we followed to validate the model.

Model calculations and measured data were compared in terms of ρ' (the reflectance), α or ψ_r (the angle of polarization for the beam after reflection from the target), and P (the percentage of polarization of the reflected beam).

Measured data for materials of different properties (color and roughness) were used to demonstrate the model's performance. The materials are designated as A02018-001 and A02018-002 and are not included in the previous compilation[1, 2]. Material A02018-001 is a green paint and material A02018-002 is a tan paint. These materials were supplied by the Army Ballistic Research Laboratories for the purpose of developing the non-Lambertian diffuse component of the model. They were used for validation because an unusually extensive set of measurements could be made on them. Model parameters are listed in Table I. (See Section 7 for definitions of model parameters.) The overall discussion of the model fitting is divided into four parts:

(1) ρ' for A02018-001

(2) ρ' for A02018-002

(3) polarization angle (α or ψ_r) for A02018-001

(4) percent polarization (P) for A02018-001 and A02018-002

In what follows, the orientation of the source polarizer in the measurements of materials A02018-001 and A02018-002 was not actually perpendicular, parallel, nor at 45° to the plane of incidence but instead was offset by 5° in each case. Specifically, the appropriate correspondences, shown in Table II, should be recognized. These shifts were taken into account when the validation calculations were made on the computer; however, we continue to refer to "perpendicular," "parallel," and "45°."

6.1. REFLECTANCE FOR SAMPLE MATERIAL A02018-001

Material A02018-001 is a green painted surface. The zero bistatic measurement with 5° polarization angle (i.e., almost perpendicular polarization) is shown in Fig. 4. (The zero bistatic data with parallel-polarized source, although not shown, have identical characteristics.) The zero bistatic plot is sharply peaked at 0°, falling off rapidly to a constant value at about

TABLE I. MODEL PARAMETERS FOR SAMPLE PAINTS

Parameter	Material A02018-001	Material A02018-002
n	1.65	1.65
k	0	0
$\rho_{\chi 1}$	---*	0.044
$\rho_{\chi 2}$	---*	0.044
ρ_v	0.007	0.05**
τ	15	15
Ω	40	40
$f(\beta)$	1	1
$g\left(\theta_{\hat{n}}\right)$	1	1
$\rho'\left(\theta_{\hat{n}}, \theta_{\hat{n}}; \theta_{\hat{n}}, \theta_{\hat{n}}\right) \cos^2 \theta_{\hat{n}}$	----	----
λ	1.06 μm	1.06 μm

*This material is run with the non-Lambertian volume model; therefore ρ_χ values are not necessary.

**Material 2018-002 was run with the Lambertian volume model; therefore ρ_v should not be used.

TABLE II. TRUE SOURCE POLARIZATION ANGLES

Receiver Azimuth Plane	Nominal Angles $\perp(0^\circ)$	$\parallel(90^\circ)$	$+45^\circ$	-45°
0°-180°, 30°-210°, 60°-240°	5°	-85°		-40°
90°-270°	5°	$+95^\circ$	$+50^\circ$	
Fixed Bistatic	5°	$+95^\circ$	$+50^\circ$	

A02018 001

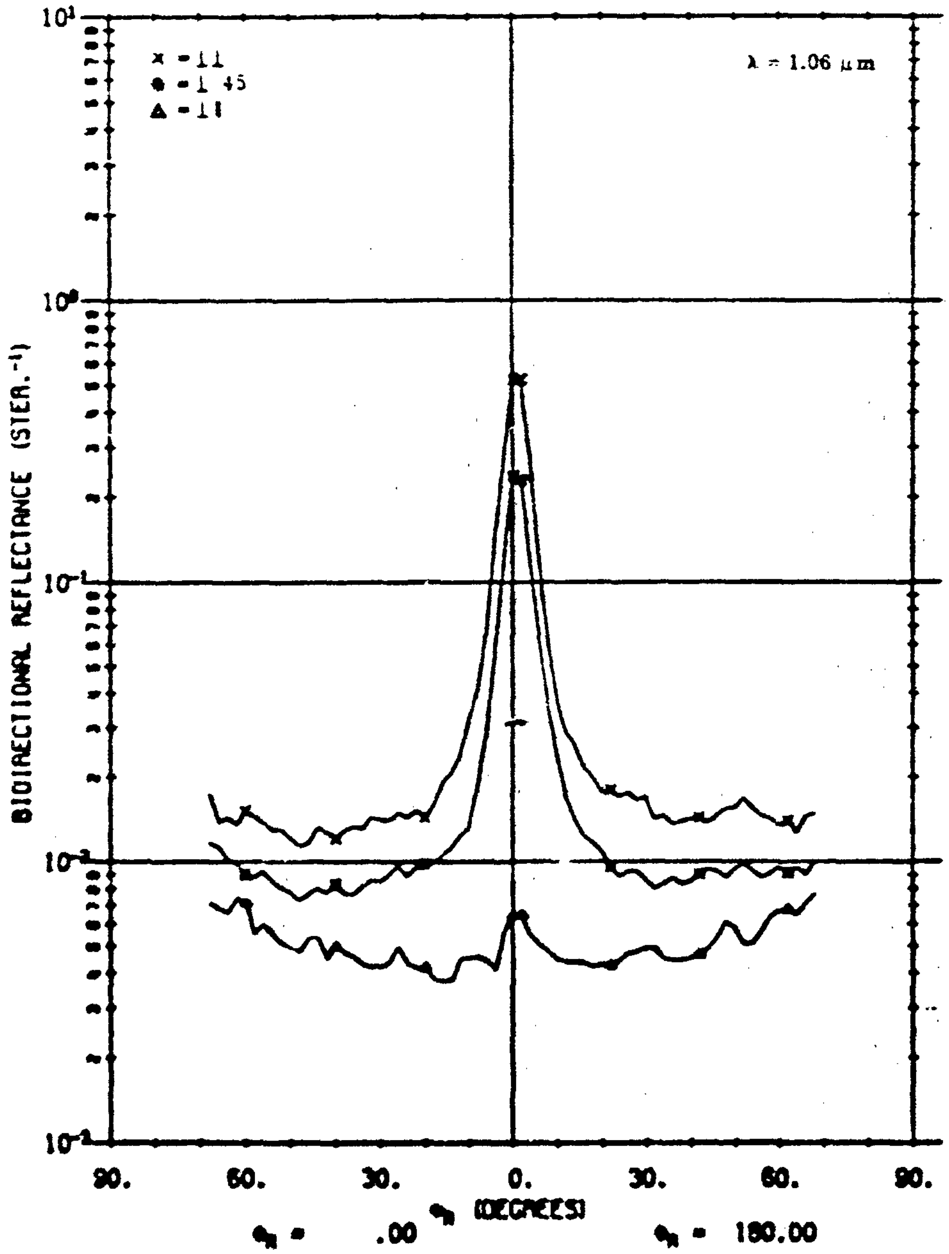

FIGURE 4. FIXED BISTATIC ρ' FOR A02018-001

20°. In all receiver polarizations, ρ' shows an angular dependence clearly departing from Lambertian behavior. The table of values for $\rho'\left(\theta_{\hat{n}}, \phi_{\hat{n}}; \theta_{\hat{n}}, \phi_{\hat{n}}\right) \cos^2 \theta_{\hat{n}}$ used in the model was obtained from this measurement by reading off $\rho'_{\perp\perp}$ and $\rho'_{\perp\parallel}$ at each angle and then calculating $(\rho'_{\perp\perp} - \rho'_{\perp\parallel}) \cos^2 \theta_{\hat{n}}$ where $\theta_{\hat{n}}$ is the angle that the normal to the reflecting facet makes with the fixed z-axis. In zero bistatic scans, $\theta_i = \theta_r = \theta_{\hat{n}}$ (see Fig. 1). (Physically the source and receiver were separated by 1.8°. Thus, both were 0.9° from the true $\theta_{\hat{n}}$. In the calculations, the axis was translated to bring the x-axis into correspondence with $\theta_{\hat{n}} = 0$.) The subtraction, $\rho'_{\perp\perp} - \rho'_{\perp\parallel}$ eliminates the diffuse contribution which would distort the value for $\rho'\left(\theta_{\hat{n}}, \phi_{\hat{n}}; \theta_{\hat{n}}, \phi_{\hat{n}}\right)$ which is what must be measured (recall Eq. 9).

In Figs. 5, 7, 9 and 11,* plots of measured data are shown for $\theta_i = 40$, $\phi_i = 180^{\circ}$ and where θ_r is scanned in azimuth planes represented by $\phi_r = 0^{\circ}, 180^{\circ}; 90^{\circ}, 270^{\circ}; 30^{\circ}, 210^{\circ}; 60^{\circ}, 240^{\circ}$. Each measurement plot is followed by plots of data generated, respectively, by the Lambertian model with no shadowing and obscuration factor, by the non-Lambertian model with no shadowing and obscuration factor, and by the non-Lambertian model <u>with</u> the shadowing and obscuration factor. For example, Fig. 6 shows the calculated ρ' data for $\theta_i = 40^{\circ}$ and θ_r as scanned in the 0° and 180° azimuth planes for the above variations of the model. The simulated source is taken to have a "perpendicular" polarization angle. In these in-plane scans ($\phi_r = 0^{\circ}, 180^{\circ}$), the main peak is in the 0° azimuth plane which is the forward direction for the source angle of $\phi_i = +180^{\circ}$. Note the rise (in the plot of <u>measured</u> data) at large zenith angles for the cross-polarized component. This is a characteristic which suggests the need for the non-Lambertian volume model.

<u>Surface Plus Lambertian Volume Model with No Shadowing and Obscuration Correction.</u> Figure 6 plots (in solid lines) the model calculation using the surface model plus the Lambertian volume model with no correction for shadowing and obscuration. The following characteristics should be noted:

(1) In the $\phi_r = 0$ (forward scattering) azimuth plane, the model fits the measured data very well between $\theta_r = 0$ and $\theta_r = 50^{\circ}$ for matched polarization of source and receiver. At $\theta_r = 60^{\circ}$, the calculated curve suddenly diverges. This is thought to be the result of the failure to account for shadowing and obscuration as discussed earlier. At $\theta_r = 0^{\circ}$ and on into the backscattered ($\phi_r = 180^{\circ}$) direction, the calculated values lie above the measured values and this, too, is believed to be the result of the lack of a shadowing and obscuration correction.

(2) In the cross-polarization component ($\perp\parallel$), the model predicts a flat response except for a slight bump under the specular peak. The measured data, however, show a clear angular dependence on θ_r.

*Note: On all reprints of original computer plots, the symbols θ_r and ϕ_r are represented by Θ_R and Φ_R respectively.

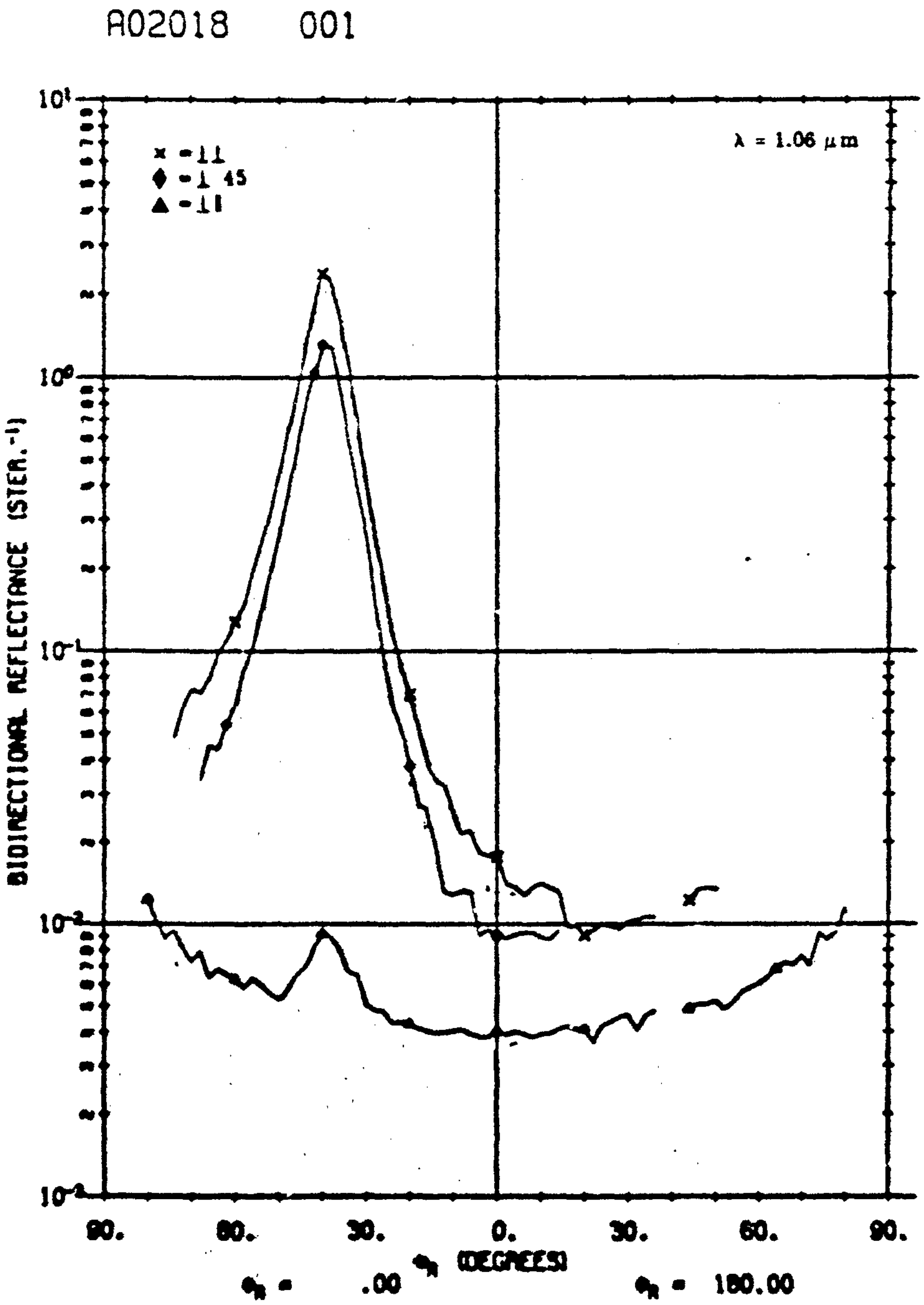

FIGURE 8. MEASURED ρ' FOR A02018-001. $\theta_i = 40^0$, $\phi_r = 0, 180^0$.

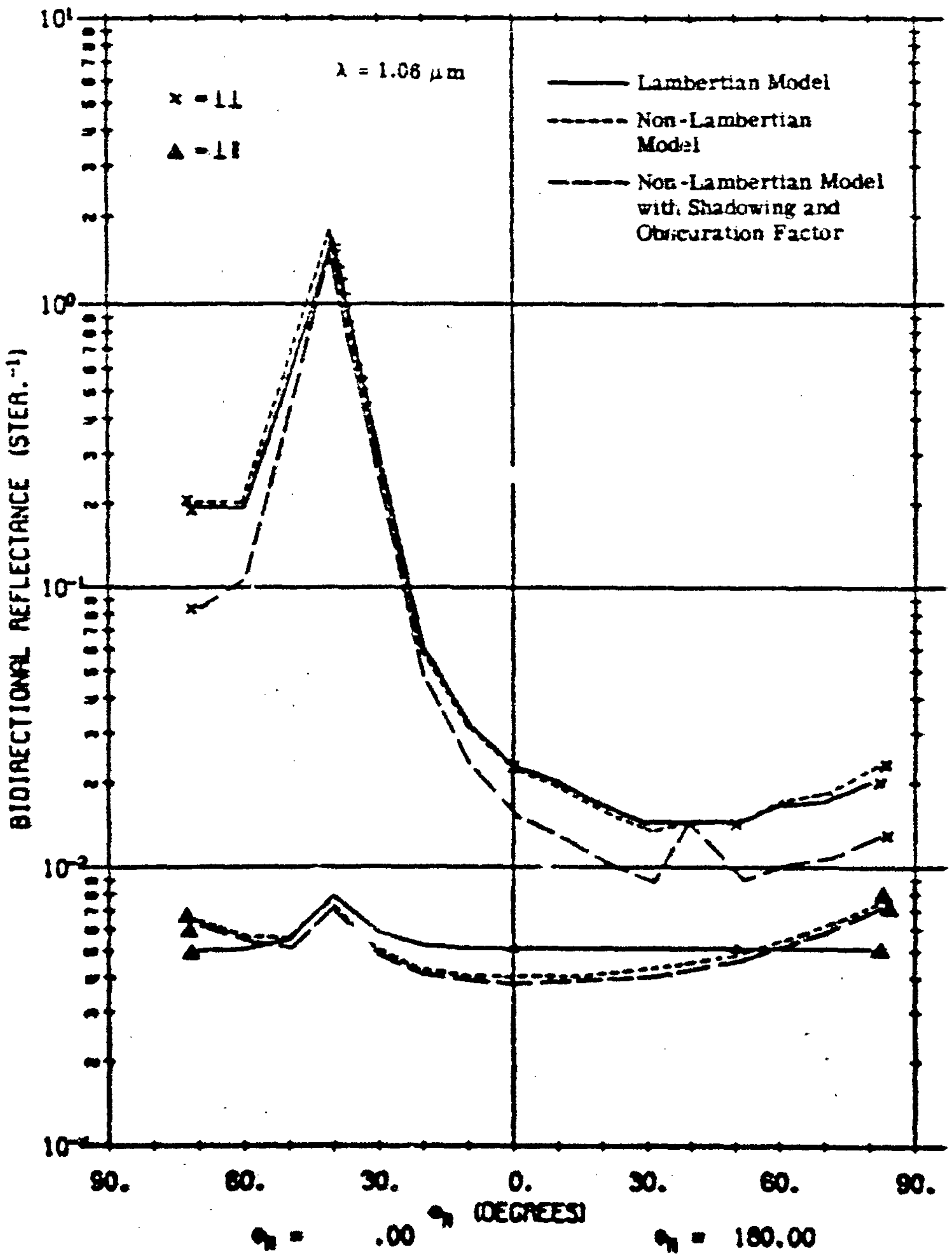

FIGURE 6. CALCULATED ρ' FOR A02018-001 USING LAMBERTIAN VOLUME MODEL AND NON-LAMBERTIAN MODEL WITH AND WITHOUT SHADOWING AND OBSCURATION FACTOR. $\theta_i = 40^\circ$, $\phi_r = 0^\circ, 180^\circ$.

With the exception of these two characteristics, however, the surface plus Lambertian volume model with no shadowing and obscuration correction fits the measured data fairly well.

Non-Lambertian Volume Model with No Shadowing and Obscuration Correction. The dotted lines in Fig. 6 show a model plot using the same parameters, except that the non-Lambertian volume model is now used. Keep in mind that one may use the non-Lambertian volume scattering as a model by itself or in conjunction with a specular component. The latter is used here. In the like-polarized component, nothing has changed from the previous case. However, the cross-polarized component now fits the measured data much more closely. It rises steadily at large angles, both in the back-scattered and forward-scattered directions—a result of $1/(\cos\theta_i + \cos\theta_r)$ dependence shown in Eq. (28) for the volume model. However, the response for the like-polarized component does not drop sharply enough at either side of the peak, and at high angles in the forward-scattered direction, the awkward divergence still appears at 60°.

Thus, the non-Lambertian volume model improves the cross-polarized fit (with respect to material A02018-001) over that of the Lambertian volume model and, apart from anomalies at high angles and near 0°, provides a reasonable fit to the measurements.

Non-Lambertian Volume Model with Shadowing and Obscuration Correction. The dashed-line curves in Fig. 6 show results with the shadowing and obscuration correction applied to the non-Lambertian volume model calculation. The cross-polarized component is unaffected. The net effect on the match-polarized component is to reduce the reflectance everywhere except at the specular peak and at the direct backscattering peak (i.e., at $\beta = 0$). In particular, it lowers the forward-scatter contributions beyond 50°, bringing the model closer to measured data in this region. Overall, the fit obtained using the volume model with a shadowing and obscuration correction agrees closely with measurements.

The foregoing discussion applies to "in plane" receiver scans—those in the $\phi_r = 0$ and $\phi_r = 180^{\circ}$ azimuth planes. The azimuth plane perpendicular to the 0°, 180° plane is the 90°, 270° plane and is referred to as "out-of-plane". The plane we are in or out of is the plane of incident beam and target normal, or the target incidence plane. (See Fig. 1.)

In Fig. 7 we have the plot of measured data for the out-of-plane situation with perpendicular-polarized source again. In this case, however, the incidence plane is perpendicular to the reflection plane. At $\theta_i = 0$, therefore, $\rho'_{\perp\perp}$ in plane is the same as $\rho'_{\perp\parallel}$ out of plane. For this reason, the reflectances of match-polarized and cross-polarized components seem to exchange behaviors in the out-of-plane configuration, as is verified by the plotted measurements as well as by the model calculations. Figure 8 presents plots of a Lambertian model without the shadowing and obscuration factor, a surface plus non-Lambertian volume model without the shadowing and obscuration factor, and the surface plus non-Lambertian volume model with the shadowing and obscuration factor. As before, it is apparent that the use of the non-Lambertian volume model plus the shadowing and obscuration factor improves agreement between model and measurements so that, apart from a possible overall scale factor, the agreement is within measurement fluctuation.

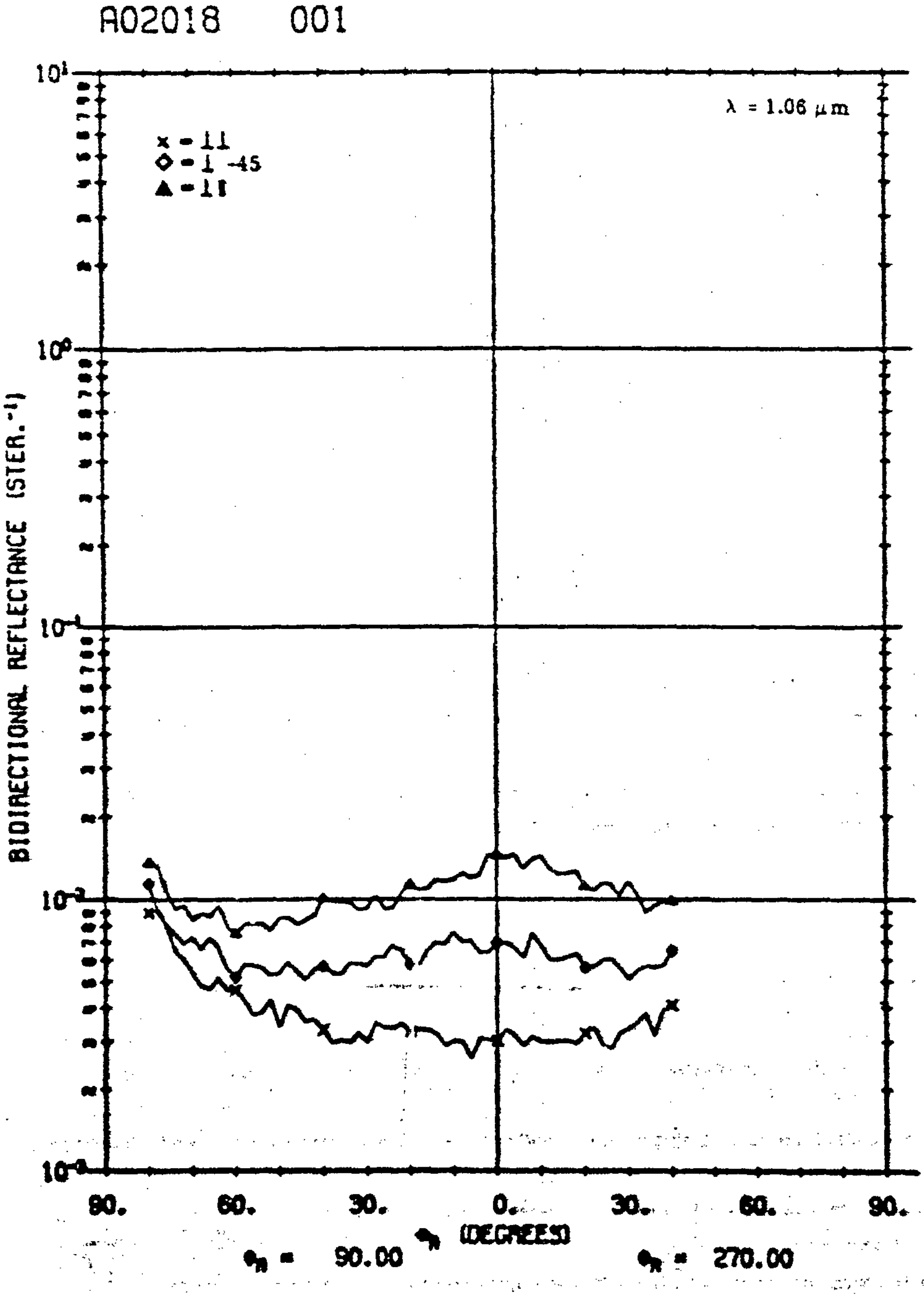

FIGURE 7. MEASURED ρ' FOR A02018-001. $\theta_i = 40^0$, $\phi_i = 180^0$, $\phi_r = 90^0, 270^0$.

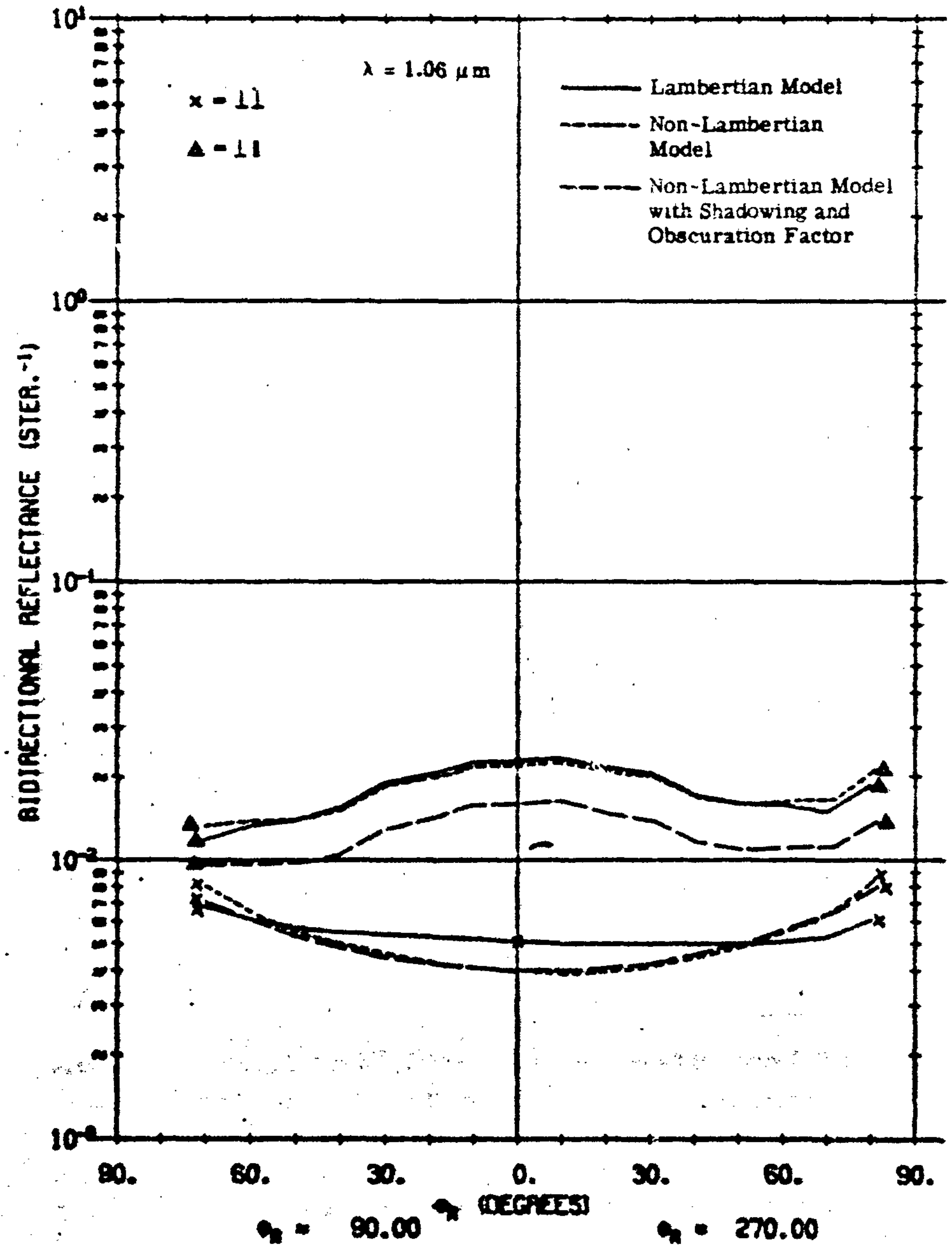

FIGURE 9. CALCULATED ρ' FOR A02018-001 USING LAMBERTIAN VOLUME MODEL AND NON-LAMBERTIAN VOLUME MODEL WITH AND WITHOUT SHADOWING AND OBSCURATION FACTOR. $\theta_i = 40^o$, $\phi_i = 180^o$; $\phi_r = 90^o, 270^o$.

For additional validation, plots are shown for the 30°, 210° azimuth planes (Figs. 9 and 10) and for the 60°, 240° azimuth planes (Figs. 11 and 12). The characteristics of calculated and measured curves, apart from a scale factor, are in excellent agreement. Figures 13 through 20 represent similar comparisons for the case when the source polarizer is set for -45° (in the 0°, 180° azimuth plane) and set parallel (in the 30°, 210°; 60°, 240°; and 90°, 270° planes). Measured plots are presented with the calculated plot to represent the surface plus non-Lambertian volume model and to include the shadowing and obscuration factor.

6.2. REFLECTANCE FOR SAMPLE MATERIAL A02018-002

Material A02018-002 consists of a tan painted surface.

Based on the zero bistatic scan, Fig. 21, material A02018-002 appears to be somewhat brighter than material A02018-001. Whereas the non-Lambertian volume model was clearly the best choice for material A02018-001, it is not in the case of A02018-002. In this latter case, the best choice is the Lambertian model.

The lack of angular dependence in the reflectance of the cross-polarized component could have a number of explanations. Multiple scattering increases for rougher surfaces. Since such scattering may not be angular dependent, it could become a large enough factor to swamp the angular dependence which is otherwise present. Moreover, the difference in color between the green and tan certainly alters the absorption and, consequently, can alter the angular dependence as well.

In any case, the appropriate model to use can be determined by looking at the cross-polarized component of the fixed bistatic scan. If a clear angular dependence is present, the non-Lambertian model should be used. But if there is little or no apparent angular dependence, as with material A02018-002, then the Lambertian model is more appropriate.

In Figs. 22 through 29, plots are provided for different azimuth planes, beginning with the plot for measured data, followed immediately by the corresponding plot from model calculations. In this group of illustrations, Figs. 22 through 25 represent perpendicular source polarization, while Figs. 26 through 29 represent a source parallel polarization for the 0°, 180° azimuth plane and for the 90°, 270° azimuth plane.

In all cases the fit appears to be excellent, except for occasional anomalies at large azimuth angles. Further modification of the shadowing and obscuration factor should decrease these present anomalies.

6.3. POLARIZATION ANGLE (ψ_r) FOR SAMPLE MATERIAL A02018-001

The reflectances of the perpendicular and parallel components of a linearly polarized beam vary as functions of the source-receiver angles and the index of refraction of the target material. (See, for example, the Fresnel equations, Ref. 3.) Based on observations, the index of refraction varies little over a wide range of paint surfaces. For the particular materials

A02018 001

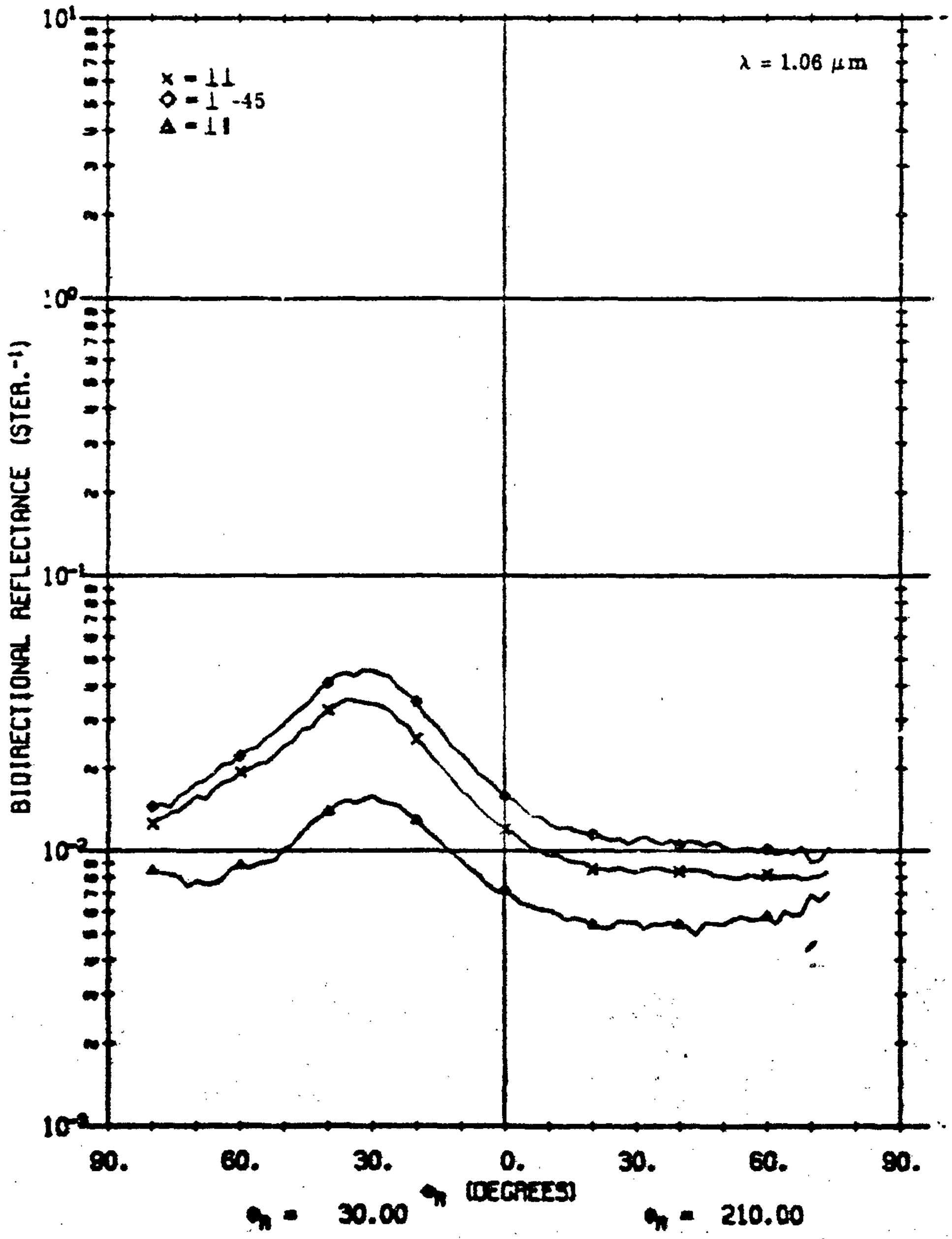

FIGURE 9. MEASURED ρ' FOR A02018-001. $\theta_i = 40^\circ$, $\phi_i = 180^\circ$, $\phi_r = 30^\circ, 210^\circ$.

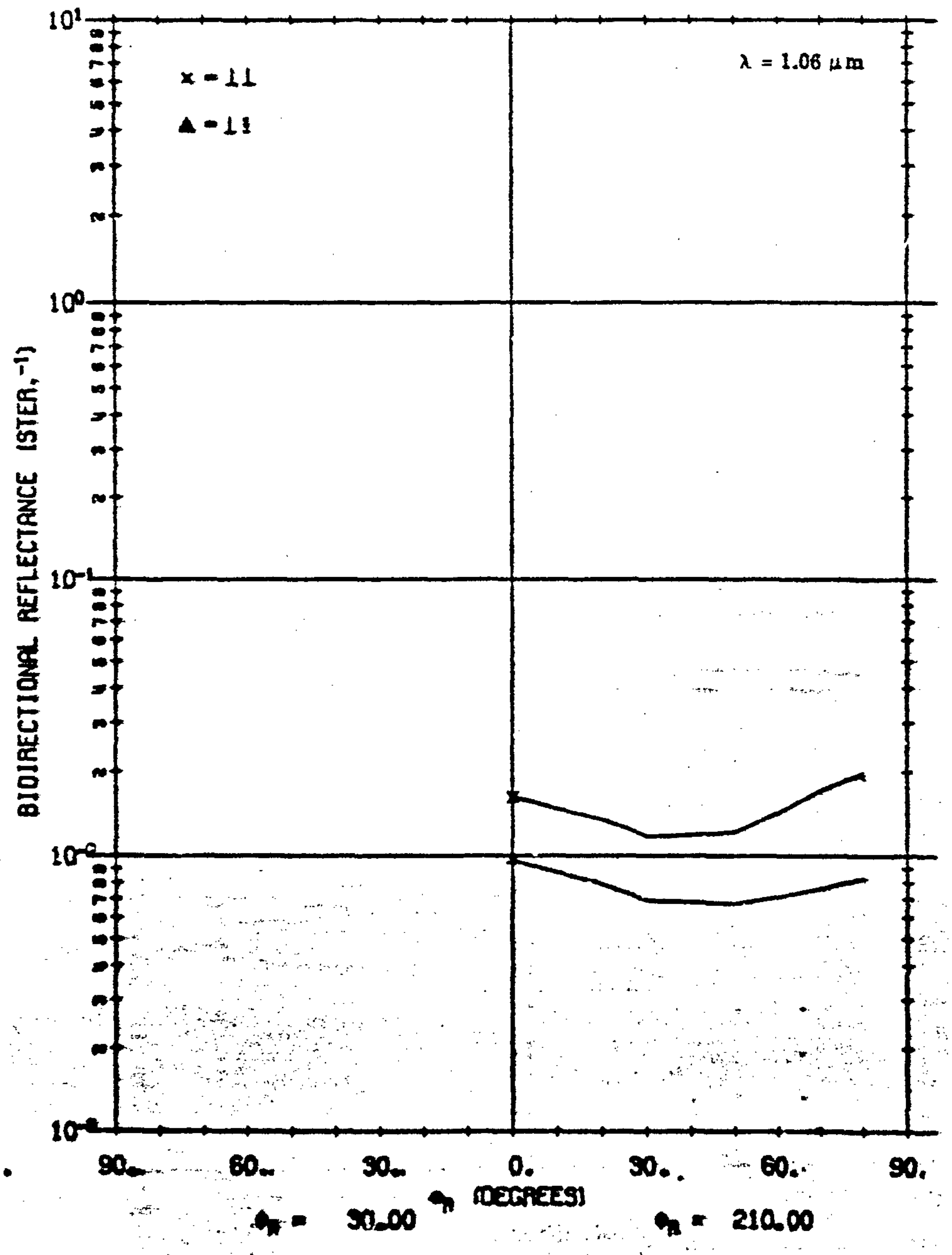

FIGURE 10. CALCULATED ρ' FOR A02018-001 USING NON-LAMBERTIAN VOLUME MODEL WITH SHADOWING AND OBSCURATION FACTOR. $\theta_i = 40^0$, $\phi_i = 180^0$, $\phi_r = 30^0$, 210^0.

A02018 001

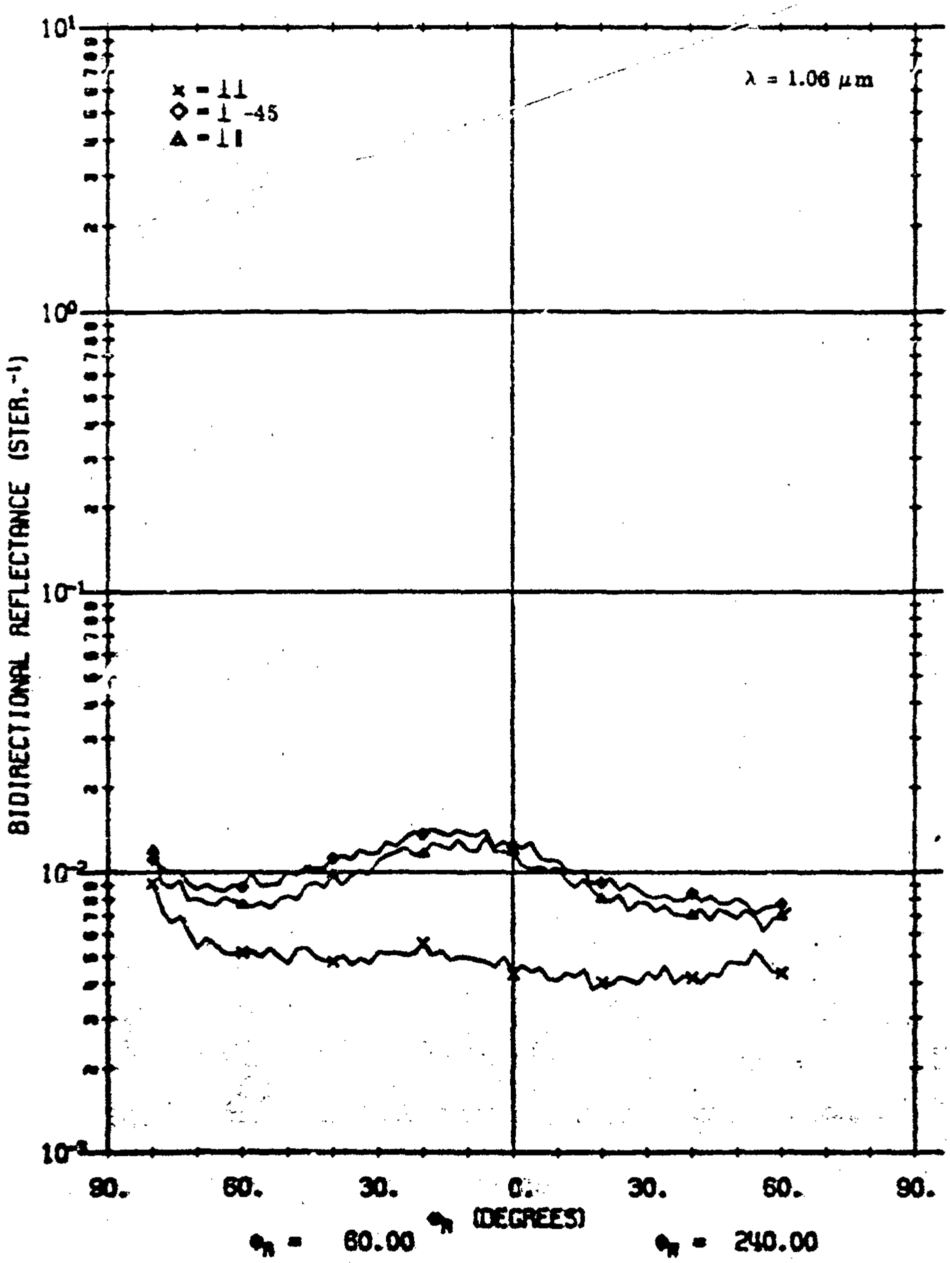

FIGURE 11. MEASURED ρ' FOR A02018-001. $\theta_i = 40^0$, $\phi_i = 180^0$, $\phi_r = 60^0$, 240^0.

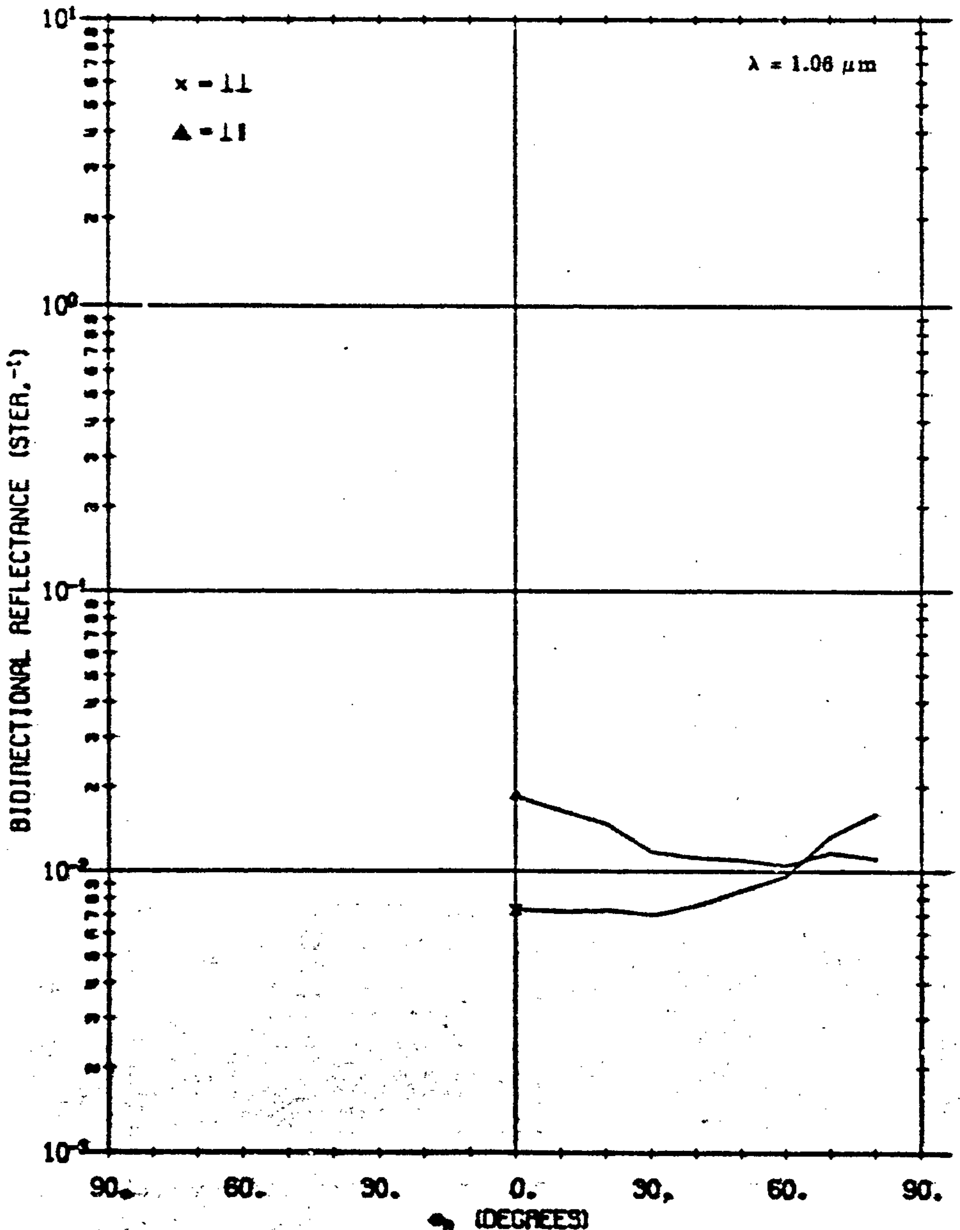

FIGURE 12. CALCULATED ρ' FOR A02018-001 USING NON-LAMBERTIAN VOLUME MODEL WITH SHADOWING AND OBSCURATION FACTOR. $\theta_i = 40^\circ$, $\phi_i = 180^\circ$, $\phi_r = 60^\circ, 240^\circ$.

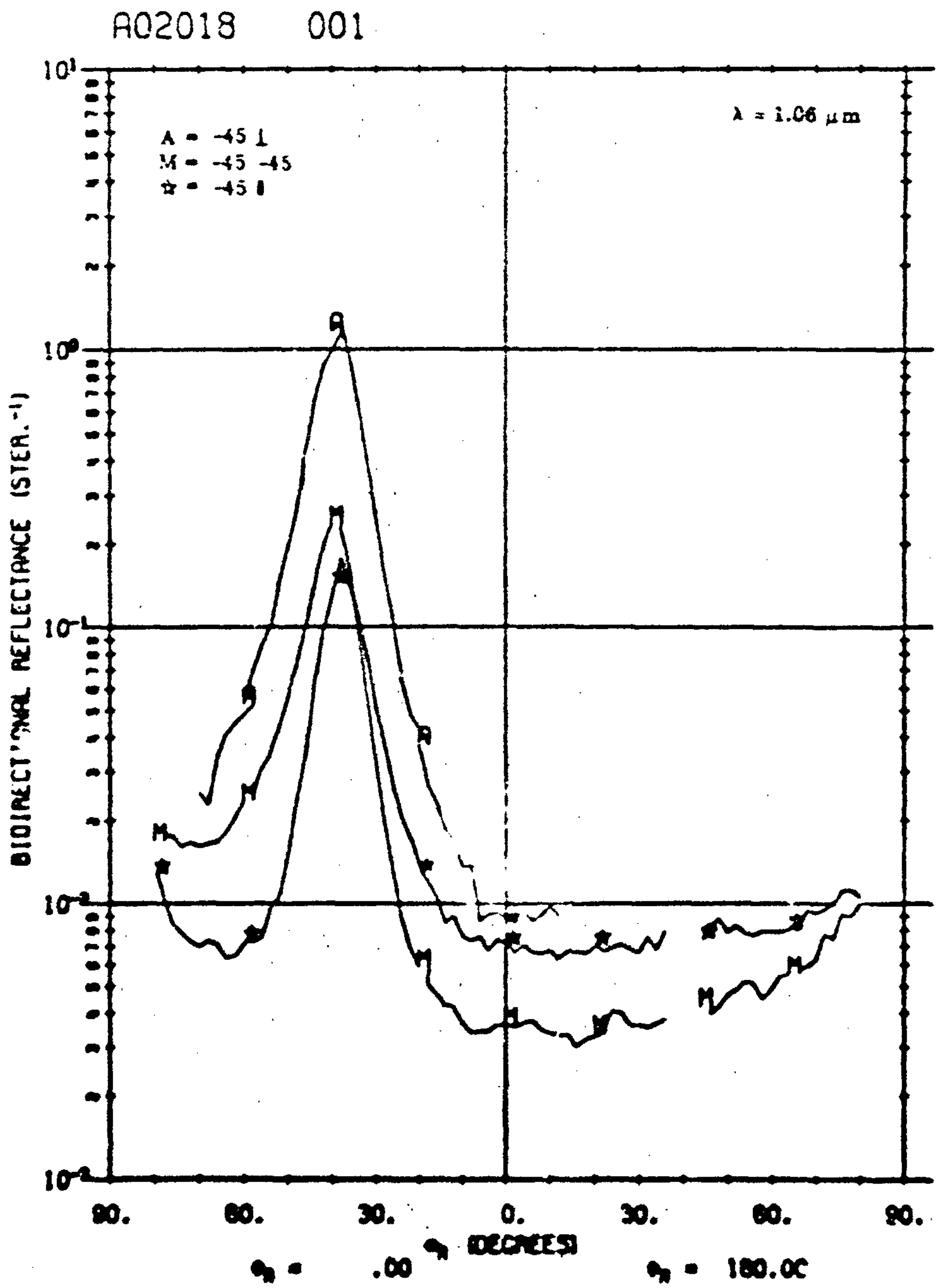

FIGURE 13. MEASURED ρ' FOR A02018-001. $\theta_i = 40°$, $\phi_i = 180°$, $\phi_r = 0°$, $180°$.

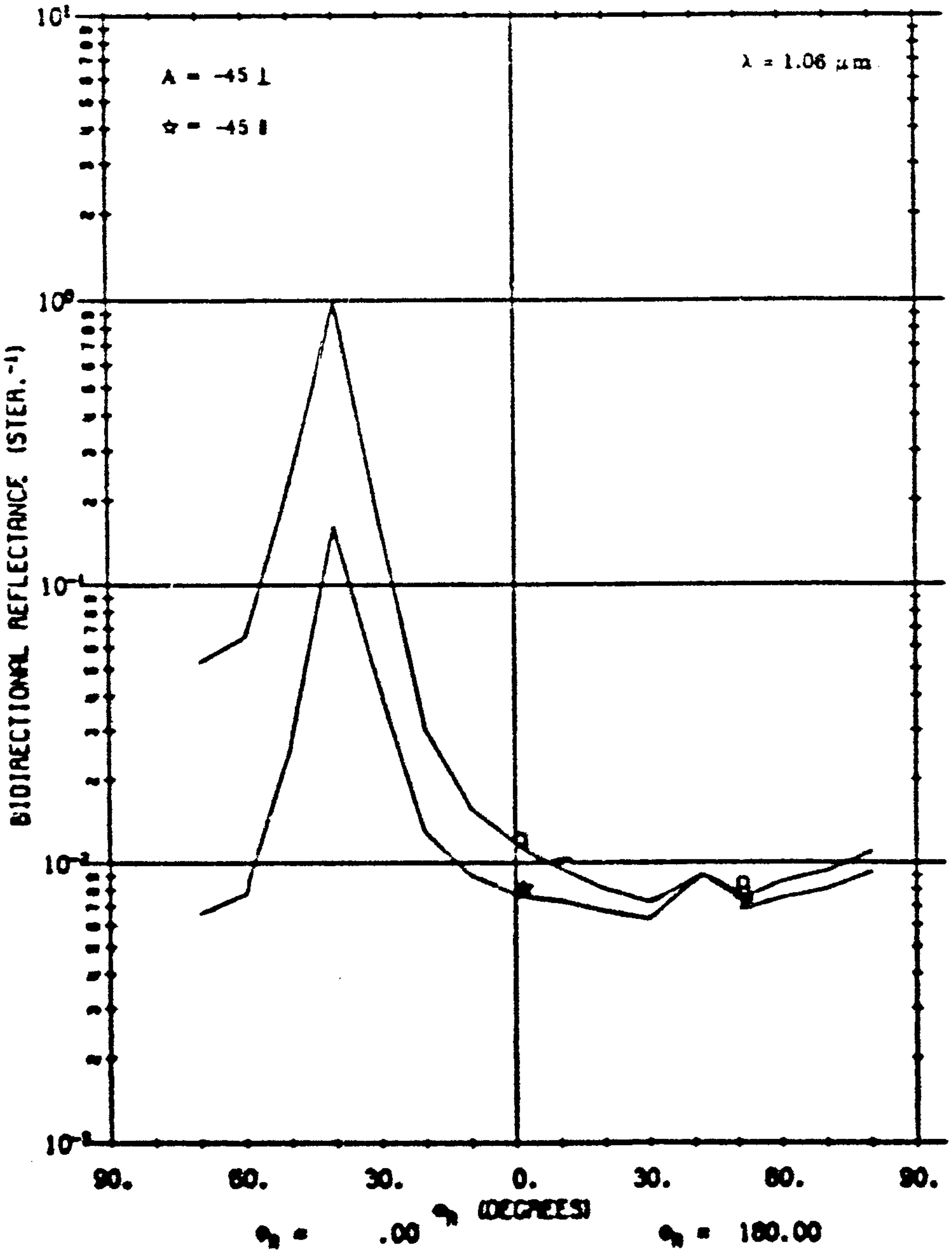

FIGURE 14. CALCULATED ρ' FOR A02018-001 USING NON-LAMBERTIAN VOLUME MODEL WITH SHADOWING AND OBSCURATION FACTOR. $\theta_i = 40^\circ$, $\phi_i = 180^\circ$, $\phi_r = 0^\circ, 180^\circ$.

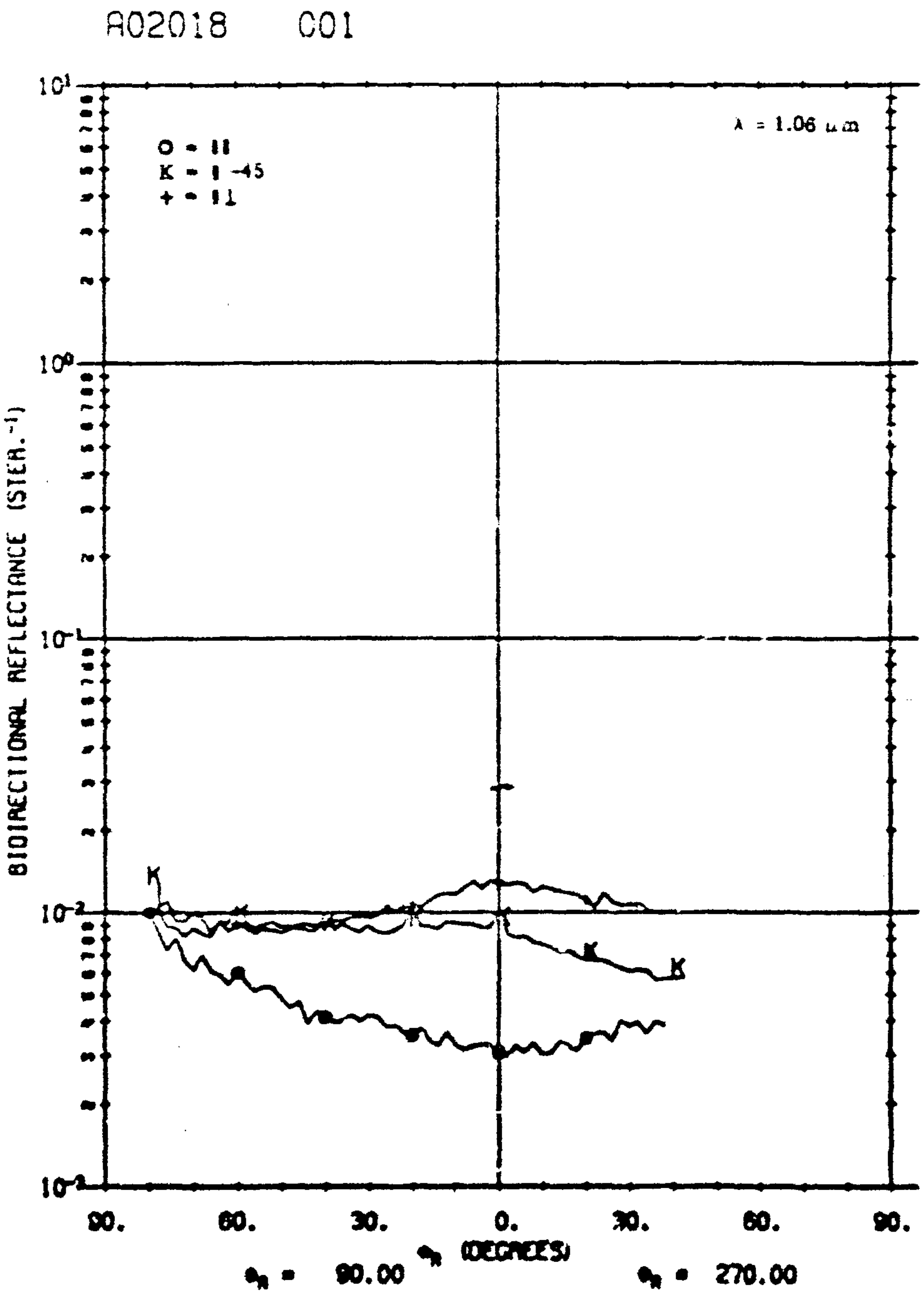

FIGURE 15. MEASURED ρ' FOR A02018-001. $\theta_i = 40^{\circ}$, $\phi_i = 180^{\circ}$, $\phi_r = 90^{\circ}, 270^{\circ}$.

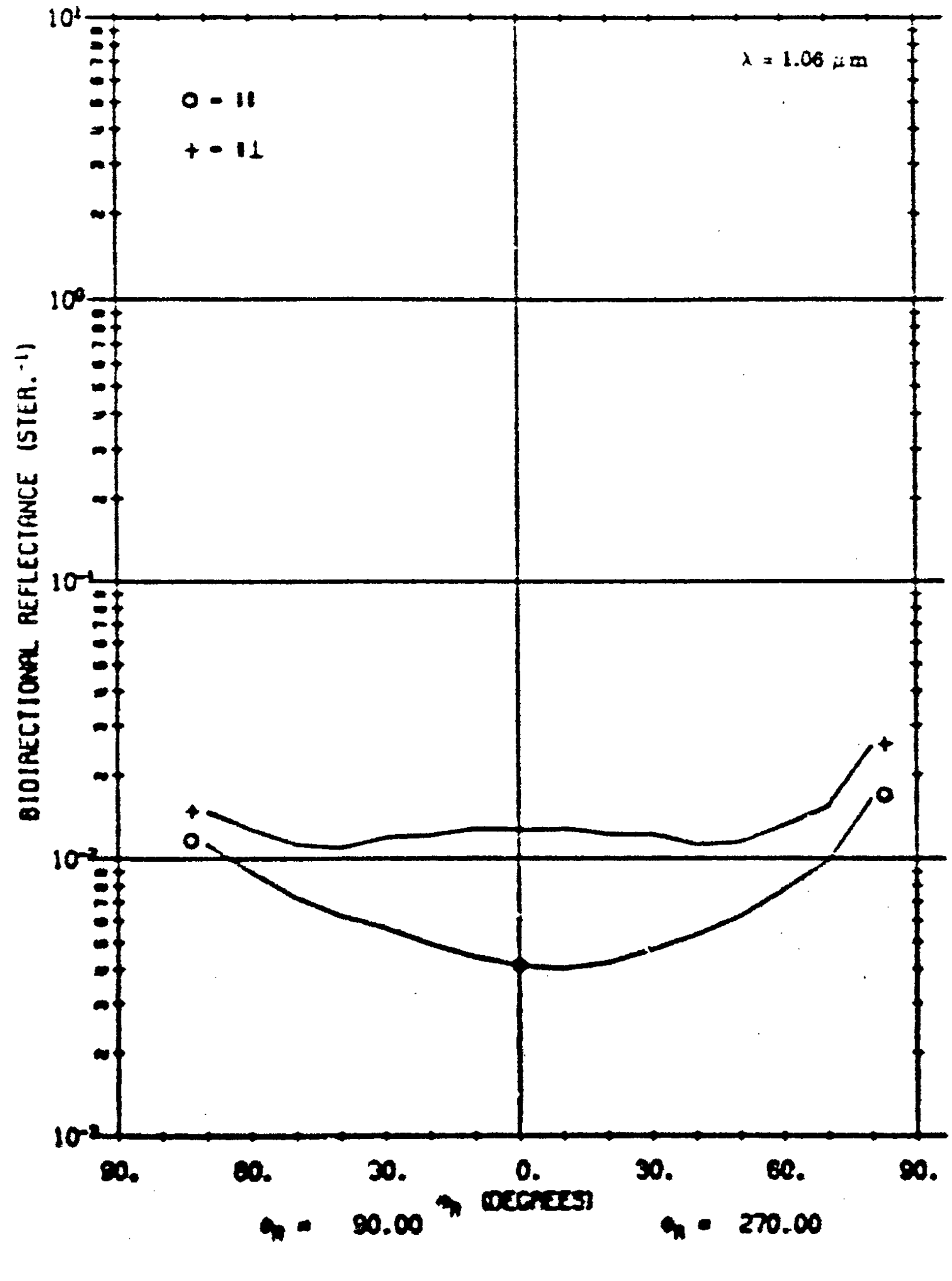

FIGURE 18. CALCULATED ρ' FOR A02018-001 USING NON-LAMBERTIAN VOLUME MODEL WITH SHADOWING AND OBSCURATION FACTOR. $\theta_i = 40^{\circ}$, $\phi_i = 180^{\circ}$, $\phi_r = 90^{\circ}, 270^{\circ}$.

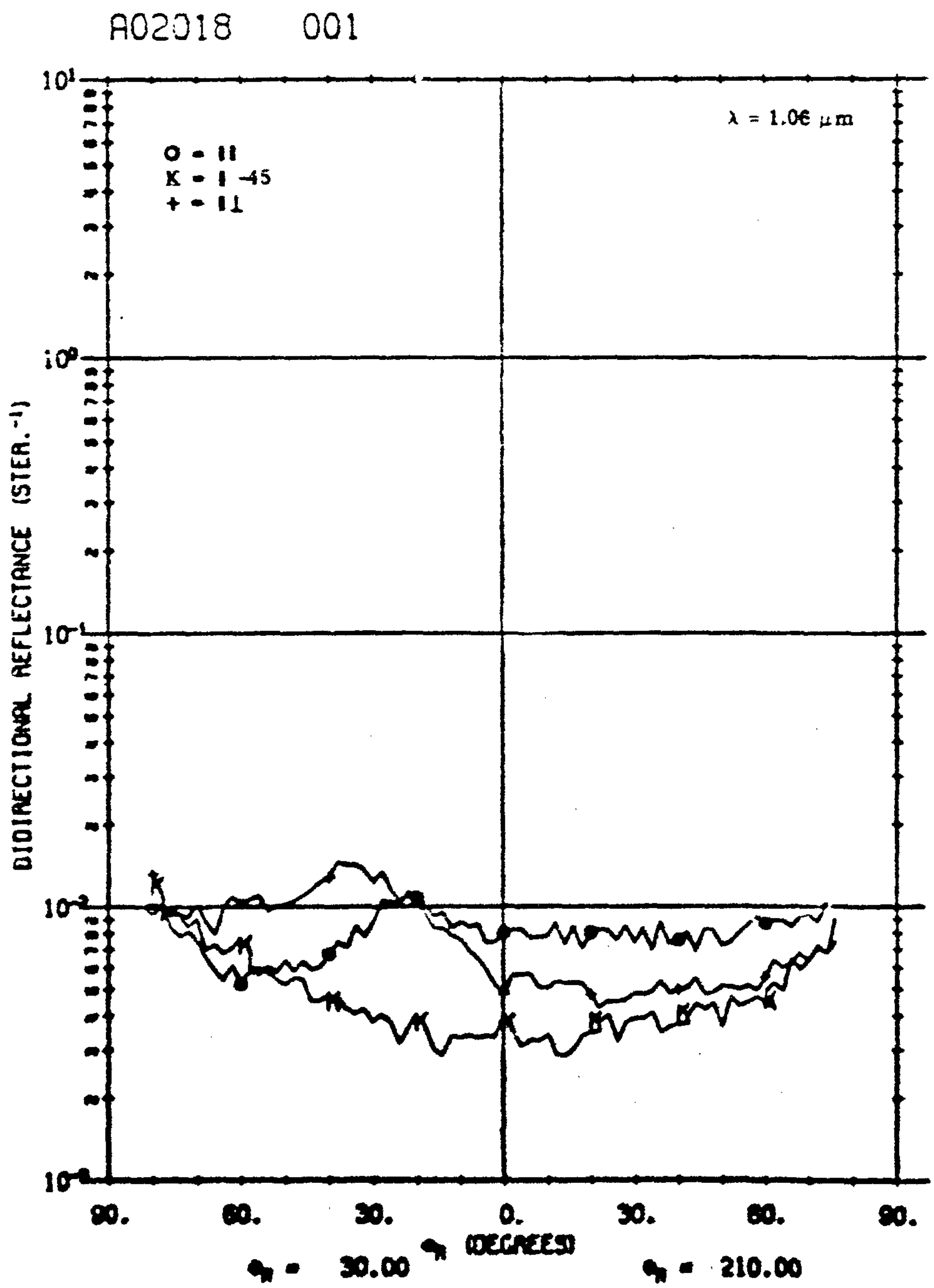

FIGURE 17. MEASURED ρ' FOR A02018-001. $\theta_i = 40^{\circ}$, $\phi_i = 180^{\circ}$, $\phi_r = 30, 210^{\circ}$.

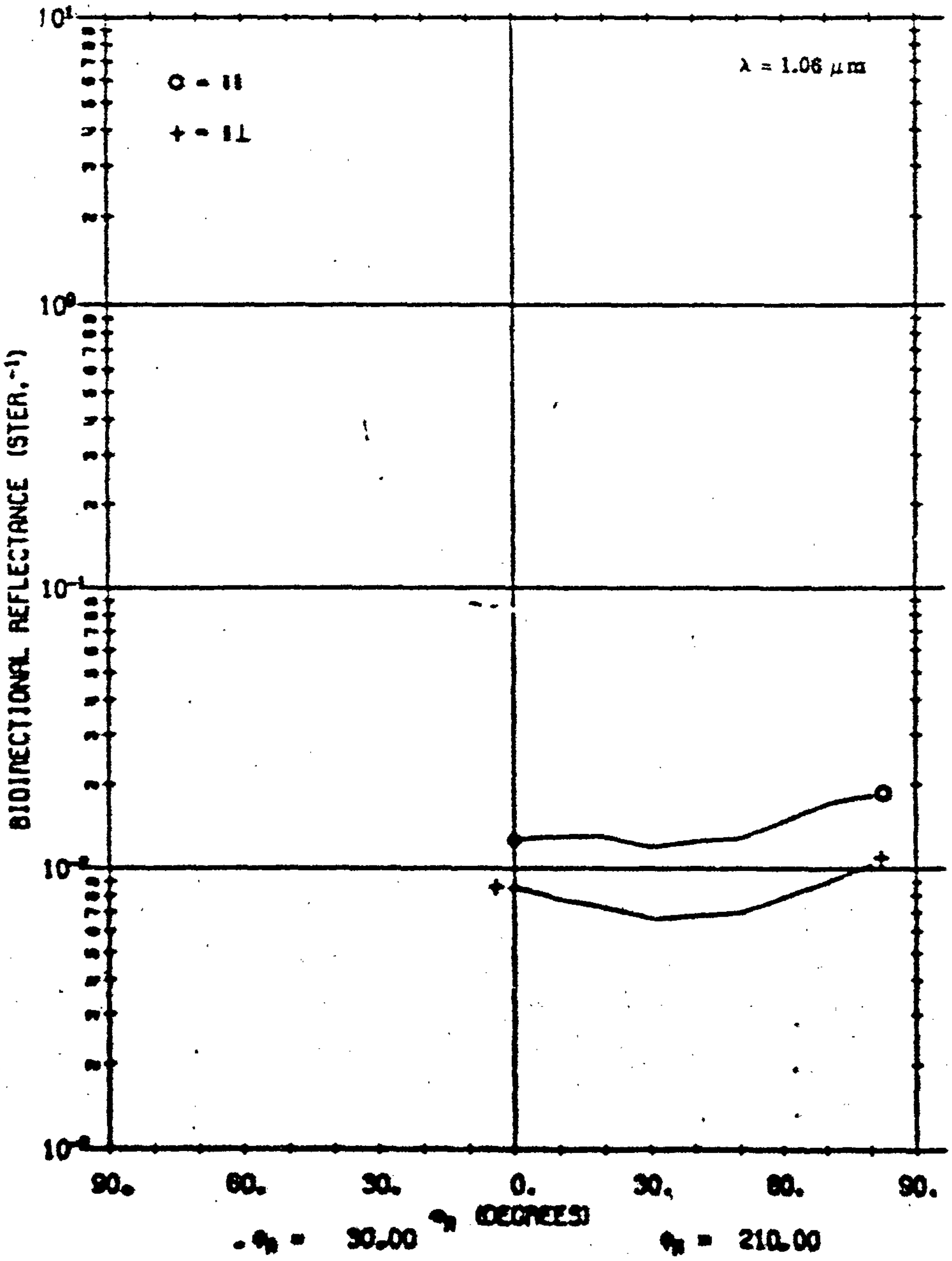

FIGURE 18. CALCULATED ρ' FOR A02018-001 USING NON-LAMBERTIAN VOLUME MODEL WITH SHADOWING AND OBSCURATION FACTOR. $\theta_i = 40^{\circ}$, $\phi_i = 120^{\circ}$, $\phi_r = 30^{\circ}, 210^{\circ}$.

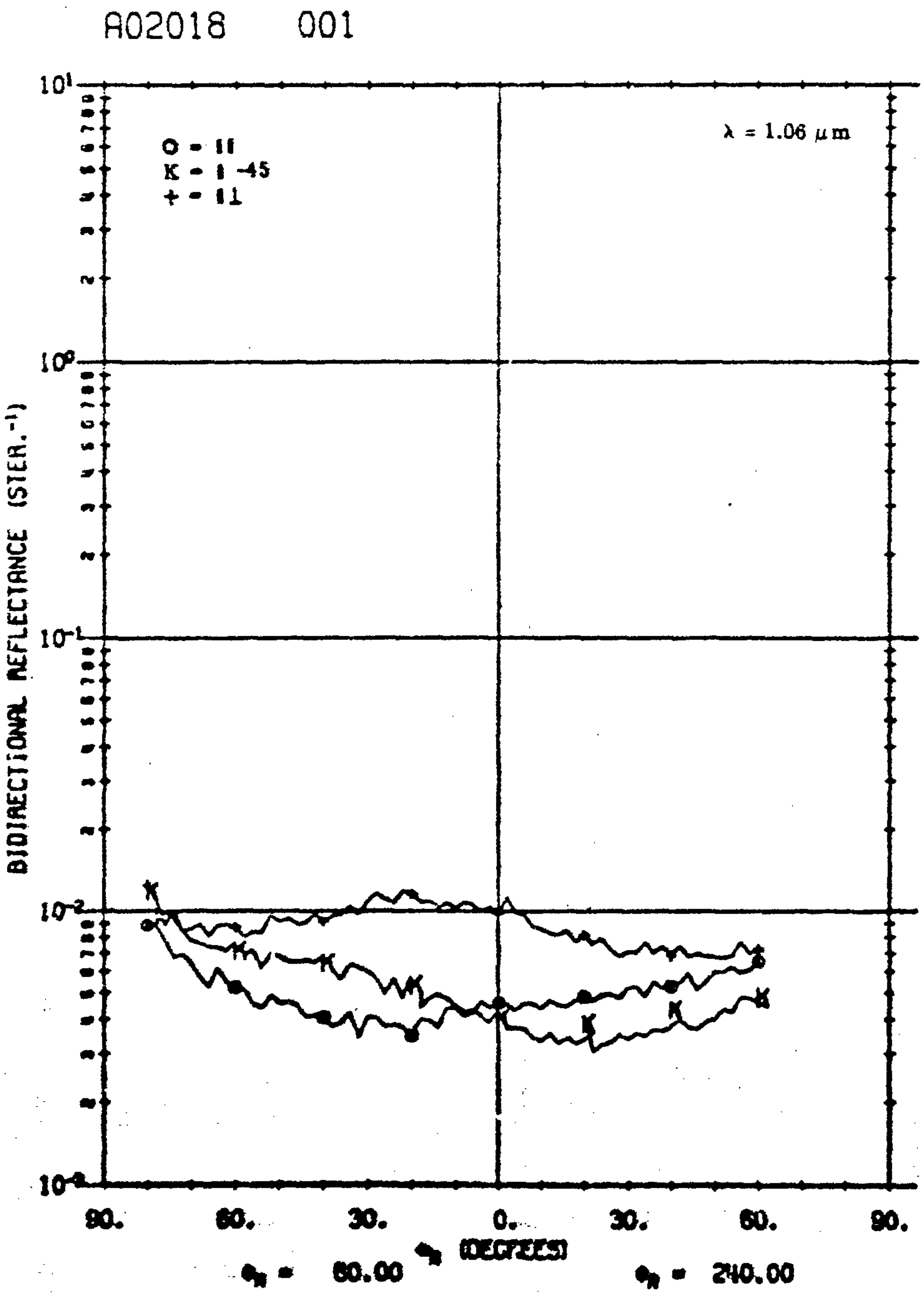

FIGURE 19. MEASURED ρ' FOR A02018-001. $\theta_i = 40°$, $\phi_i = 180°$, $\phi_r = 60°, 240°$.

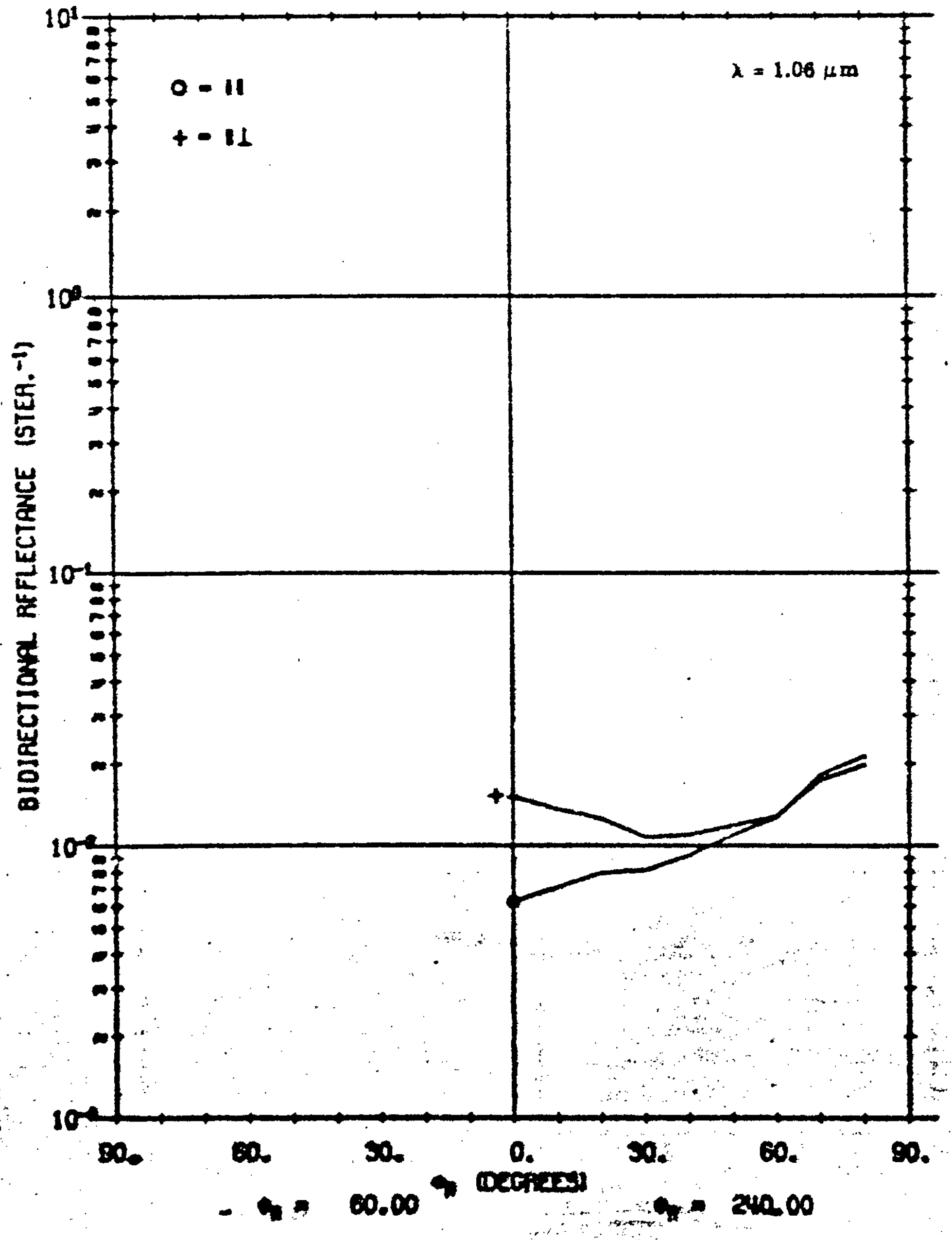

FIGURE 20. CALCULATED ρ' FOR A02018-001 USING NON-LAMBERTIAN VOLUME MODEL WITH SHADOWING AND OBSCURATION FACTOR. $\theta_i = 40^\circ$, $\phi_i = 180^\circ$, $\phi_r = 60^\circ, 240^\circ$.

A02018 002

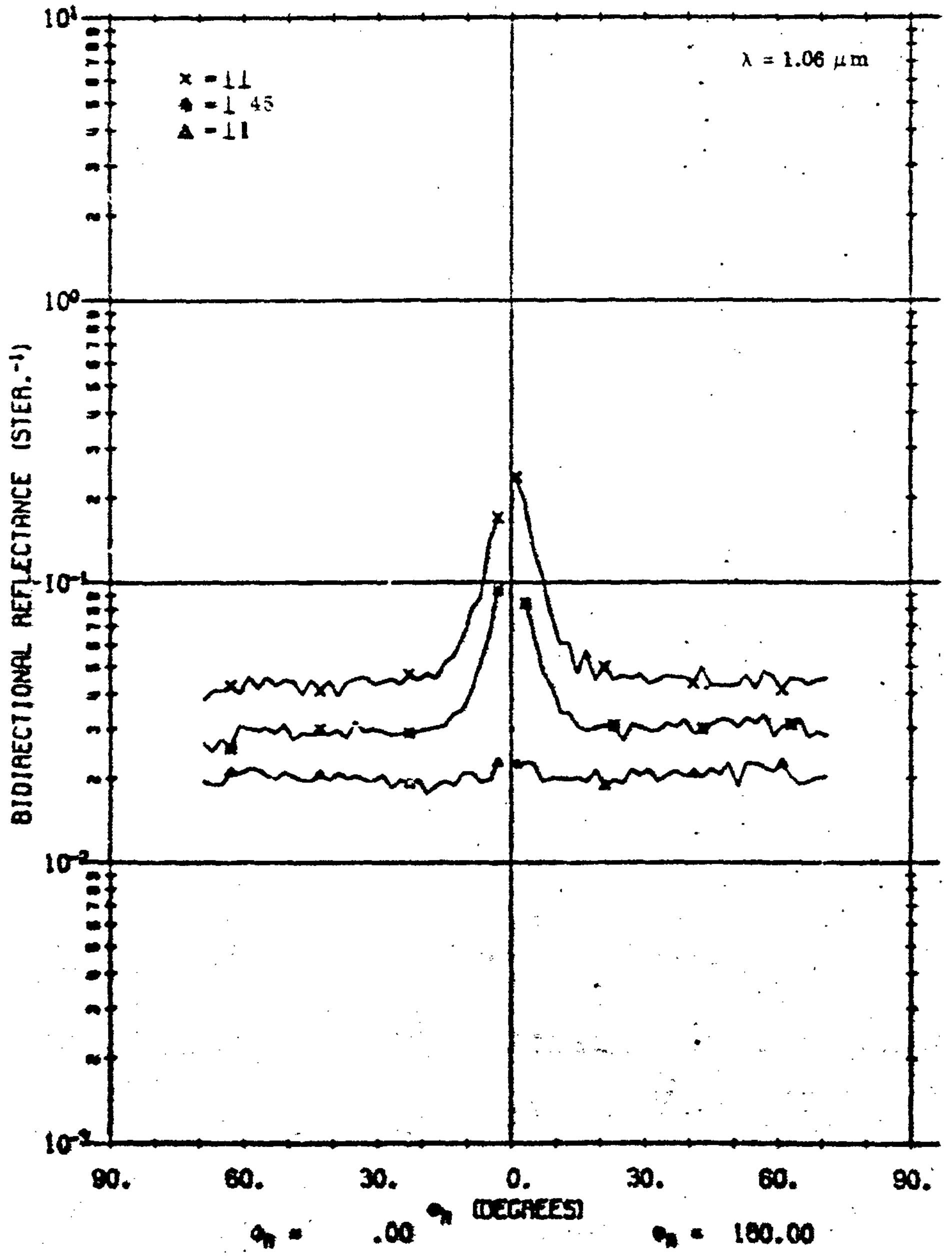

FIGURE 21. FIXED-BISTATIC ρ' FOR A02018-002

A02018 0C2

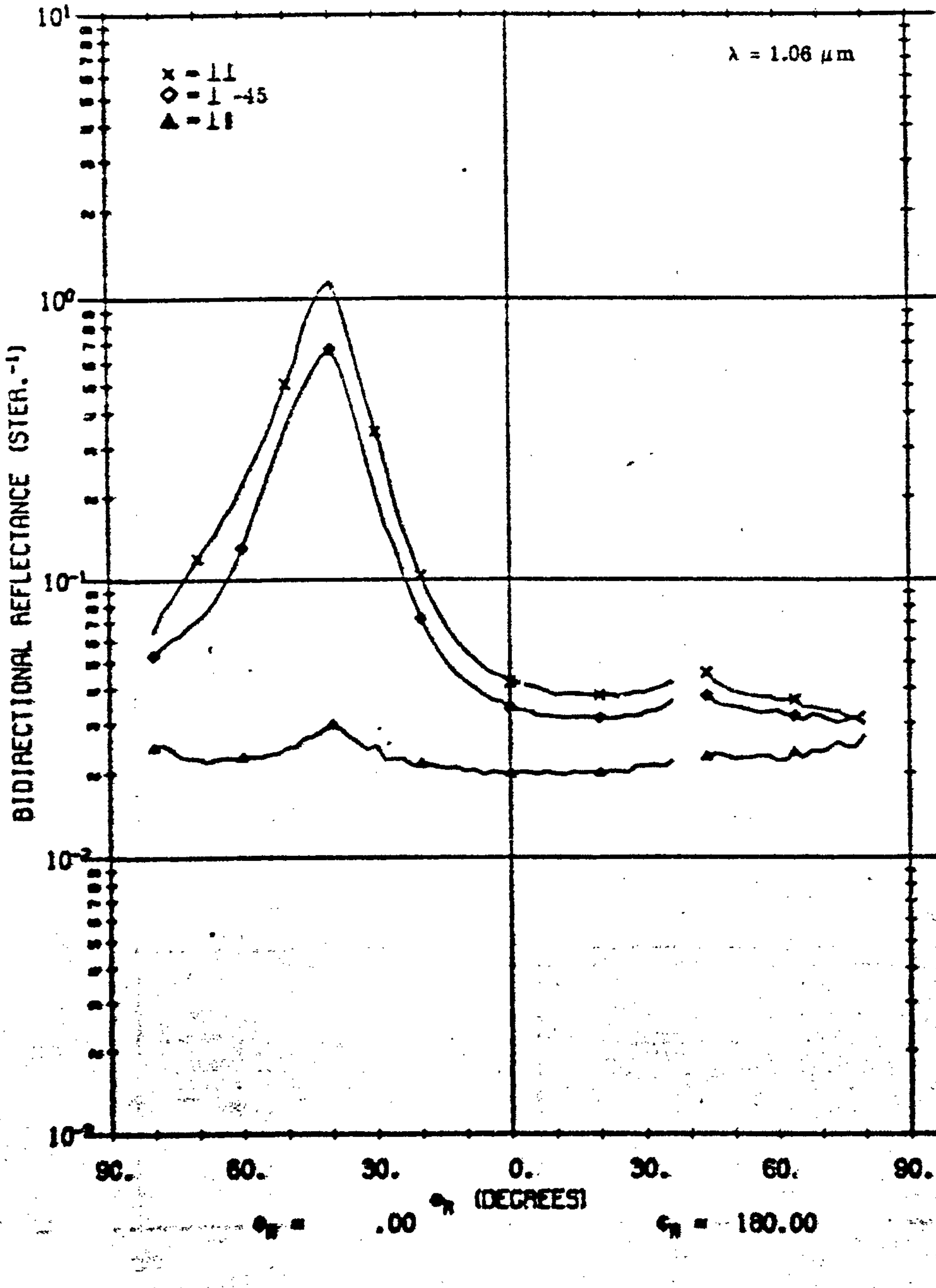

FIGURE 22. MEASURED ρ' FOR A02018-002. $\theta_i = 40^0$, $\phi_i = 180^0$, $\phi_r = 0^0, 180^0$.

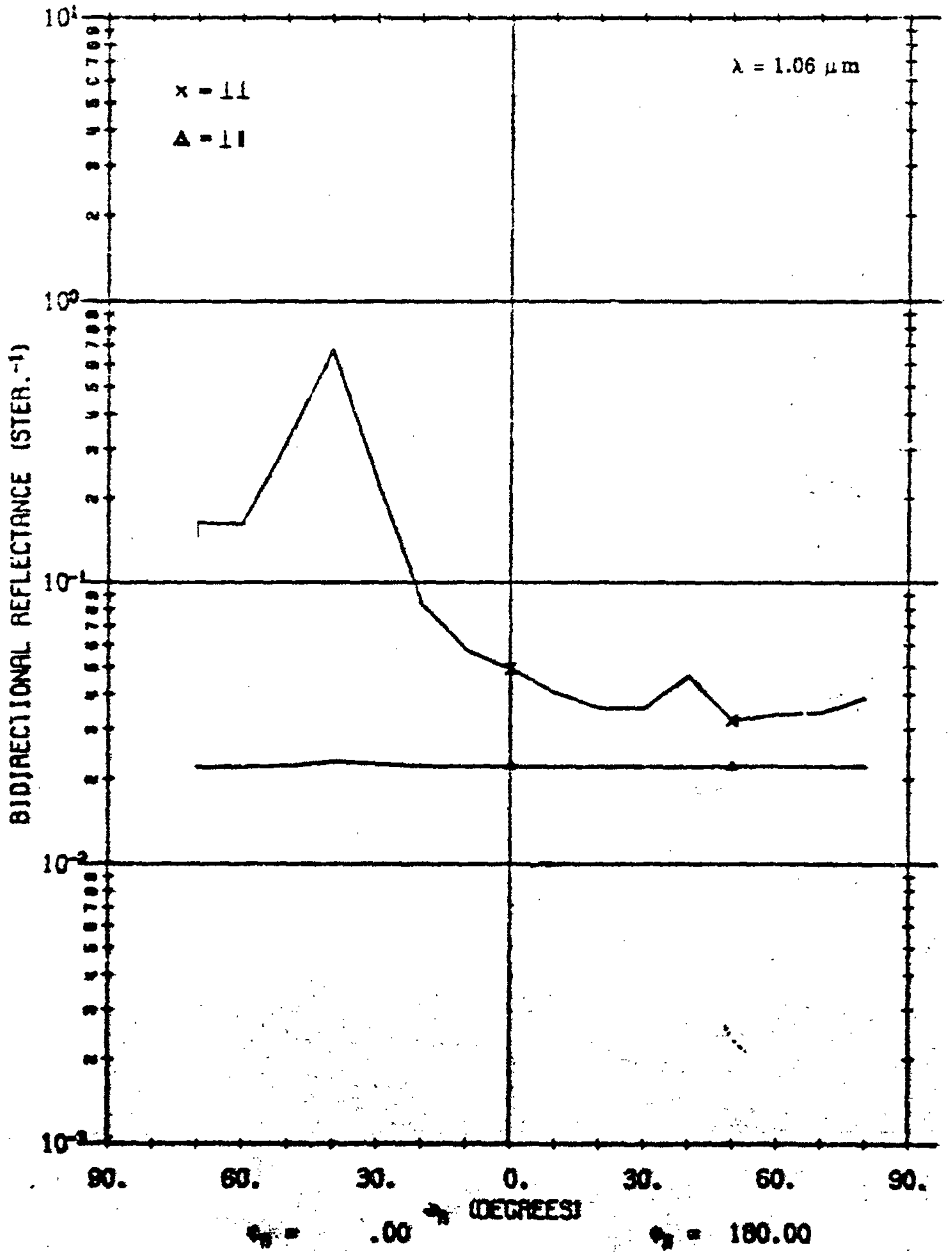

FIGURE 23. CALCULATED ρ' FOR A02018-002 USING LAMBERTIAN VOLUME MODEL.
$\theta_i = 40^\circ$, $\phi_i = 180^\circ$, $\phi_r = 0^\circ, 180^\circ$.

A02018   002

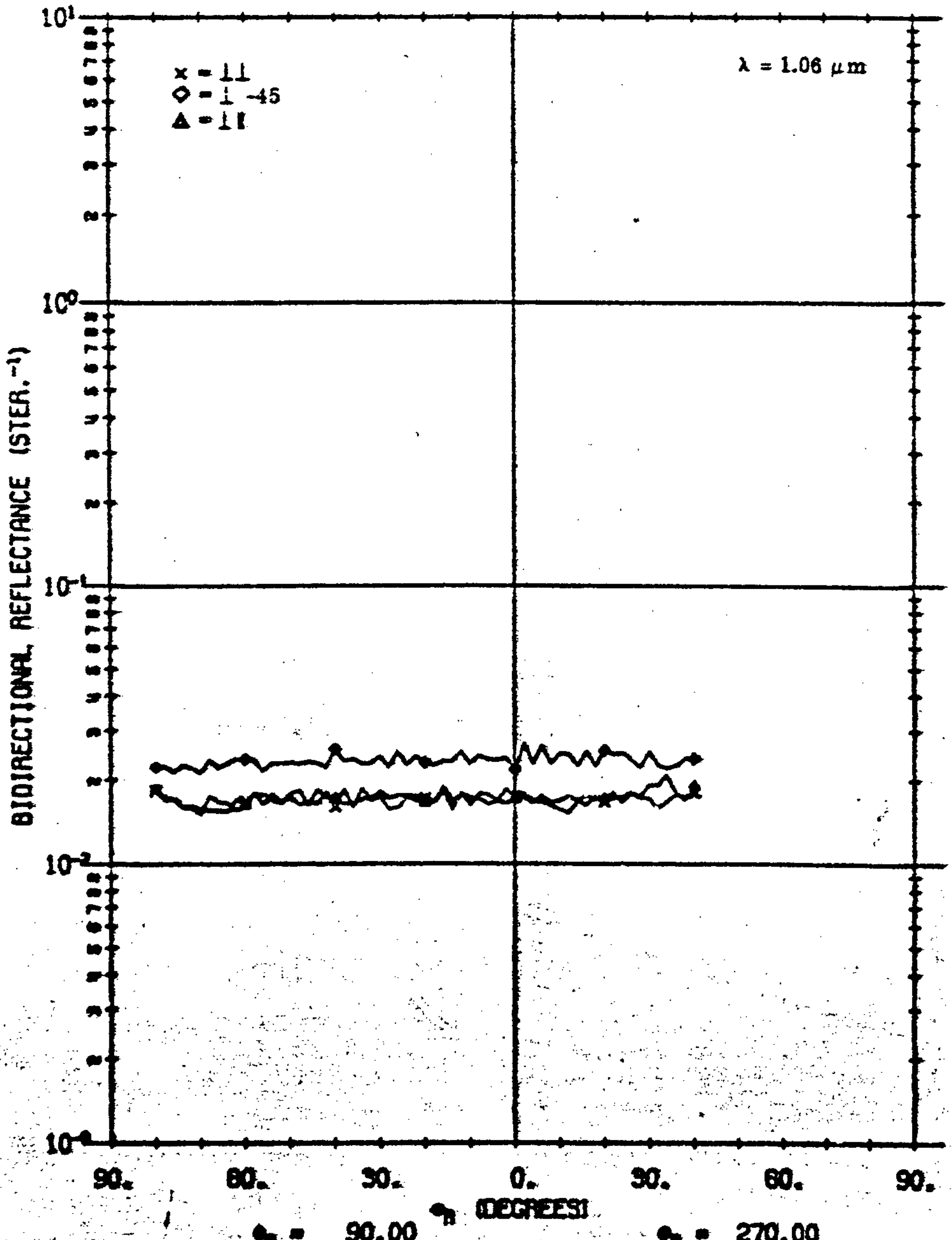

FIGURE 24. MEASURED ρ' FOR A02018-002. $\theta_i = 40^o$, $\phi_i = 180^o$, $\phi_r = 90^o, 270^o$.

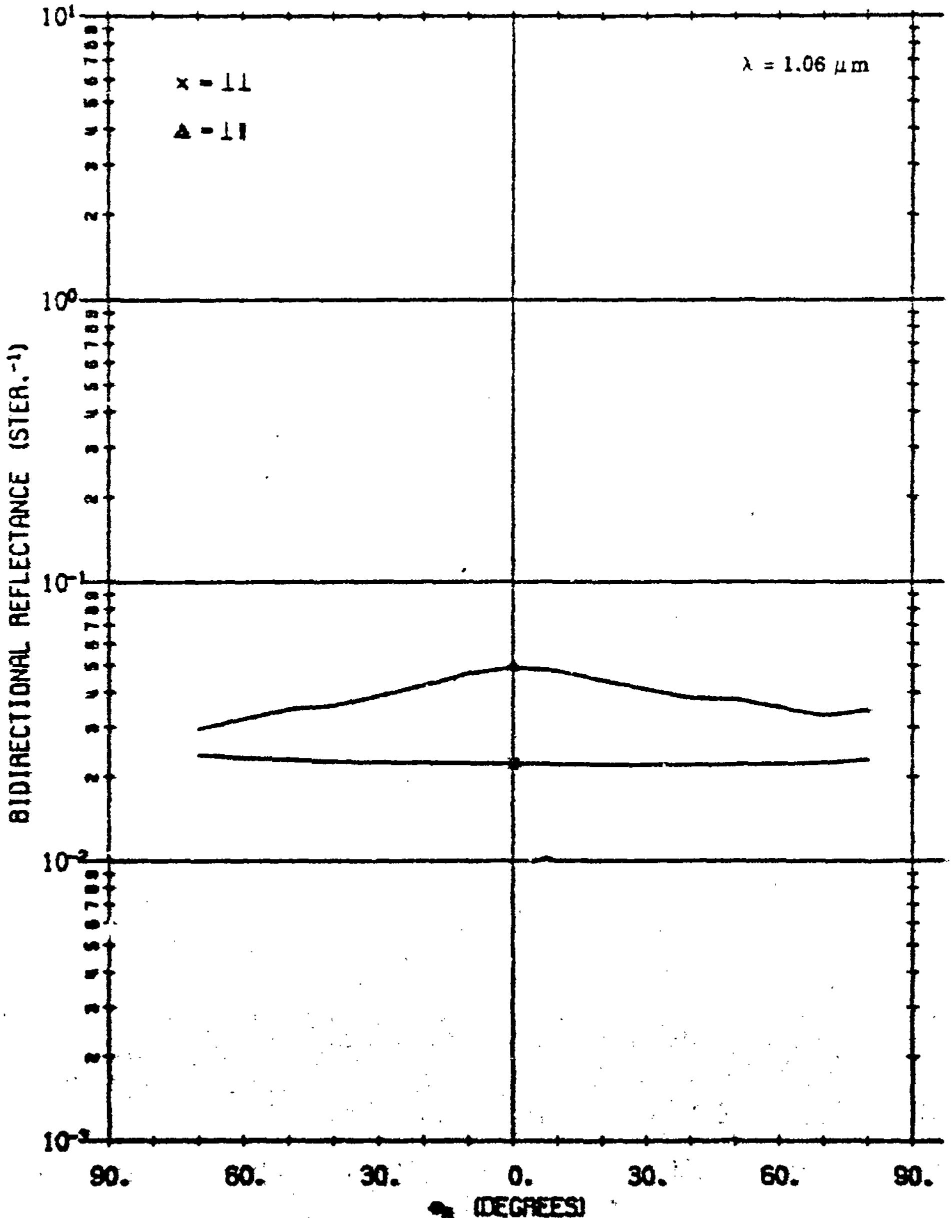

FIGURE 25. CALCULATED ρ' FOR A02018-002 USING LAMBERTIAN VOLUME MODEL. $\theta_i = 40^0$, $\phi_i = 180^0$, $\phi_r = 90^0, 270^0$.

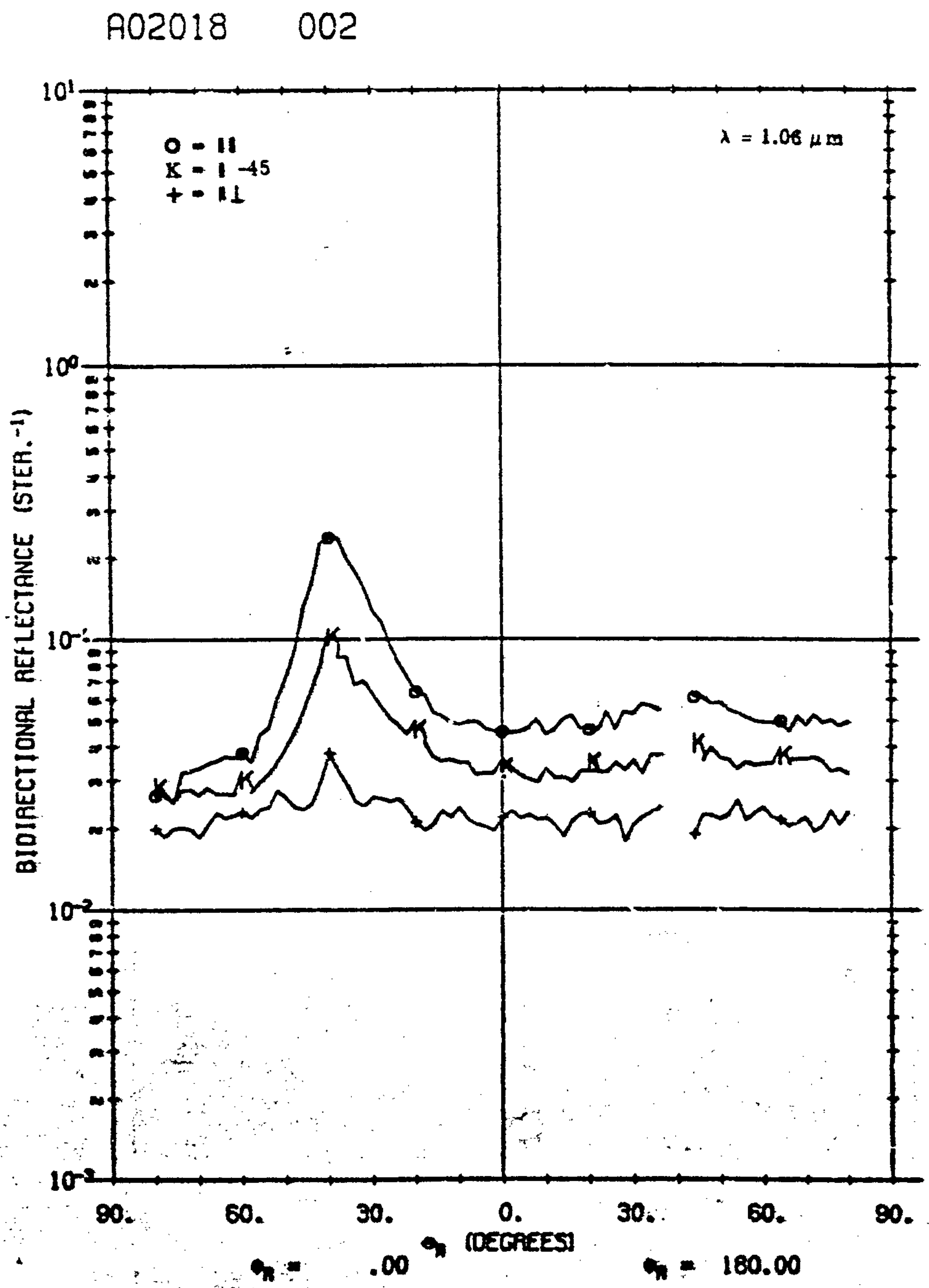

FIGURE 26. MEASURED ρ' FOR A02018-002. $\theta_i = 40^{\circ}$, $\phi_i = 180^{\circ}$, $\phi_r = 0^{\circ}, 180^{\circ}$.

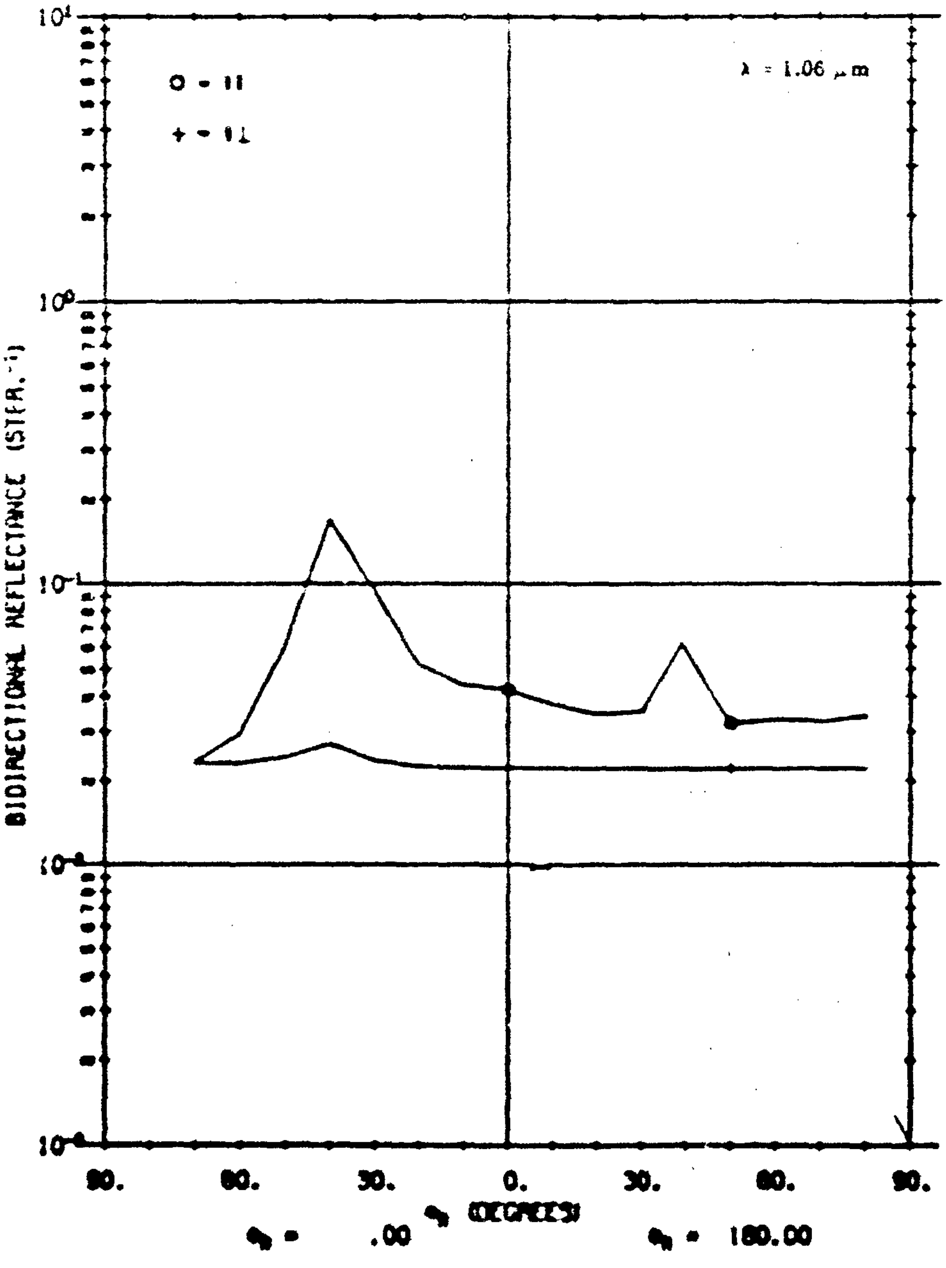

FIGURE 27. CALCULATED ρ' FOR A02018-002. θ_i = 60°, ϕ_i = 180°, ϕ_r = 0°, 180°.

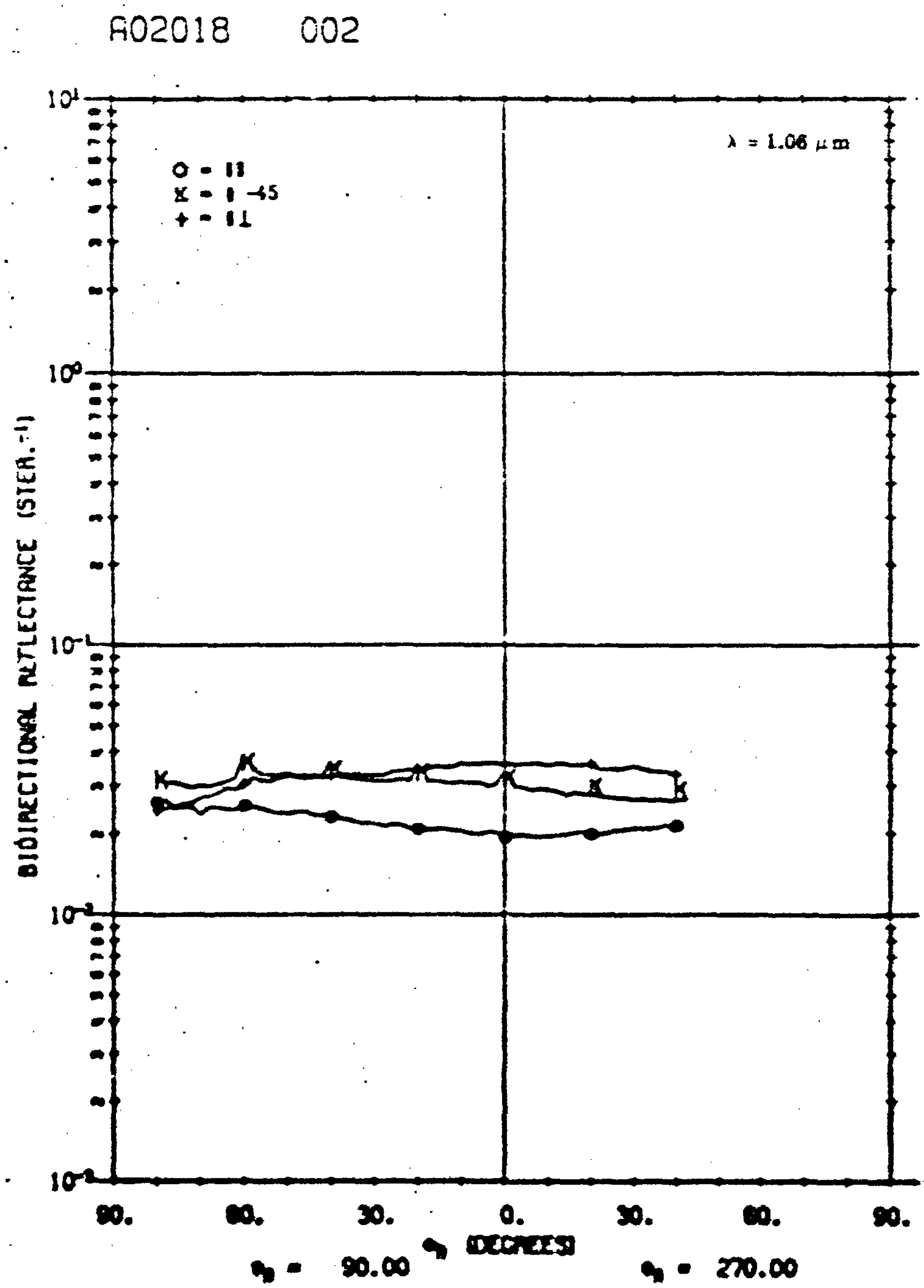

FIGURE 28. MEASURED ρ' FOR A02018-002. $\theta_i = 60°$, $\phi_i = 180°$, $\phi_r = 90°, 270°$.

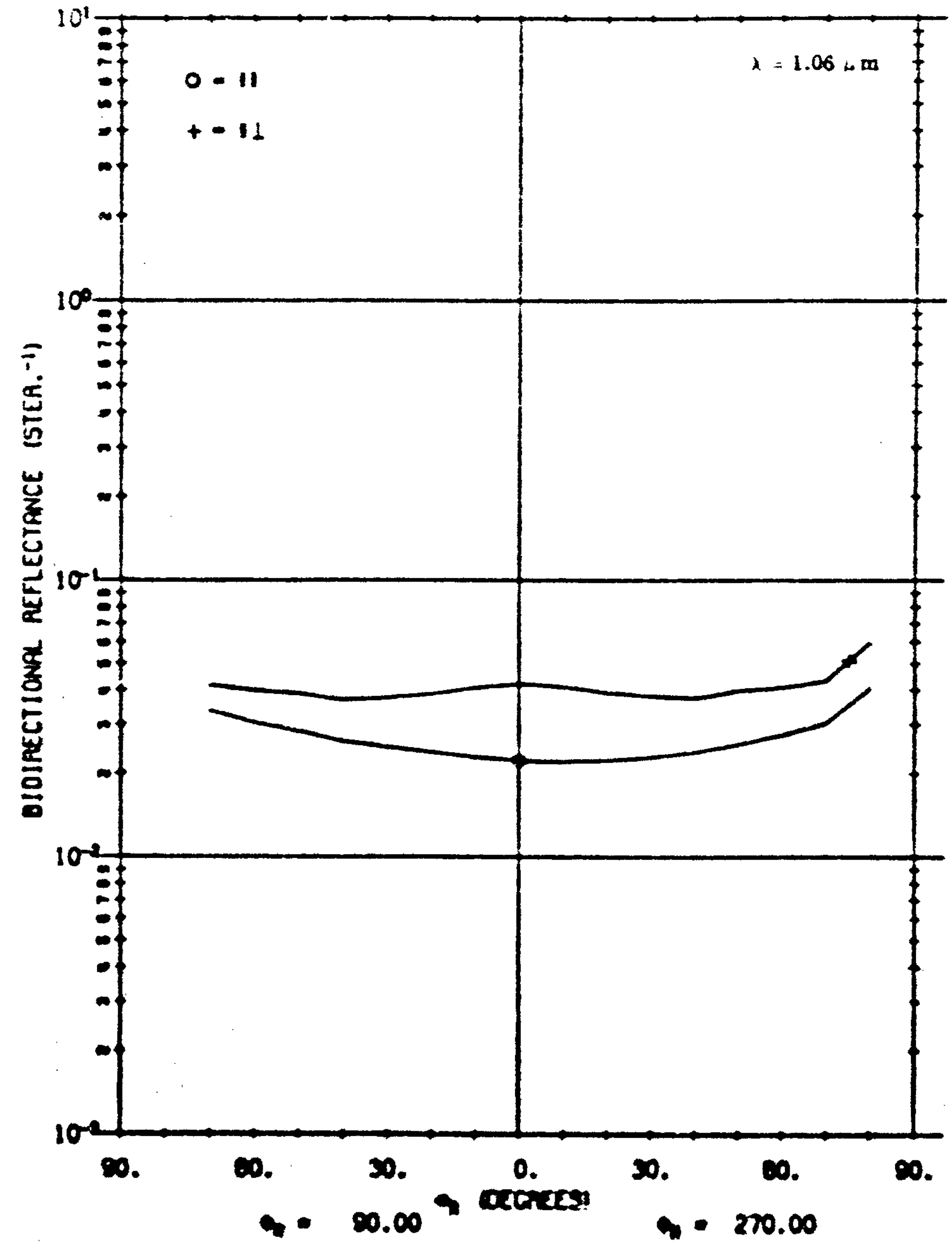

FIGURE 29. CALCULATED ρ' FOR A02018-002 USING LAMBERTIAN VOLUME MODEL.
$\theta_i = 40^\circ$, $\phi_i = 180^\circ$, $\phi_r = 90^\circ, 270^\circ$.

covered in this report, the variation is considered to be zero. Therefore, for these surfaces, polarization angle is essentially a function only of source-receiver positions.

As additional validation for the model, predicted polarization angles are compared with polarization angles extracted from the measured data. Figures 30 through 33 show plots obtained for the 0°, 180°; 90°, 270°; 30°, 210°; and 60°, 240° azimuth planes. Measured data represent material A02018-001. In all cases, agreement between measurements and calculations is excellent, with the average disparity not more than 10%. In particular, the dramatic agreement between measurements and model in the 30°, 210° and 60°, 240° azimuth planes constitutes powerful verification of the model and affirms its usefulness in arbitrary source-receiver positions.

6.4. PERCENT POLARIZATION FOR SAMPLE MATERIALS A02018-001 AND A02018-002

Percent polarization (P) validates the ratio of surface-to-volume contributions to reflectance. Percent polarization depends on both polarized reflectance and angle of polarization, both validated in earlier sections of this report. In this section, we compare model predictions with percent polarization values extracted from measured data.

Figures 34 and 35 illustrate degree of polarization for scans of material A02018-002, for perpendicular and parallel sources, respectively. The validity of the model is supported by the close correlation between the behavior of values extracted from measured data and those calculated with the model.

Additional confirmation of the model is provided in Figs. 36 through 38 where percent polarization plots are given for material A02018-001 in the 0°, 180° and 90°, 270° azimuth angle planes.

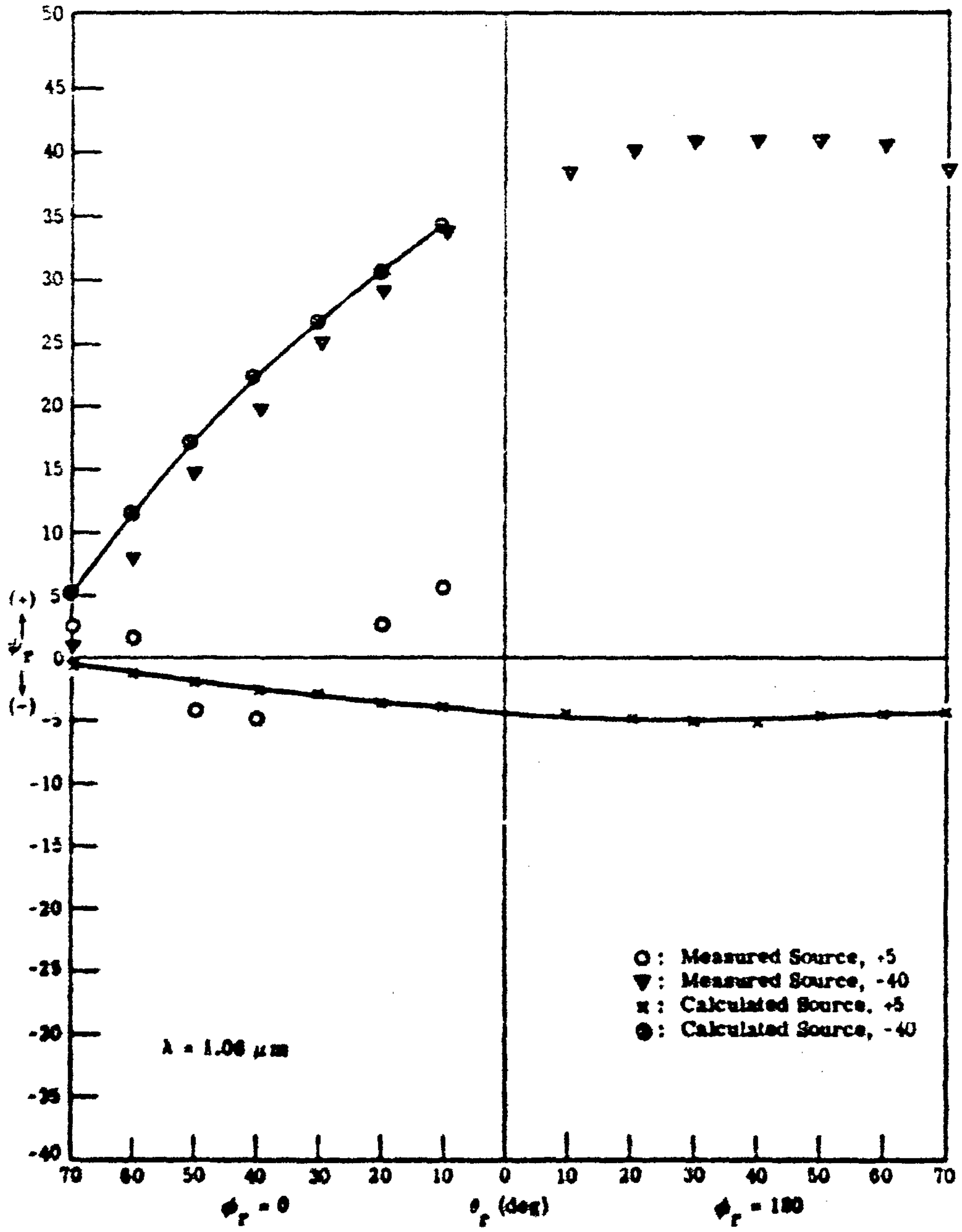

FIGURE 30. VARIATION OF POLARIZATION ANGLE OF REFLECTED RADIANCE AS FUNCTION OF SOURCE-RECEIVER POSITION. $\theta_i = 40°$, $\phi_i = 180°$, $\phi_r = 0°, 180°$.

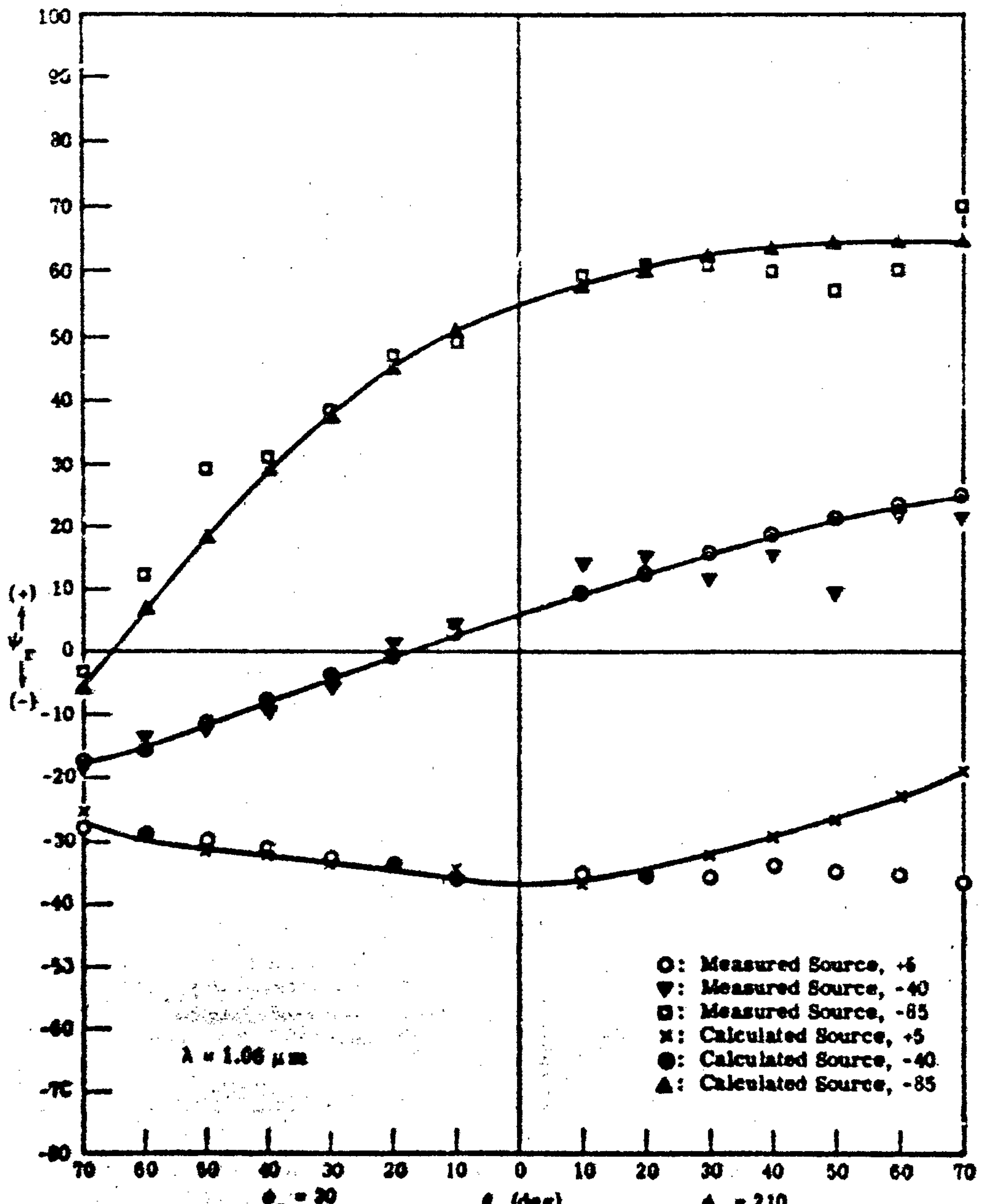

FIGURE 31. VARIATION OF POLARIZATION ANGLE OF REFLECTED RADIANCE AS FUNCTION OF SOURCE-RECEIVER POSITION. $\theta_i = 40°$, $\phi_i = 180°$, $\phi_r = 30°, 210°$.

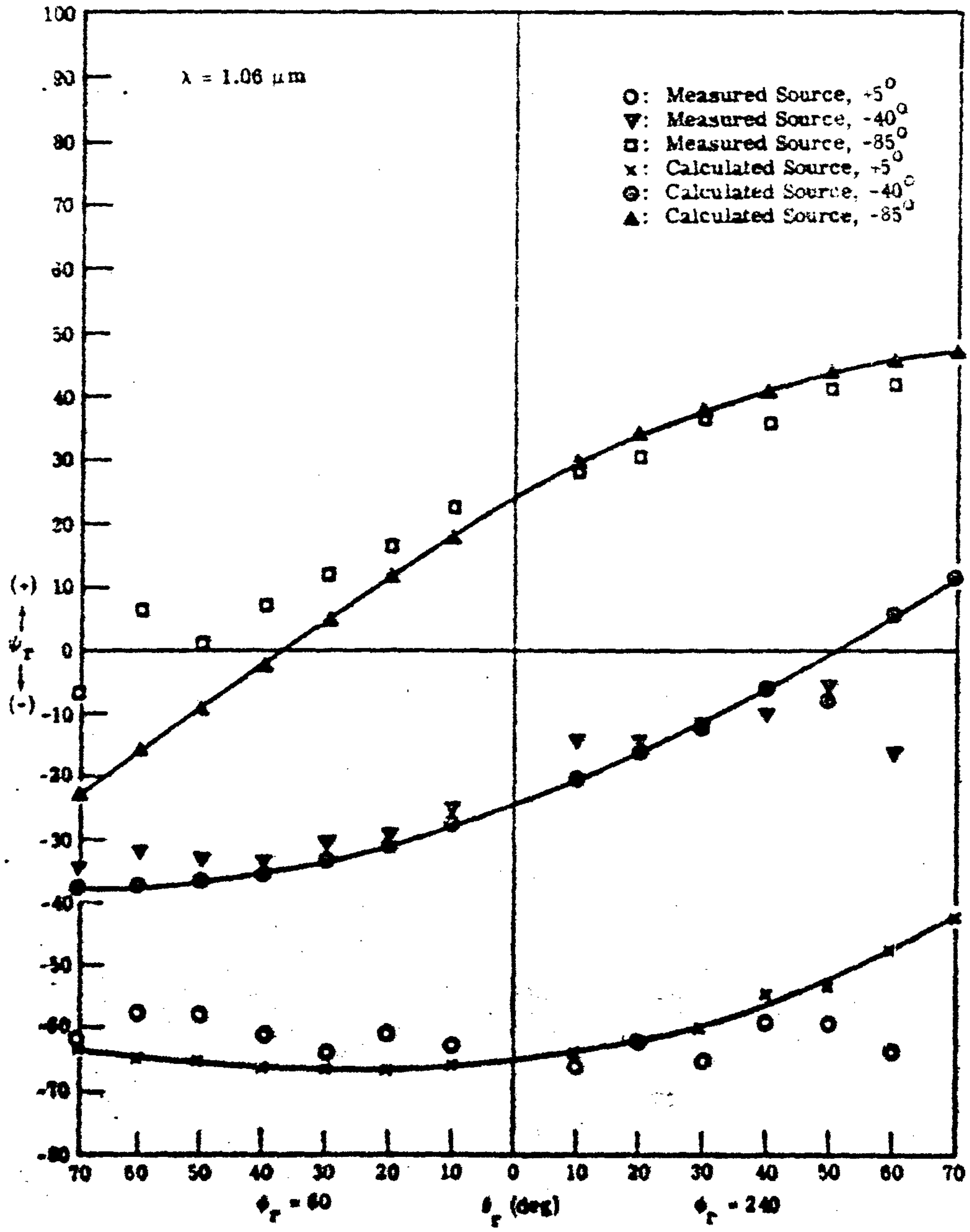

FIGURE 32. VARIATION OF POLARIZATION ANGLE OF REFLECTED RADIANCE AS FUNCTION OF SOURCE-RECEIVER POSITION. $\theta_i = 40°$, $\phi_i = 180°$, $\phi_r = 60°, 240°$.

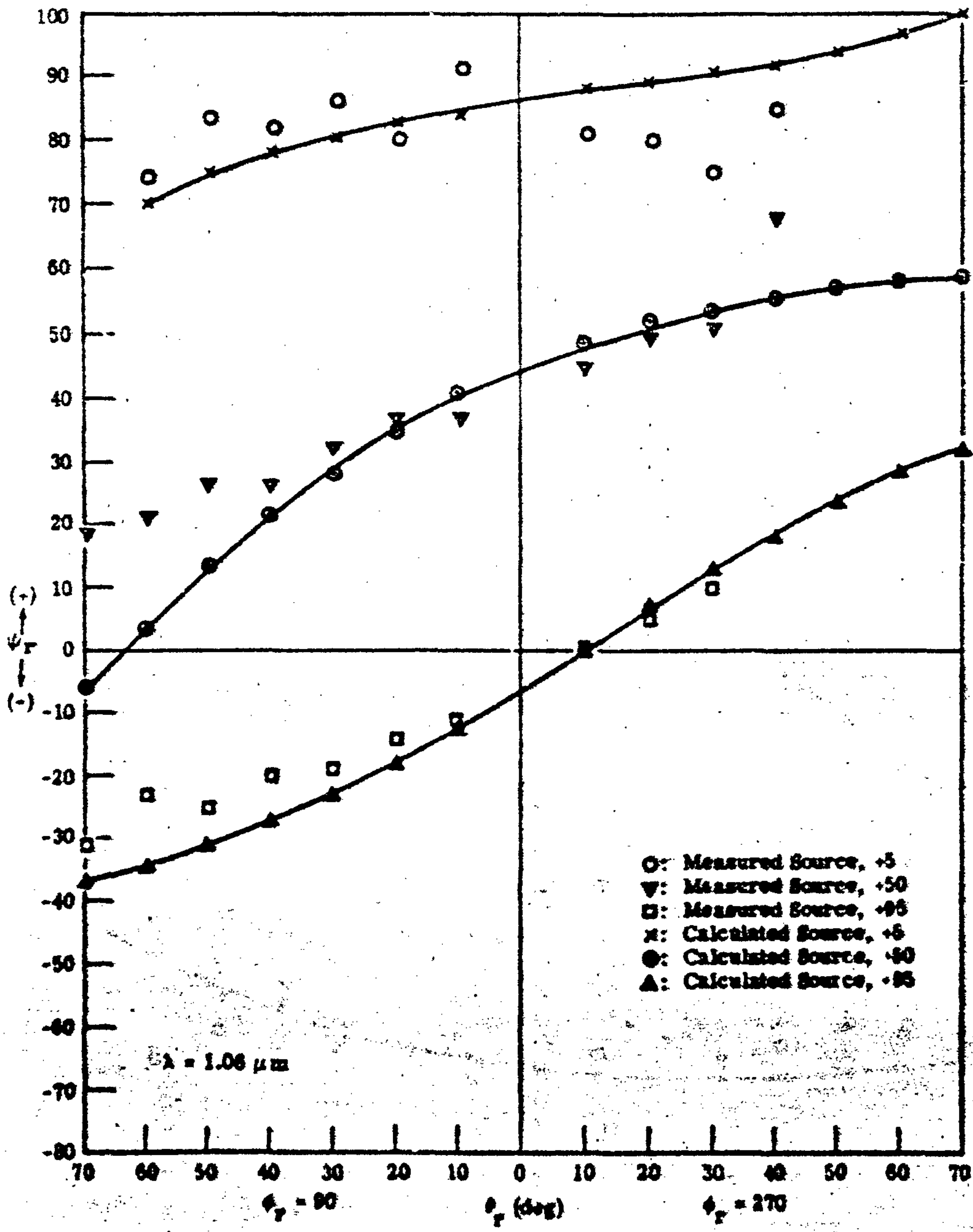

FIGURE 33. VARIATION OF POLARIZATION ANGLE OF REFLECTED RADIANCE AS FUNCTION OF SOURCE-RECEIVER POSITION. $\theta_i = 40^0$, $\phi_i = 180^0$, $\phi_r = 90^0, 270^0$.

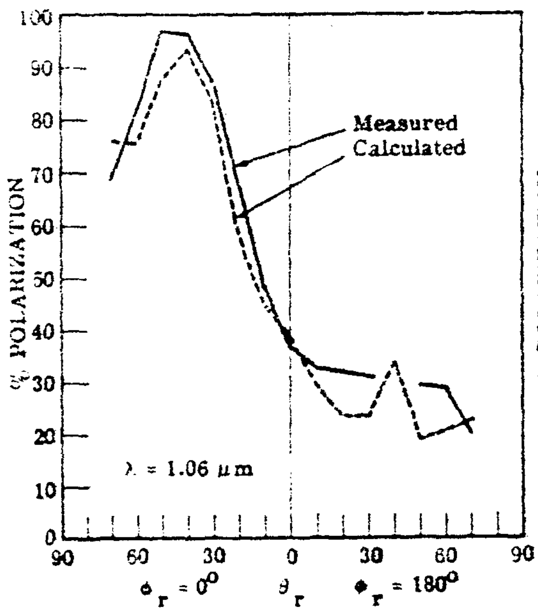

FIGURE 34. PERCENT POLARIZATION VARIATION FOR A02018-002 AS FUNCTION OF SOURCE-RECEIVER POSITION. $\theta_i = 40^o$, $\phi_i = 180^o$, $\phi_r = 0^o$, 180^o; perpendicular source.

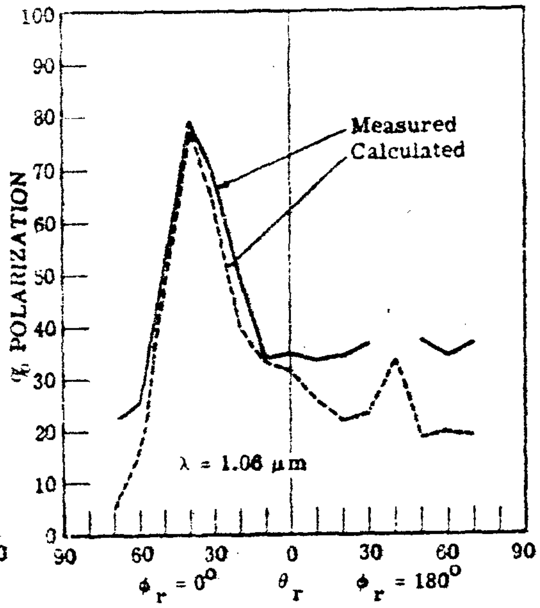

FIGURE 35. PERCENT POLARIZATION VARIATION FOR A02018-002 AS FUNCTION OF SOURCE-RECEIVER POSITION. $\theta_i = 40^o$, $\phi_i = 180^o$, $\phi_r = 0^o$, 180^o; parallel source.

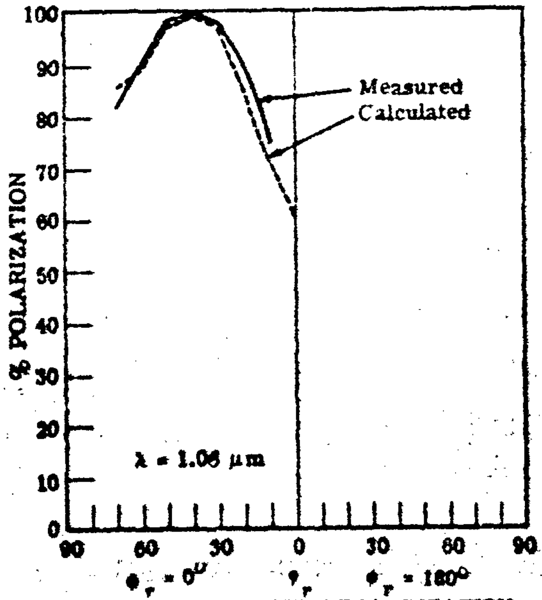

FIGURE 36. PERCENT POLARIZATION VARIATION FOR A02018-001 AS FUNCTION OF SOURCE-RECEIVER POSITION. $\theta_i = 40^o$, $\phi_i = 180^o$, $\phi_r = 0^o$, 180^o; perpendicular source.

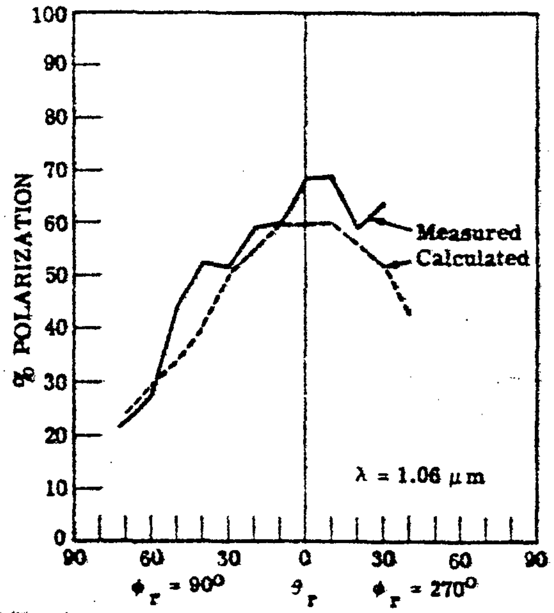

FIGURE 37. PERCENT POLARIZATION VARIATION FOR A02018-001 AS FUNCTION OF SOURCE-RECEIVER POSITION. $\theta_i = 40^{\circ}$, $\phi_i = 180^{\circ}$, $\phi_r = 90^{\circ}$, 270°.

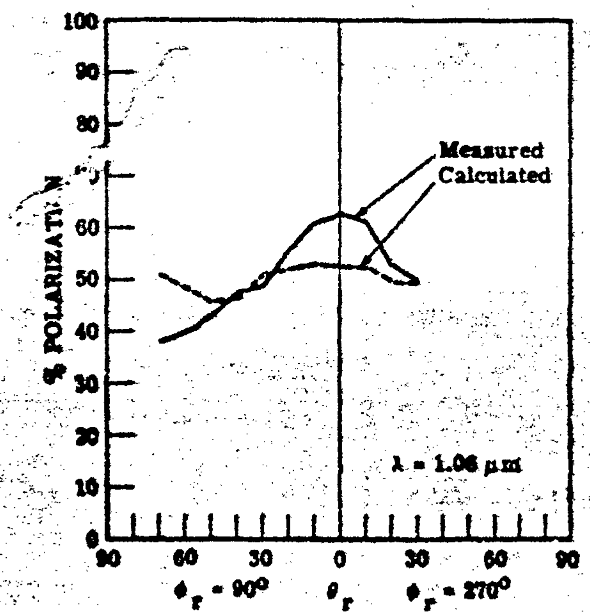

FIGURE 38. PERCENT POLARIZATION VARIATION FOR A02018-001 AS FUNCTION OF SOURCE-RECEIVER POSITION. $\theta_i = 40^{\circ}$, $\phi_i = 180^{\circ}$, $\phi_r = 90^{\circ}$, 270°.

7

MODEL PARAMETERS

This section briefly describes the model parameters that can be used in the bidirectional reflectance program and explains how their values are derived. The choice of parameters for use in the program depends to some extent on the mode of the model being run. Basically, the model is run in three different modes:

(1) Surface and Lambertian volume components
(2) Non-Lambertian volume component (no surface contribution included)
(3) Surface and non-Lambertian volume components

Therefore, we have grouped the model parameters as follows:

(1) Polarization parameters
(2) Surface model parameters
(3) Lambertian volume model parameters
(4) Non-Lambertian volume model parameters
(5) Parameters used to generate typical data for comparison purposes (see Sec. 8)

7.1. SOURCE POLARIZATION PARAMETERS

The present model has been designed to account for polarization dependence in both surface and volume components.

In the surface component, polarization is accounted for automatically in the Fresnel reflectance coefficients. In the most general case, such polarization can be elliptical and can be decomposed into linear and circular components. To date, only a linearly polarized source and receiver have been used in measurements. However, for some applications, circularly polarized sources or receivers may be of interest. Therefore, in the model, we have provided program subroutines which take into consideration the ellipticity and handedness (i.e., direction of rotation in an elliptically polarized source) of both incident and reflected beam.

For volume components in both Lambertian and non-Lambertian cases, it is assumed that reflectance will be depolarized to some extent. In both cases, in fact, we assume total depolarization. Therefore, although a depolarization factor has been included in the non-Lambertian volume model for future flexibility, we assume $DP(\beta) = 1$.

The source polarization may most generally be defined as partially polarized with the polarized component elliptically polarized. The state of polarization of the source will be defined by its degree of polarization, P, and parameters A, B, ψ, and H to define the elliptical polarization of the polarized component. Here, A and B are the intensities along the semi-major and semi-minor axes, respectively. The angle ψ is the angle between the semi-major axis of the ellipse and the direction normal to the plane of incidence, measured looking into the source beam; ψ is equivalent to α except that $0^0 \le \psi \le 180^0$ and $-90^0 \le \alpha \le 90^0$. The handedness H $= \pm 1$.

The Stokes vectors provide a convenient formalism for defining the polarization state of the reflected radiance. (Reference [5] provides a general discussion of Stokes vectors in this context.)

$$S = \begin{bmatrix} I_p + I_u \\ I_p \cos 2\chi \cos 2\psi \\ I_p \cos 2\chi \sin 2\psi \\ I_p \sin 2\chi \end{bmatrix}$$

where I_p and I_u are the polarized and unpolarized components, respectively, in the reflected radiance. The degree of polarization in the reflected radiance is $P = I_p/(I_p + I_u)$. Angles χ and ψ define the polarization state of the reflected radiance: ψ is the angle between the semi-major axis of the ellipse and the direction normal to the plane of reflection; $\tan \chi = \pm\sqrt{B/A}$ where A and B are the intensities along the semi-major and semi-minor axes of the polarization ellipse and $\tan \chi \begin{smallmatrix} < 0 \\ > 0 \end{smallmatrix}$ for $\begin{smallmatrix} \text{left-} \\ \text{right-} \end{smallmatrix}$handed elliptically polarized radiation.

The RHOPRIME program produces the Stokes vector S for unit irradiance in the input beam; the area may also be defined to be unity and then S represents a reflectance Stokes vector. The program also produces the components of the reflected radiance transmitted with a receiver polarization analyzer oriented parallel or perpendicular to the reflectance plane for computing $\rho'_{\psi,\parallel}$ and $\rho'_{\psi,\perp}$.

7.2. SURFACE MODEL PARAMETERS

One of the quantities in Eq. (9) from which $\rho'(\theta_i,\phi_i; \theta_r,\phi_r)$ is determined is $\rho'\left(\theta_{\hat{n}},\phi_{\hat{n}}; \theta_{\hat{n}},\phi_{\hat{n}}\right) \cos^2 \theta_{\hat{n}}$. As previously discussed, $\rho'\left(\theta_{\hat{n}},\phi_{\hat{n}}; \theta_{\hat{n}},\phi_{\hat{n}}\right)$ is obtained from zero bistatic data. Values for $\rho'\left(\theta_{\hat{n}},\phi_{\hat{n}}; \theta_{\hat{n}},\phi_{\hat{n}}\right)\cos^2 \theta_{\hat{n}}$ must be calculated (preferably for increments of two degrees) and made into a table which is one of the model inputs.

<u>n and k</u>. These are the real and imaginary parts of the refractive index. As discussed earlier in this report, they are used for the determination of $R(\beta)$, the Fresnel reflectance. Values for n and k are estimated for the paint surfaces in this study. Moreover, the surface is assumed to be essentially nonconducting so that $k = 0$. Based on experience with similar paint samples, n is taken to be 1.65. For a given sample, n and k can be determined accurately by measuring the Brewster angle and calculating n and k as outlined in Section 4 on the surface model. At the present time the program used, RHOPRIME, does not do this.

<u>τ and Ω</u>. These parameters are used in the function which provides a correction to the program to account for shadowing and obscuration effects resulting from the roughness of the surface. Values for τ and Ω have been selected, based on observed characteristics of reflectance properties. They have been established as $\tau = 15$ and $\Omega = 40$.

7.3. LAMBERTIAN VOLUME MODEL PARAMETERS

$\underline{\rho_{\chi 1} \text{ and } \rho_{\chi 2}}$. These are the cross components of polarized radiation used in the model to account for the diffuse contribution, $\rho_{\chi 1} = 2\rho_{\parallel\perp}$ and $\rho_{\chi 2} = 2\rho_{\perp\parallel}$, where $\rho_{\perp\parallel}$ and/or $\rho_{\parallel\perp}$ is determined by taking the average value of the cross component from the measured data. According to the reciprocity theorem, $\rho_{\chi 1} = \rho_{\chi 2}$ [Ref. 6]. It is important to remember that ρ_χ values only used when the volume scatter model is <u>not</u> used. When the volume model <u>is</u> used, $\rho_{\chi 1} = \rho_{\chi 2} = 0$.

7.4. NON-LAMBERTIAN VOLUME MODEL PARAMETERS

$\underline{\rho_V}$. This represents the non-Lambertian volume scatter component; it is determined by extracting $\rho'_{\perp\parallel}$ or $\rho'_{\parallel\perp}$ at the point which would lie under the peak of the zero bistatic scan if the measured curve were smooth; $\rho_V = 2\rho'_{\perp\parallel} = 2\rho'_{\parallel\perp}$ at the peak point. (The fact that a hump sometimes occurs on the measured cross component curve is discussed in the section on Model Validations.)

Here again, it is important to remember that when the Lambertian volume model is used, $\rho_V = 0$ and $\rho_\chi \neq 0$. When the non-Lambertian volume model is used, $\rho_V \neq 0$ and $\rho_\chi = 0$. Also, ρ_V and ρ_χ are never simultaneously nonzero in models which have been validated to date.

$\underline{DP(\beta), f(\beta), g\left(\theta_{\hat{n}}\right)}$. Integral parts of SUBROUTINE FUNC, these parameters currently are all set equal to 1. They have been included to provide flexibility for later model modifications.

7.5. PARAMETERS USED TO GENERATE TYPICAL DATA FOR COMPARISON PURPOSES

As will be discussed in Section 8, available data representing typical material parameters are sometimes useful. For this reason, the model contains a subroutine which can generate zero bistatic data, given a suitable set of input parameters. The parameters are: σ, RPO, Q1, and Q2. Normally, however, actual zero bistatic measured data are used, and $\sigma = 0$; RPO = 0; Q1 = Q2 = 1.

8
REFLECTANCE ESTIMATION METHOD

If one has sufficient information about the target material, reflectance data can be estimated without the use of a computer. In particular, as discussed earlier, the index of refraction and a fixed bistatic curve are the necessary elements from which to extract the necessary parameters. For the sample paints used for the data compilation, the index of refraction is assumed to be totally real with $n = 1.65$ and $k = 0$.

In order to use the above information to generate reflectance data, a set of typical fixed bistatic and bidirectional reflectance curves has been generated. These curves are intended to simulate a range of paint types from which reflectance values for a particular material can be estimated by an interpolation procedure based on fixed bistatic values. Typical curves are given in Appendix II.

We first find the position of the fixed bistatic for the material of interest relative to that of two other fixed bistatics for materials on which we have complete reflectance data. We then assume that the same relationship between the three materials will be maintained in the reflectance data. Therefore, by interpolation, we determine the bidirectional reflectance of the material of interest relative to the known materials.

To proceed, we must now choose parameters that characterize the curves and provide a basis for interpolation. The parameters selected are:

(1) the ratio of peak value to that value at which the curve begins to level out or, if it begins to rise, the point of minimum reflectance (this is for the like-polarized component, i.e., $\rho'_{\perp\perp}$ or $\rho'_{\parallel\parallel}$).

(2) the width (in this case, angular distance between peak point and leveling-out or minimum point, of the fixed bistatic curve; for most materials this width is close enough to 30° to be assumed constant).

(3) the Lambertian or non-Lambertian character of the material as demonstrated by the angular dependence of the cross component in the fixed bistatic scan.

In the following subsections, we first provide a step-by-step outline of the interpolation procedure. The same step-by-step procedure is then applied in an example worked out in detail.

8.1. PROCEDURE FOR ESTIMATING REFLECTANCE VALUES BY INTERPOLATION

(1) Select the actual fixed bistatic curve for the material for which reflectances are required.

(2) Measure the reflectance at the peak value of the curve and the minimum value (or value at which the curve begins to level out from the peak). Take the ratio of these two values.

(3) Select two generated fixed bistatic curves which appear to bracket the measured curve with respect to the ratio described in step (2).

(4) Normalize all three curves to the same peak value and determine the normalization factors.

(5) If the measured curve lies between the two reference curves, select an angle close to 30° (the approximate value for minima or leveling out for most materials) and determine the position of the measured point between the points on the two artificial curves. The fraction of the distance between the two reference curve points at which the measured curve point lies is then taken as an interpolation factor, IF. This factor will be applied to the reference reflectance curves to obtain reflectance values for the material of interest. (If the measured curve does not lie between the two artificial curves, the procedure is one of extrapolation, and the derived factor will still be some fraction of the distance between the artificial curve points.)

(6) For the desired source angle ($\theta_i = 2^{\circ}, 20^{\circ}, 40^{\circ}$, or 60°), select reference reflectance curves from Appendix II which correspond to the fixed bistatic curves.

(7) Read off the reflectance values for the reference curves for each receiver (θ_r) angle.

(8) Multiply both reflectance curves by the same factor used to normalize their corresponding fixed bistatics.

(9) Using the interpolation (or extrapolation) factor, IF, derived in step (5), find the estimated reflectance value for each position of θ_r.

> Note: The above results correspond to normalized fixed bistatic values. To get the absolute reflectance value we must divide out the normalization.

(10) Divide values in step (9) by the normalizing factor (found in step 4) for the material of interest.

6.3. APPLICATION OF PROCEDURE

We will estimate five θ_r points for $\theta_i = 40^{\circ}$, using the fixed bistatic for sample A01040 as shown in Fig. 59, Appendix I. We will then compare the five estimated points with the actual measurement curve on page 118 of the Data Compilation [Ref. 2]. The whole procedure will be carried out as outlined above:

(1) Sample A01040 has been selected and the fixed-bistatic curve of Fig. 59 will be used.

(2) ρ' (peak) = 0.17

ρ' (30°) = 0.045

R = 0.17/0.045 = 3.78

(3) Select fixed bistatic curves for typical materials 2 and 3 (use Figs. 63 and 64) with R values that bracket 3.73. (It is convenient to bracket the value but not necessary.) The two values can be used to extrapolate to any value.

(4 & 5) Normalize A01640 and material 2 to the peak of material 3:

Material	θ_n	Measured Value	Normalizing Factor	Normalized Value
A01640	0^{o}	0.16	5.62	0.9
	30^{o}	0.035	5.62	0.197
2	0^{o}	0.65	1.38	0.9
	30^{o}	0.035	1.38	0.049
3	0^{o}	0.9	1	0.9
	30^{o}	0.38	1	0.38

For interpolation, use highest value as reference:

$$\text{Interpolation factor} = \text{IF} = \frac{\rho_3' - \rho_{1640}'}{\rho_3' - \rho_2'} = \frac{0.38 - 0.197}{0.38 - 0.049} = \frac{0.183}{0.331} = 0.554$$

Note that ρ_3' refers to ρ' for material 3; similar subscripting identifies ρ_{1640}' and ρ_2'.

(6) For $\theta_i = 40^{o}$, use material 2 (Fig. 79), and material 3 (Fig. 87).

(7) We use $\theta_r = 20^{o}$ and 40^{o} in the backscatter half plane, and $\theta_r = 0^{o}$, 20^{o}, and 40^{o} in the forward-scatter half plane. Values shown are for $\rho'(\theta_r, \phi_r)$ where it is understood that $\theta_i = 40^{o}$ and $\phi_i = 0^{o}$:

	$\rho'(20,0)$	$\rho'(40,0)$	$\rho'(0,0)$	$\rho'(20,180)$	$\rho'(40,180)$
Material 2:	0.03	0.035	0.048	0.23	1.8
Material 3:	0.32	0.37	0.44	0.95	2.5

(8) Normalization factor for material 2 was 1.38; for material 3 this factor was 1. Therefor:

	$\rho'(20,0)$	$\rho'(40,0)$	$\rho'(0,0)$	$\rho'(20,180)$	$\rho'(40,180)$
Material 2:	0.041	0.048	0.066	0.317	2.48
Material 3:	0.32	0.37	0.44	0.95	2.5

(9) As in step (5), $\rho_3' - \rho_{1640}' = (\text{IF})(\rho_3' - \rho_2')$, and $\rho_{1640}' = \rho_3' - (\text{IF})(\rho_3' - \rho_2')$ for each position of interest. Therefore:

	$\rho'(20,0)$	$\rho'(40,0)$	$\rho'(0,0)$	$\rho'(20,180)$	$\rho'(40,180)$
Material A01640:	0.163	0.135	0.238	0.61	2.40

(10) Dividing the results of step (9) by the normalizing factor for sample material A01640 yields the following estimated values:

$\rho'(20,0)$	$\rho'(40,0)$	$\rho'(0,0)$	$\rho'(20,180)$	$\rho'(40,180)$
0.029	0.035	0.042	0.11	0.44

We have now obtained in-plane bidirectional reflectance values at $\theta_i = 40^{o}$ for material A01640 of the Data Compilation where $\theta_r = 0^{o}$ and $\theta_r = 20^{o}$ and 40^{o} in both the backscattered and forward-scattered directions.

Since measured values for these reflectances are available in the Data Compilation [2], we can now compare them to our derived values to determine how well the interpolation method works. As page 118 of the Data Compilation shows:

$\rho'_{\perp\perp}(40,0) = 0.06$
$\rho'_{\perp\perp}(20,0) = 0.042$
$\rho'_{\perp\perp}(0,0) = 0.055$
$\rho'_{\perp\perp}(20,180) = 0.12$
$\rho'_{\perp\perp}(40,180) = 0.7$

Recall, however, that for true surface reflectance:

$$\rho'_{\perp} = \rho'_{\perp\perp} - \rho'_{\perp\parallel}$$

Therefore, the cross-components read from the same measurement curve are:

$\rho'_{\perp\parallel}(20,0) = 0.015$
$\rho'_{\perp\parallel}(40,0) = 0.018$
$\rho'_{\perp\parallel}(0,0) = 0.017$
$\rho'_{\perp\parallel}(20,180) = 0.018$
$\rho'_{\perp\parallel}(40,180) = 0.02$

Calculating $\rho'_{\perp\perp} - \rho'_{\perp\parallel}$, we obtain the following comparison:

Measurement	Estimate
$\rho'_{\perp}(20,0) = 0.027$	0.029
$\rho'_{\perp}(40,0) = 0.042$	0.035
$\rho'_{\perp}(0,0) = 0.038$	0.045
$\rho'_{\perp}(20,180) = 0.102$	0.11
$\rho'_{\perp}(40,180) = 0.68$	0.44

The agreement appears to be excellent, the largest discrepancy amounting to about 50%.

Appendix I
FIXED BISTATIC DATA FOR PAINTS FROM DATA COMPILATION

In Section 4.3 on shadowing and obscuration, we showed that Eq. (10) could be used to derive a fixed bistatic curve as a function of source-receiver position. But by so doing, one obtains some variation of fixed bistatic curves with source position. The shadowing and obscuration factor described in Section 4.3 applies a first correction to the basic calculation.

A further correction may be applied by averaging values obtained in the first correction. Fixed bistatic curves for 24 examples from the data compilation have been so derived and are included in this report as Figs. 39 through 62. Each figure includes a listing of the fixed bistatic bidirectional reflectances as a function of $\theta_{\tilde{n}}$, in correspondence with the curve.

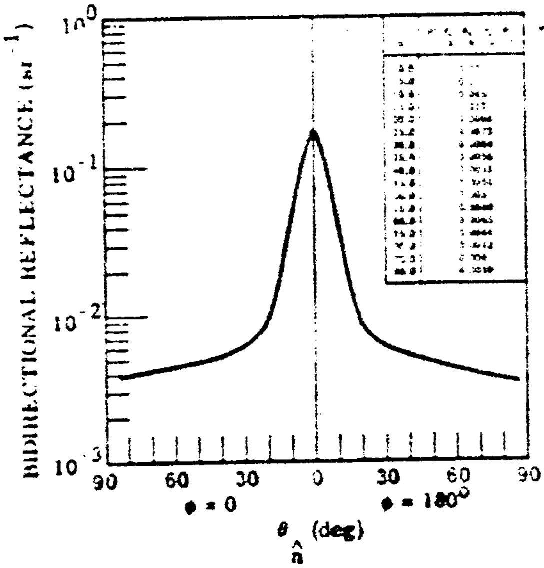

FIGURE 39. FIXED BISTATIC ρ' FOR A01027; λ = 0.63 μm.

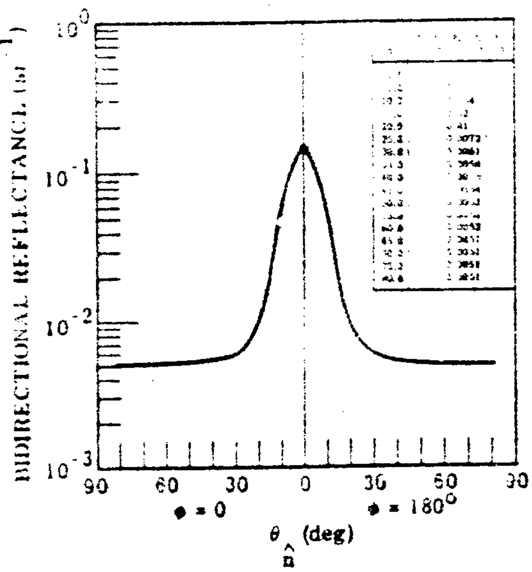

FIGURE 40. FIXED BISTATIC ρ' FOR A01044; λ = 0.63 μm.

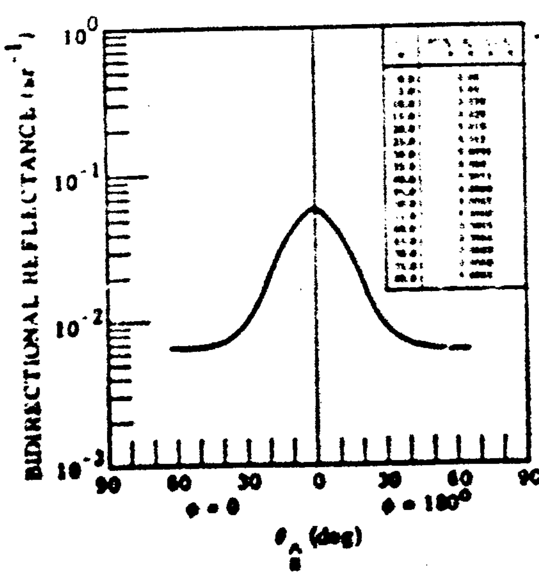

FIGURE 41. FIXED BISTATIC ρ' FOR A01047; λ = 0.63 μm.

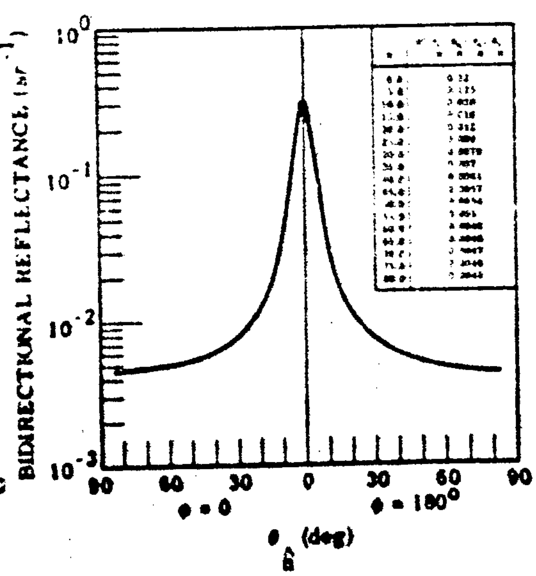

FIGURE 42. FIXED BISTATIC ρ' FOR A01224; λ = 0.63 μm.

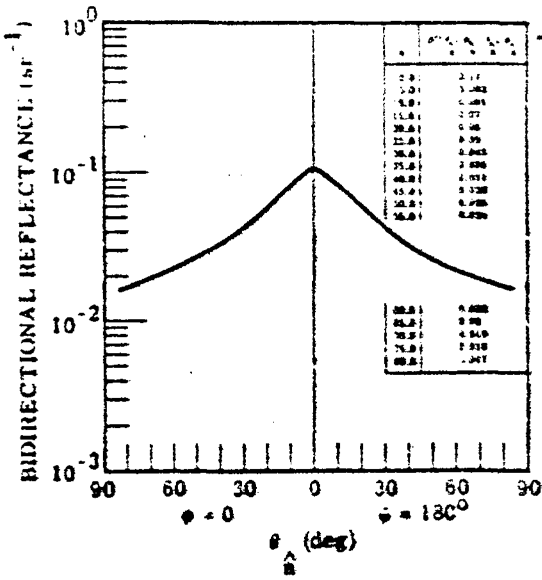

FIGURE 43. FIXED BISTATIC ρ' FOR A01295; $\lambda = 0.63\ \mu m$.

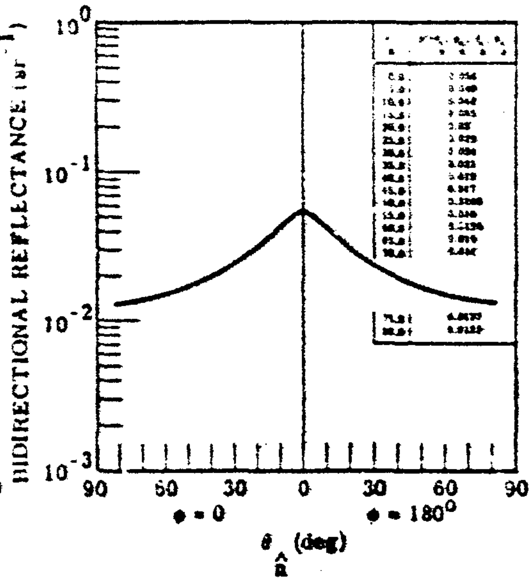

FIGURE 44. FIXED BISTATIC ρ' FOR A01341; $\lambda = 0.63\ \mu m$.

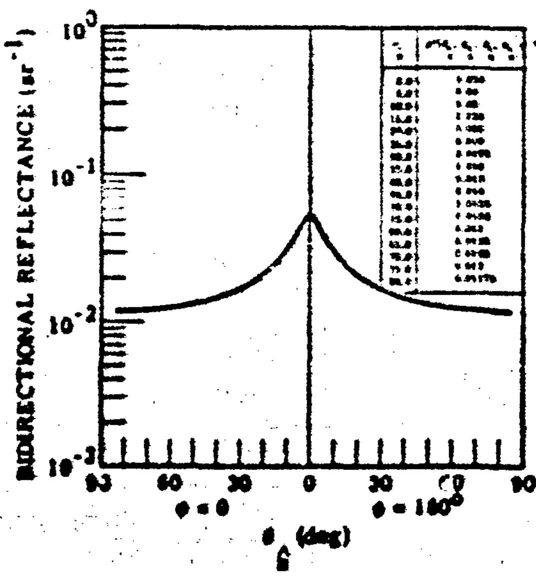

FIGURE 45. FIXED BISTATIC ρ' FOR A01342; $\lambda = 0.63\ \mu m$.

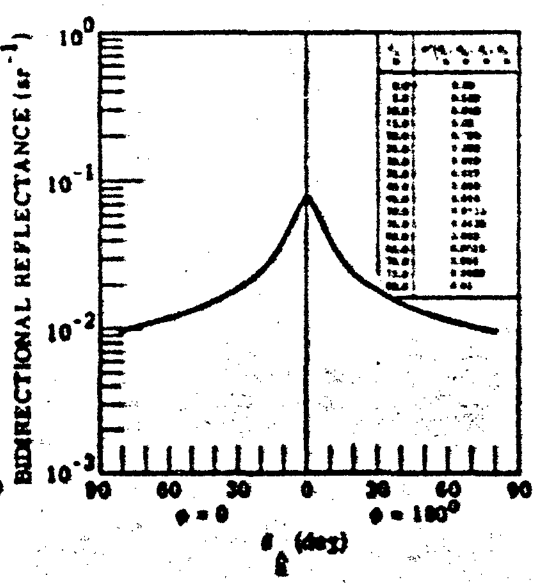

FIGURE 46. FIXED BISTATIC ρ' FOR A01343; $\lambda = 0.63\ \mu m$.

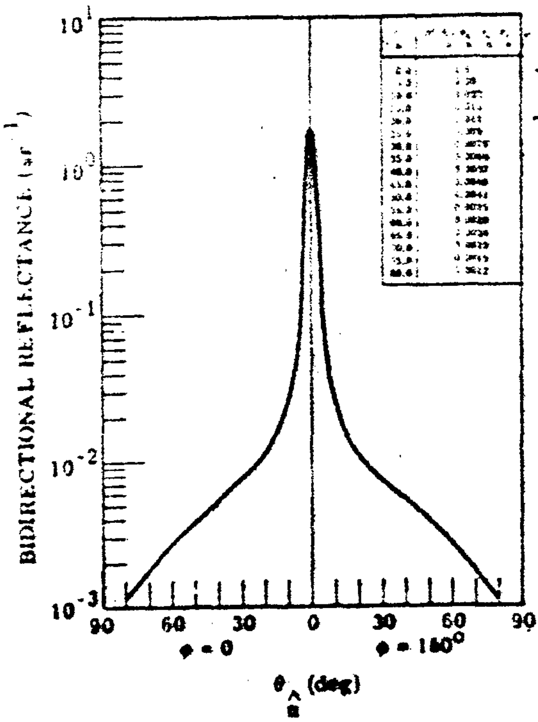

FIGURE 47. FIXED BISTATIC ρ' FOR A01444; λ = 0.67 μm.

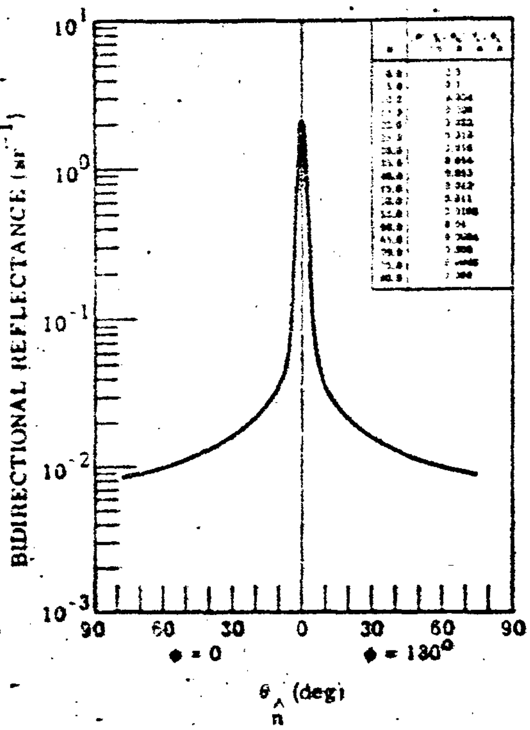

FIGURE 48. FIXED BISTATIC ρ' FOR A01444; λ = 1.06 μm.

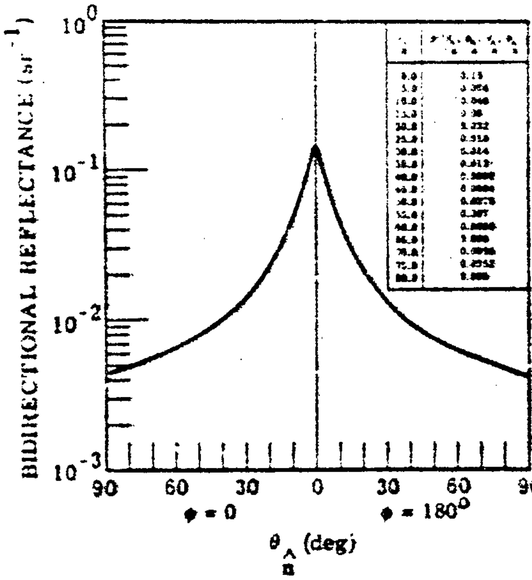

FIGURE 49. FIXED BISTATIC ρ' FOR A01453; $\lambda = 0.63\ \mu m$.

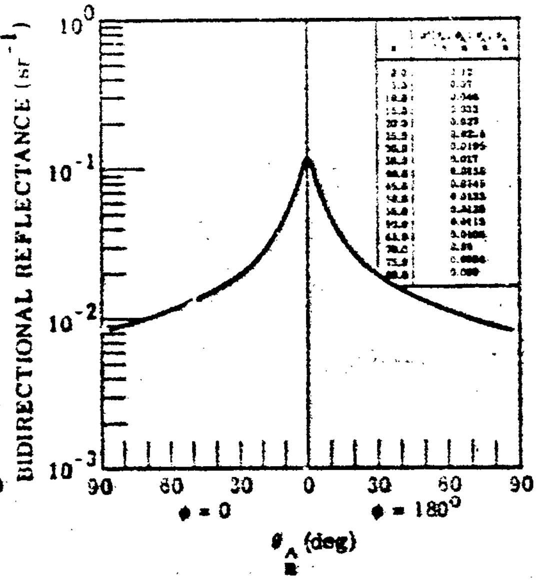

FIGURE 50. FIXED BISTATIC ρ' FOR A01453; $\lambda = 1.06\ \mu m$.

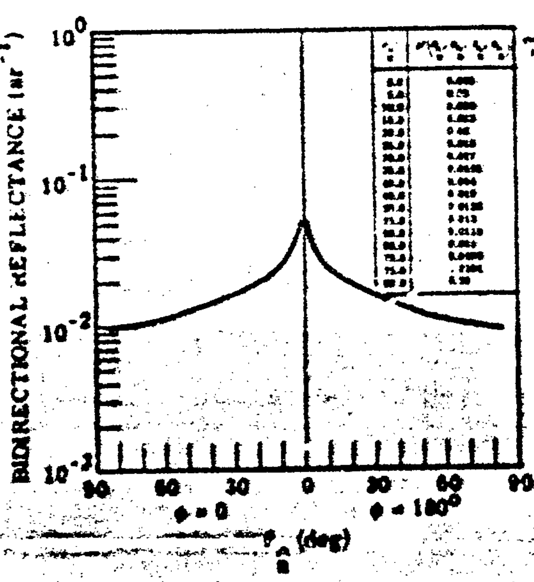

FIGURE 51. FIXED BISTATIC ρ' FOR A01454; $\lambda = 0.63\ \mu m$.

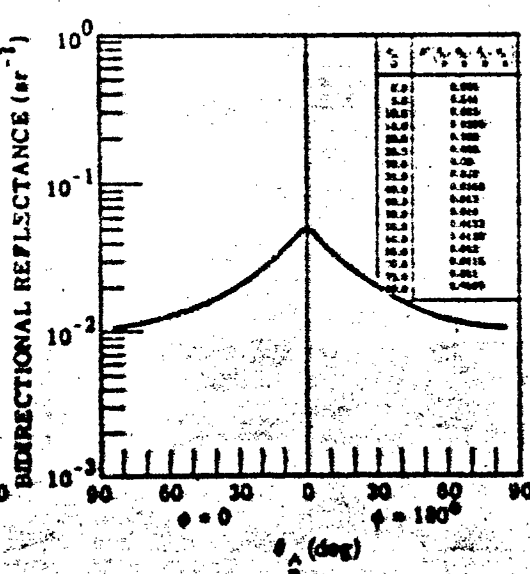

FIGURE 52. FIXED BISTATIC ρ' FOR A01404; $\lambda = 1.06\ \mu m$.

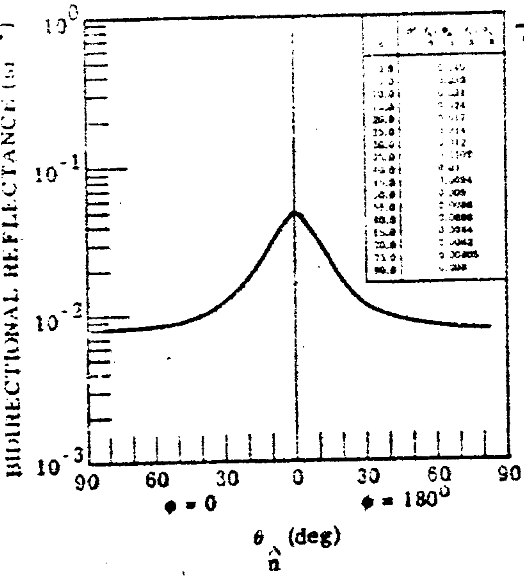

FIGURE 53. FIXED BISTATIC ρ' FOR A01455; $\lambda = 0.63\ \mu m$.

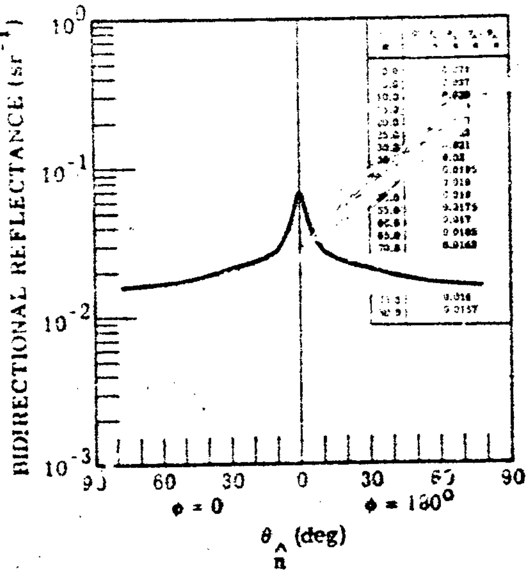

FIGURE 54. FIXED BISTATIC ρ' FOR A01456; $\lambda = 0.63\ \mu m$.

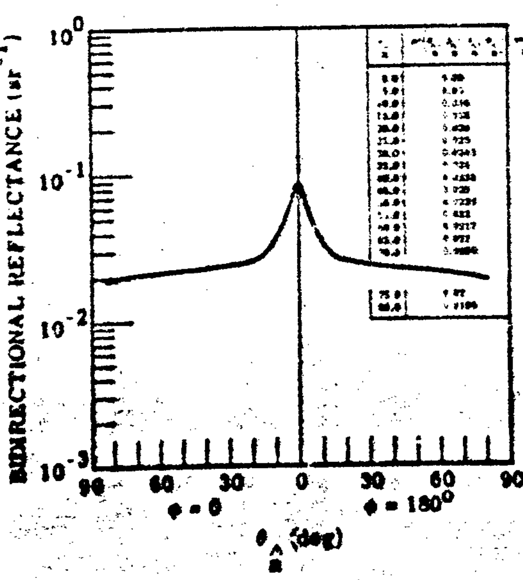

FIGURE 55. FIXED BISTATIC ρ' FOR A01456; $\lambda = 1.06\ \mu m$.

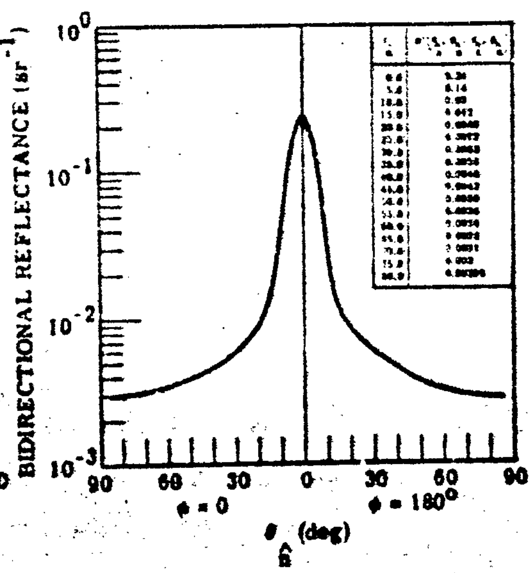

FIGURE 56. FIXED BISTATIC ρ' FOR A01608; $\lambda = 0.63\ \mu m$.

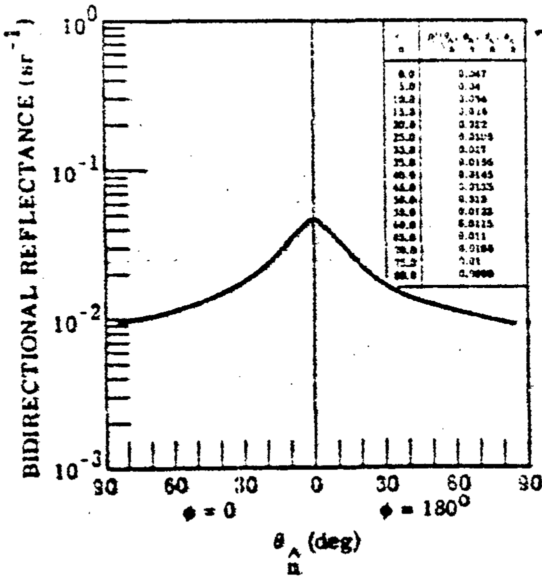

FIGURE 57. FIXED BISTATIC ρ' FOR A01629; $\lambda = 0.63\ \mu m$.

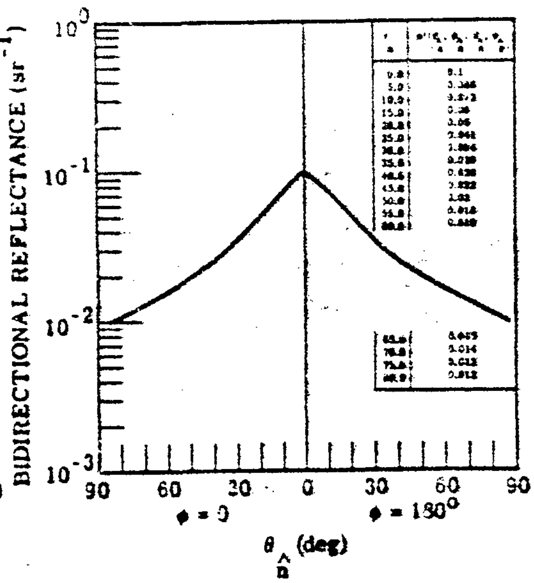

FIGURE 58. FIXED BISTATIC ρ' FOR A01638; $\lambda = 0.63\ \mu m$.

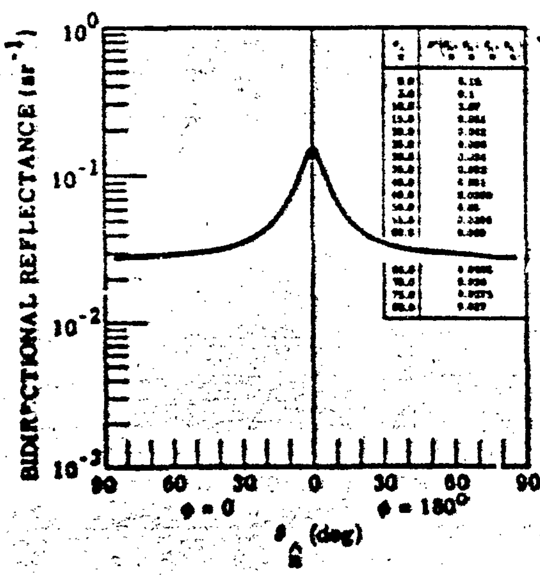

FIGURE 59. FIXED BISTATIC ρ' FOR A01640; $\lambda = 0.63\ \mu m$.

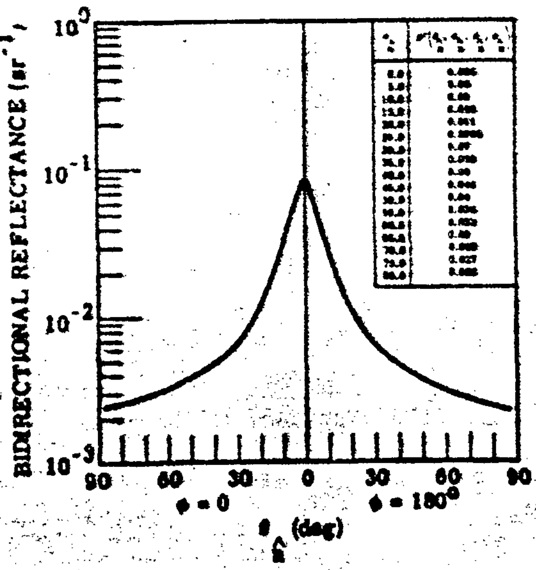

FIGURE 60. FIXED BISTATIC ρ' FOR A01701; $\lambda = 0.63\ \mu m$.

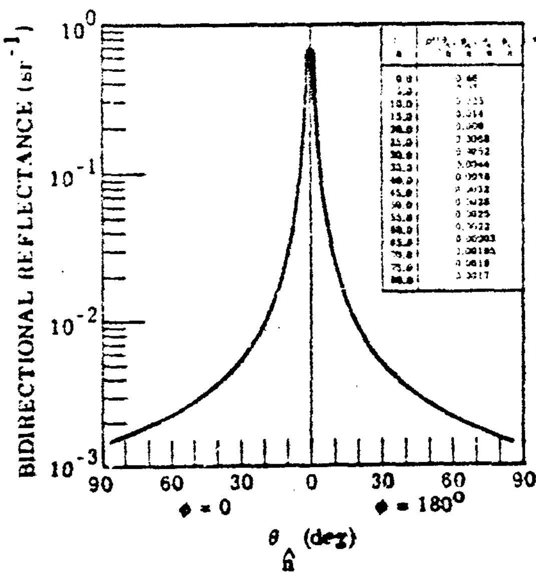

FIGURE 61. FIXED BISTATIC ρ' FOR A02001; $\lambda = 1.06$ μm.

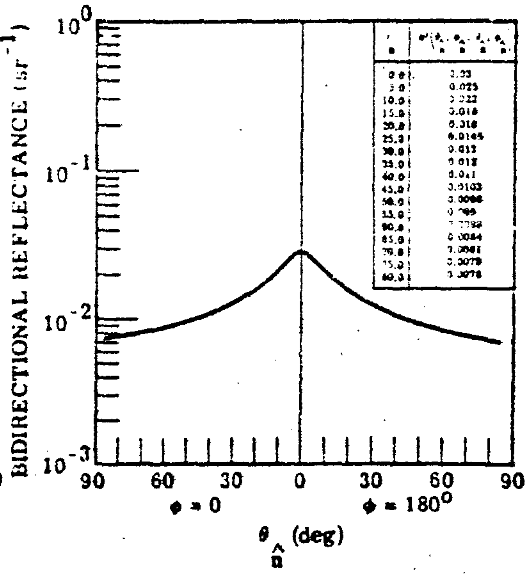

FIGURE 62. FIXED BISTATIC ρ' FOR A02004; $\lambda = 1.06$ μm.

Appendix II
BIDIRECTIONAL REFLECTANCE DATA FOR FOUR TYPICAL TYPES OF PAINT

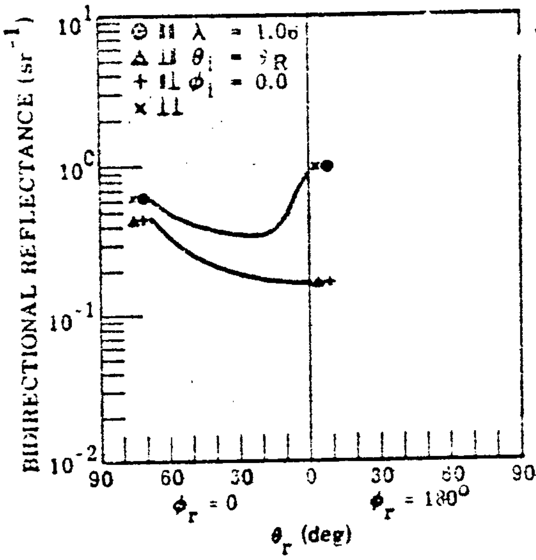

FIGURE 63. FIXED BISTATIC ρ' FOR TYPICAL MATERIAL NO. 1

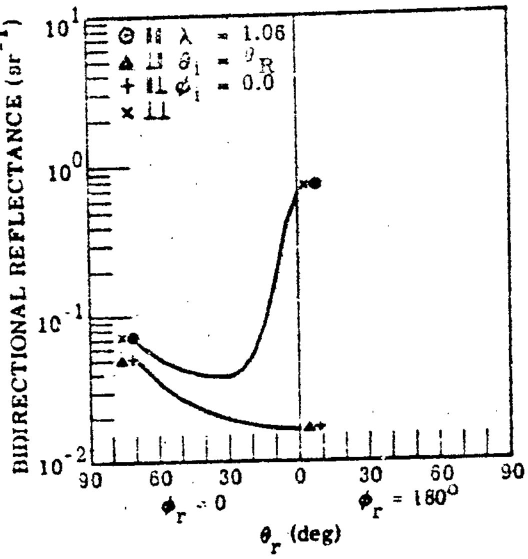

FIGURE 64. FIXED BISTATIC ρ' FOR TYPICAL MATERIAL NO. 2

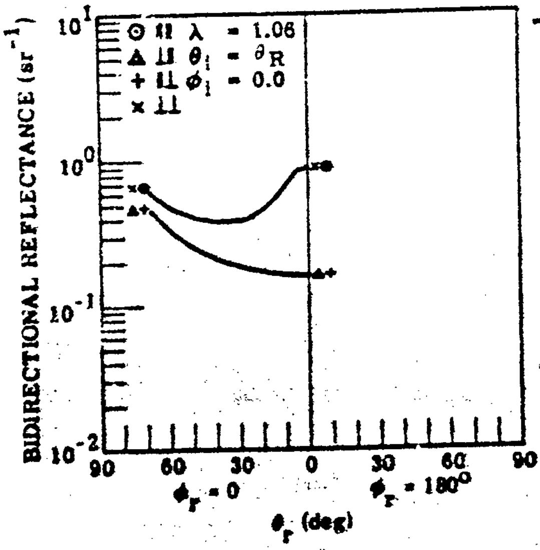

FIGURE 65. FIXED BISTATIC ρ' FOR TYPICAL MATERIAL NO. 3

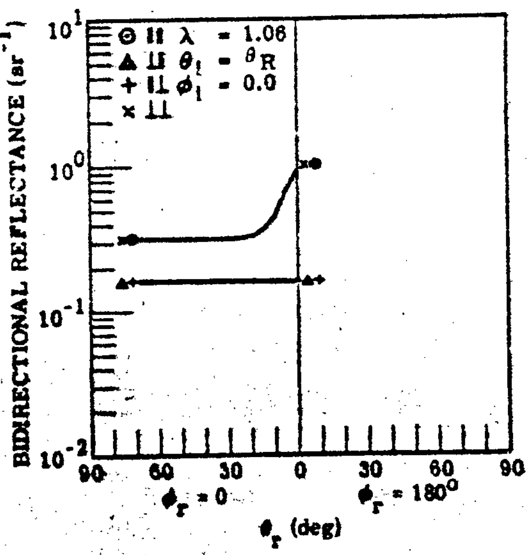

FIGURE 66. FIXED BISTATIC ρ' FOR TYPICAL MATERIAL NO. 4

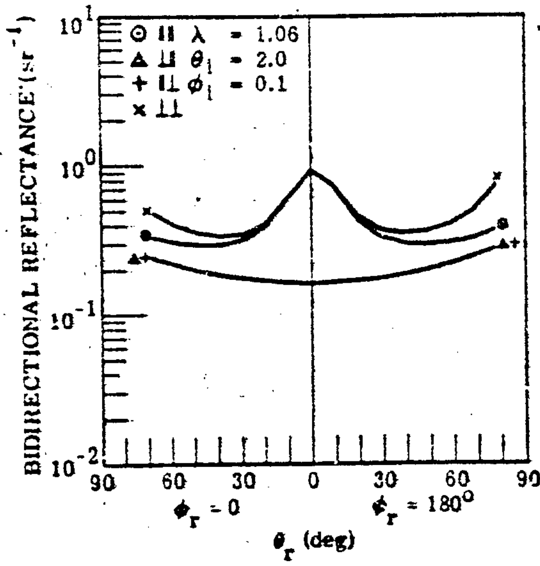

FIGURE 67. ρ' FOR MATERIAL NO. 1.
θ_i = 2° ; ϕ_r = 0°, 180°.

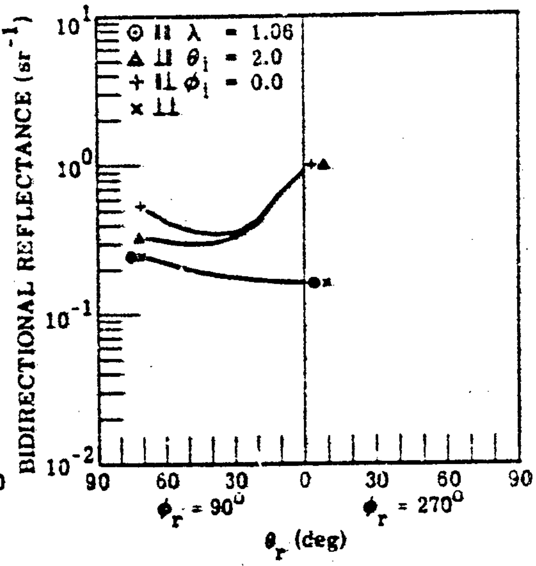

FIGURE 68. ρ' FOR MATERIAL NO. 1.
θ_i = 2° ; ϕ_r = 90°, 270°.

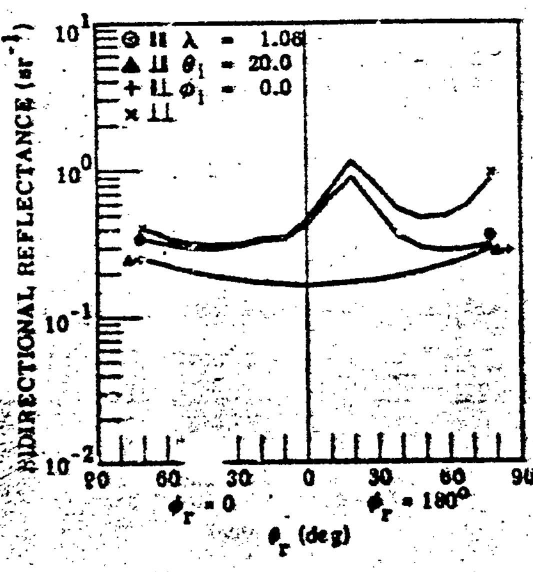

FIGURE 69. ρ' FOR MATERIAL NO. 1.
θ_i = 20°; ϕ_r = 0°, 180°.

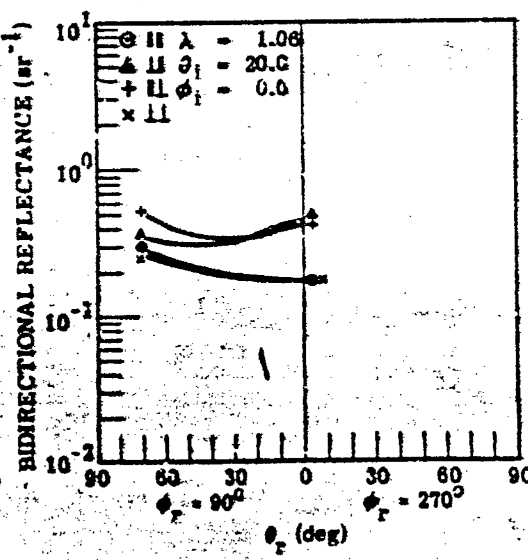

FIGURE 70. ρ' FOR MATERIAL NO. 1.
θ_i = 20°; ϕ_r = 90°, 270°.

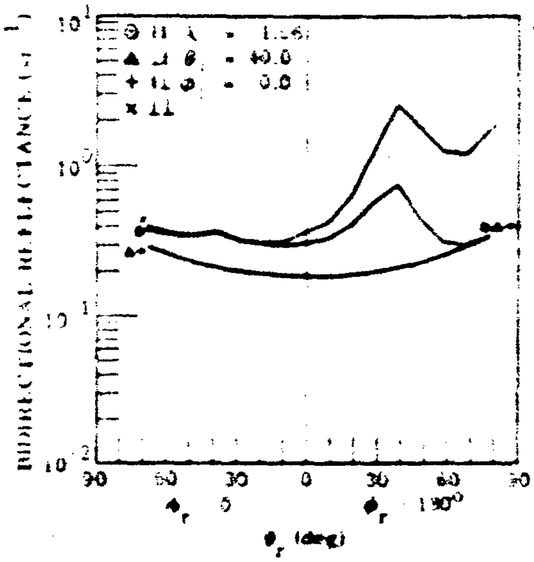

FIGURE 71. ρ FOR MATERIAL NO. 1. $\theta_i = 40°$; $\phi_r = 0°, 180°$.

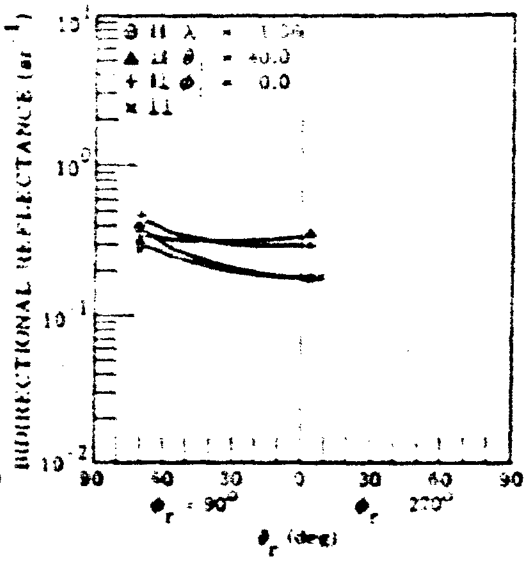

FIGURE 72. ρ FOR MATERIAL NO. 1. $\theta_i = 40°$; $\phi_r = 90°, 270°$.

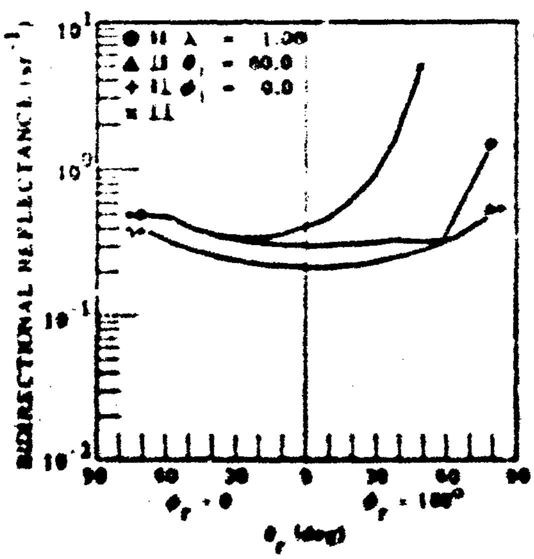

FIGURE 73. ρ FOR MATERIAL NO. 1. $\theta_i = 60°$; $\phi_r = 0°, 180°$.

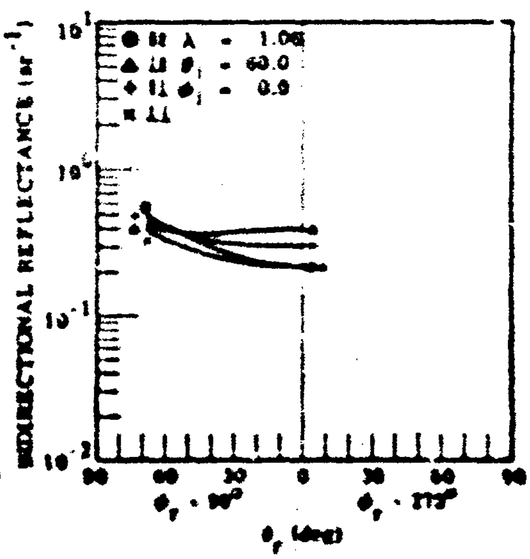

FIGURE 74. ρ FOR MATERIAL NO. 1. $\theta_i = 60°$; $\phi_r = 90°, 270°$.

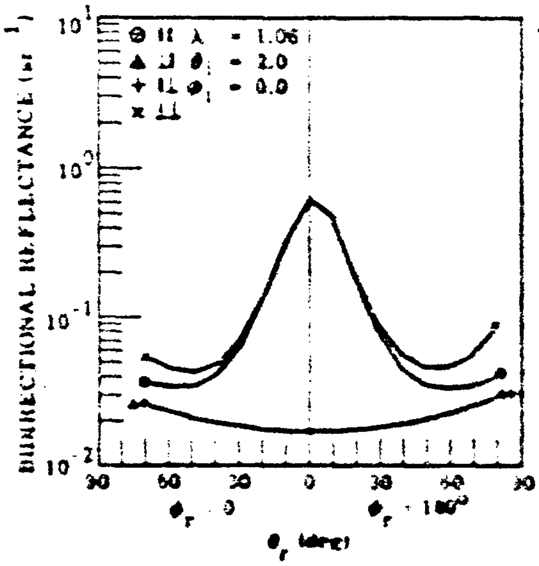

FIGURE 75. ρ' FOR MATERIAL NO. 2.
θ_i = 2°; ϕ_r = 0°, 180°.

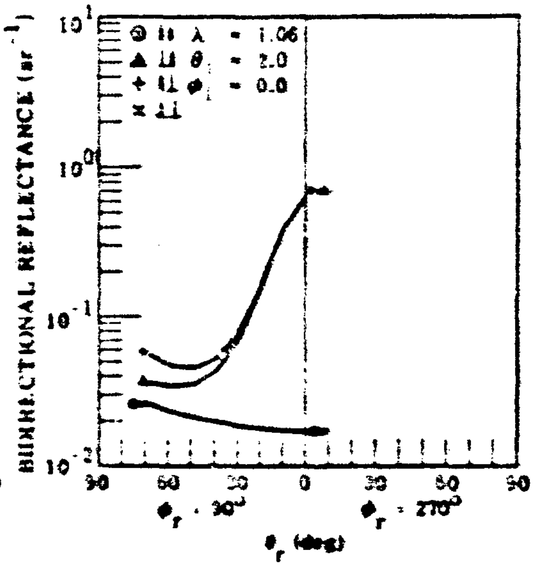

FIGURE 76. ρ' FOR MATERIAL NO. 2.
θ_i = 2°; ϕ_r = 90°, 270°.

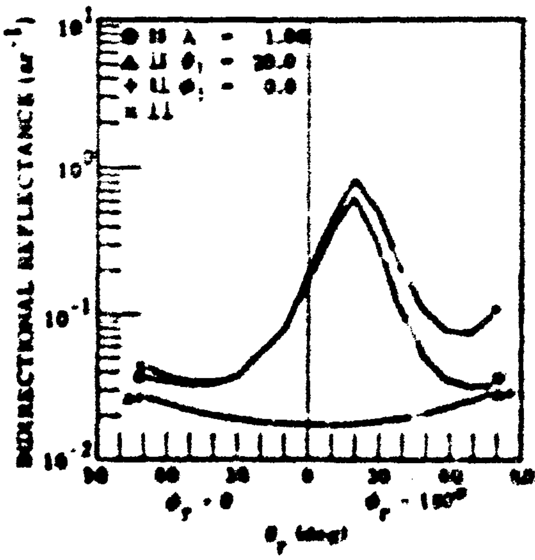

FIGURE 77. ρ' FOR MATERIAL NO. 2.
θ_i = 20°; ϕ_r = 0°, 180°.

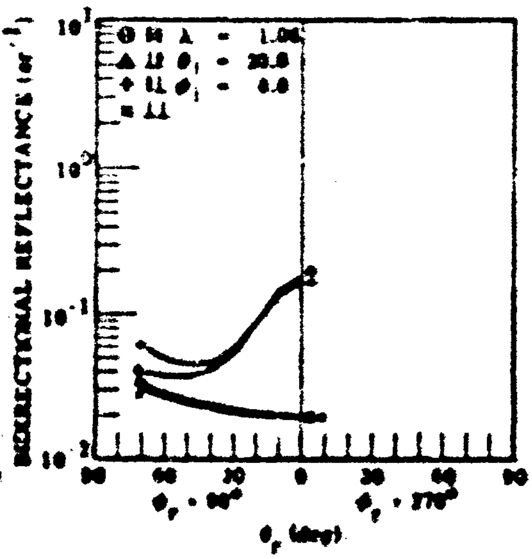

FIGURE 78. ρ' FOR MATERIAL NO. 2.
θ_i = 20°; ϕ_r = 90°, 270°.

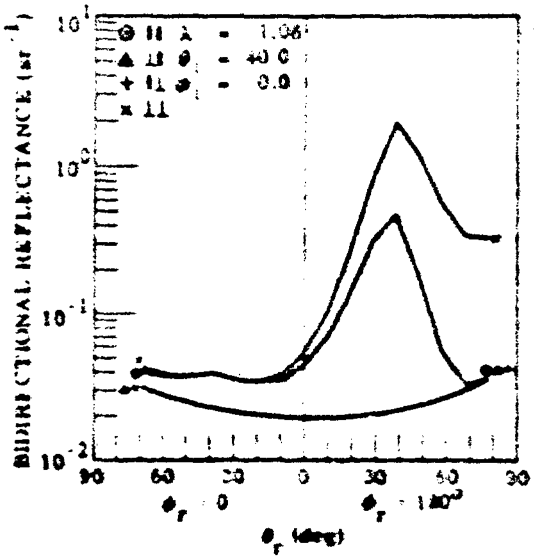

FIGURE 79. ρ' FOR MATERIAL NO. 2. $\theta_i = 40°$; $\phi_r = 0°, 180°$.

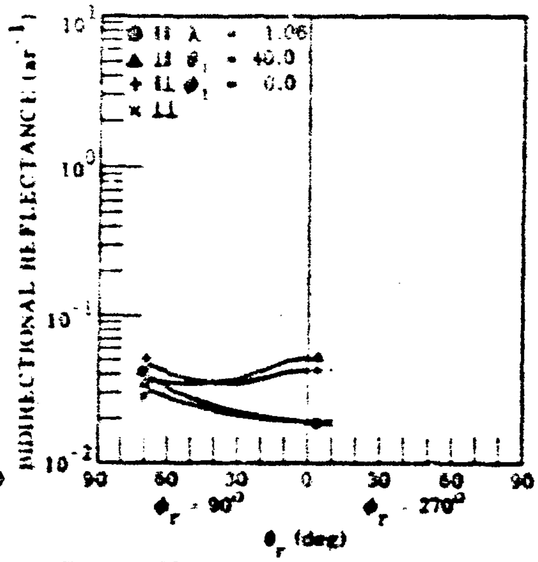

FIGURE 80. ρ' FOR MATERIAL NO. 2. $\theta_i = 40°$; $\phi_r = 90°, 270°$.

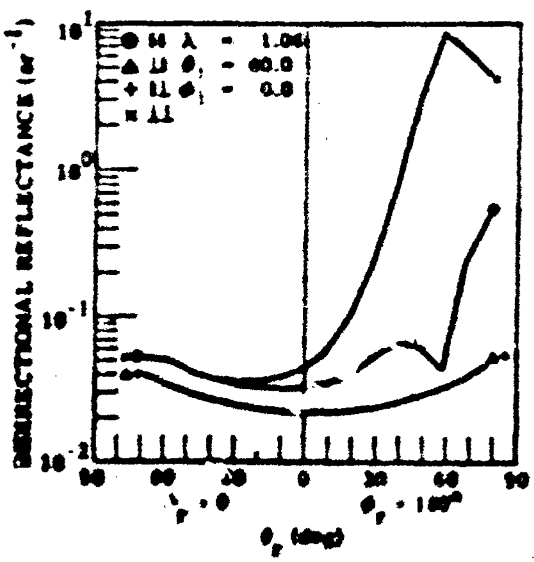

FIGURE 81. ρ' FOR MATERIAL NO. 2. $\theta_i = 60°$; $\phi_r = 0°, 180°$.

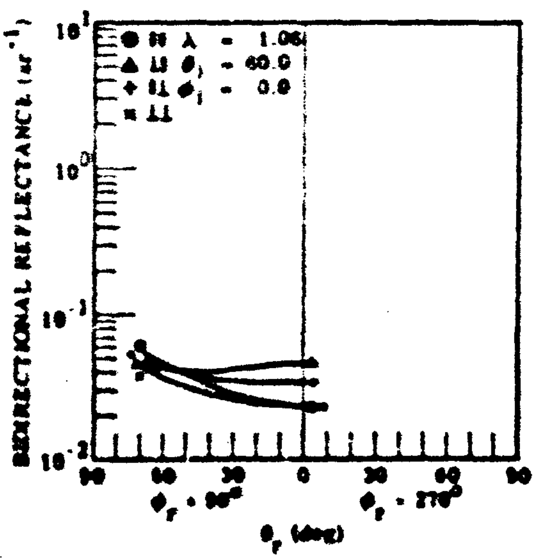

FIGURE 82. ρ' FOR MATERIAL NO. 2. $\theta_i = 60°$; $\phi_r = 90°, 270°$.

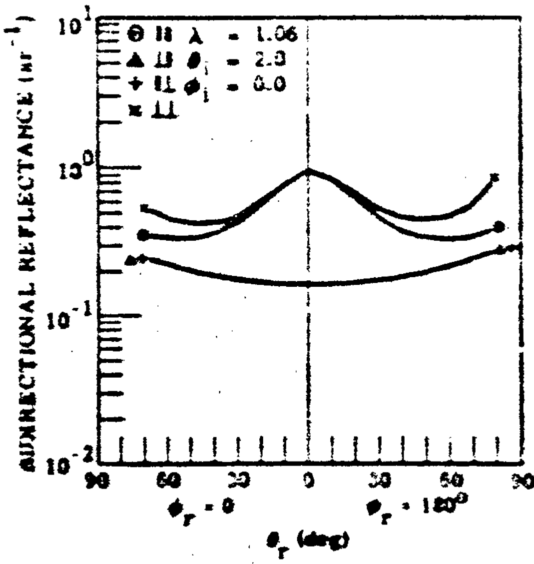

FIGURE 83. ρ' FOR MATERIAL NO. 3.
θ_i = 2°; ϕ_r = 0°, 180°.

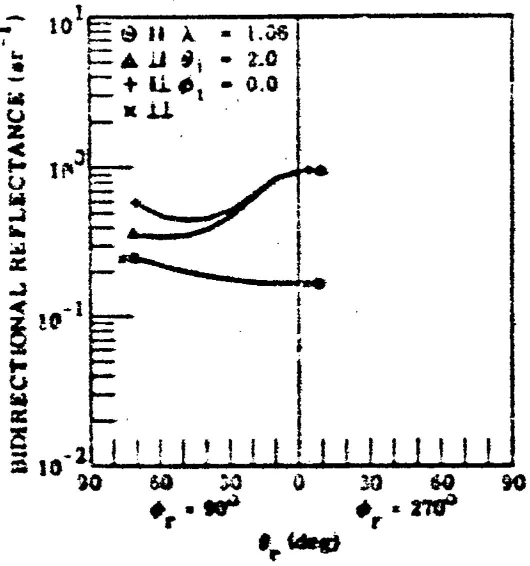

FIGURE 84. ρ' FOR MATERIAL NO. 3.
θ_i = 2°; ϕ_r = 90°, 270°.

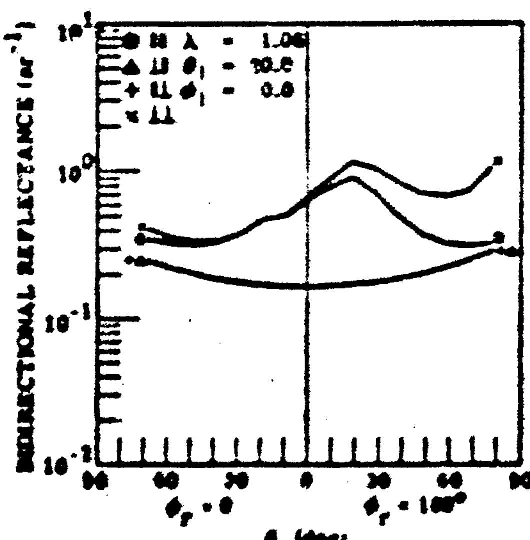

FIGURE 85. ρ' FOR MATERIAL NO. 3.
θ_i = 20°; ϕ_r = 0°, 180°.

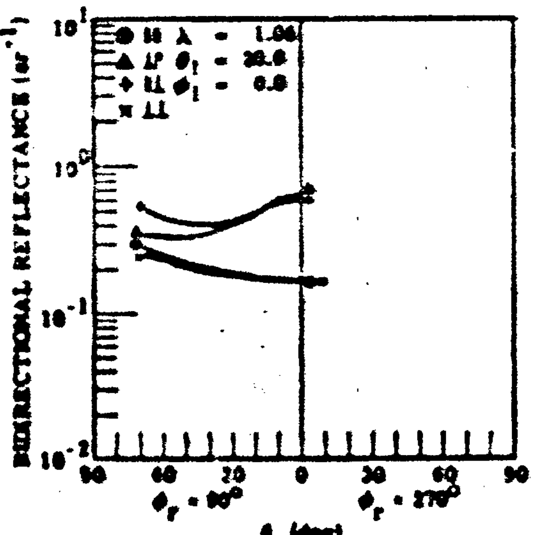

FIGURE 86. ρ' FOR MATERIAL NO. 3.
θ_i = 20°; ϕ_r = 90°, 270°.

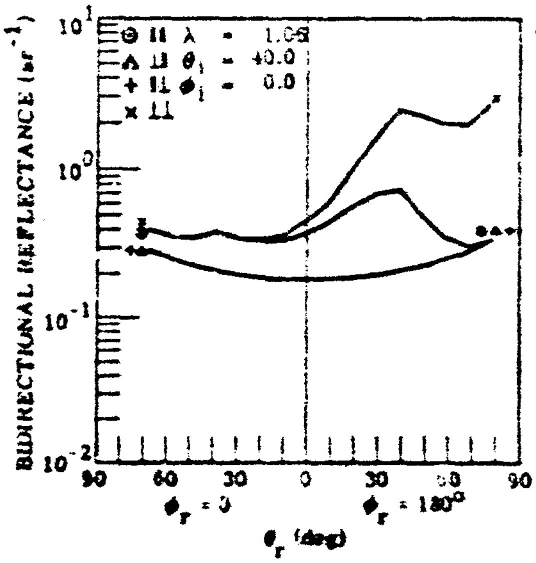

FIGURE 87. ρ' FOR MATERIAL NO. 3. $\theta_i = 40^\circ$; $\phi_r = 0^\circ, 180^\circ$.

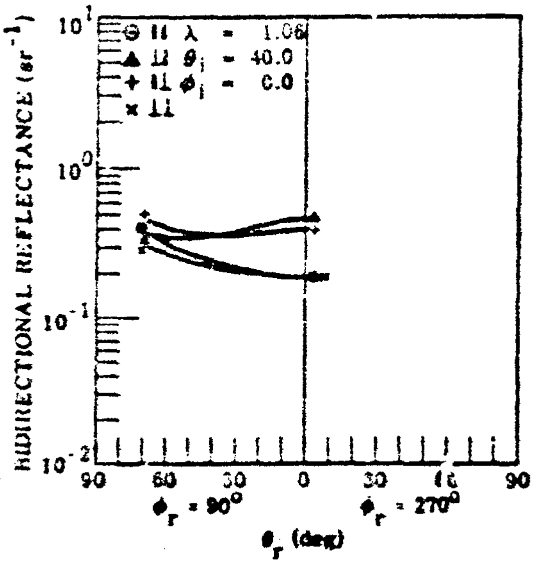

FIGURE 88. ρ' FOR MATERIAL NO. 3. $\theta_i = 40^\circ$; $\phi_r = 90^\circ, 270^\circ$.

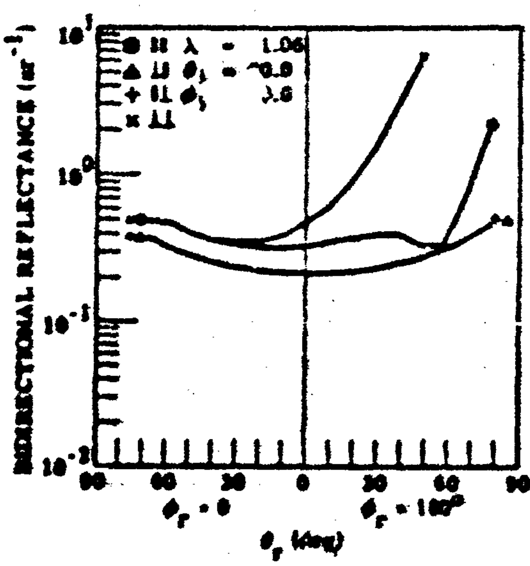

FIGURE 89. ρ' FOR MATERIAL NO. 3. $\theta_i = 60^\circ$; $\phi_r = 0^\circ, 180^\circ$.

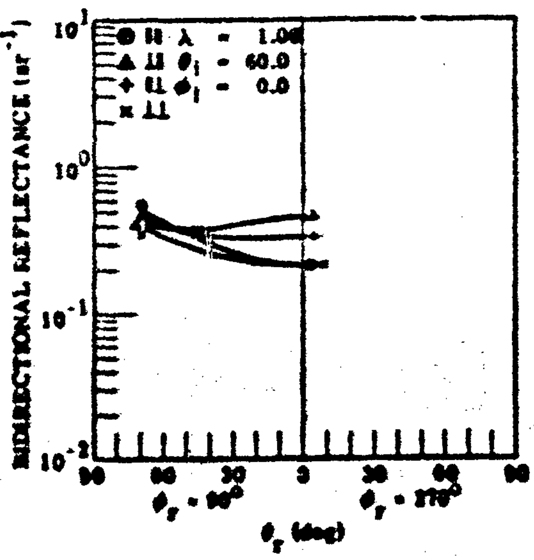

FIGURE 90. ρ' FOR MATERIAL NO. 3. $\theta_i = 60^\circ$; $\phi_r = 90^\circ, 270^\circ$.

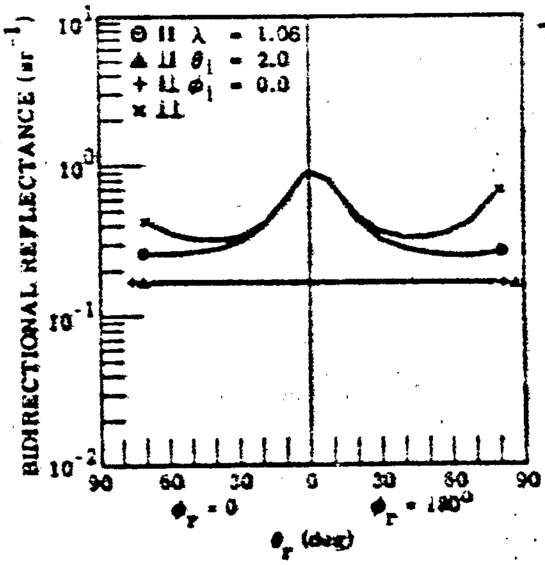

FIGURE 91. ρ' FOR MATERIAL NO. 4.
θ_i = 2°; ϕ_r = 0°, 180°.

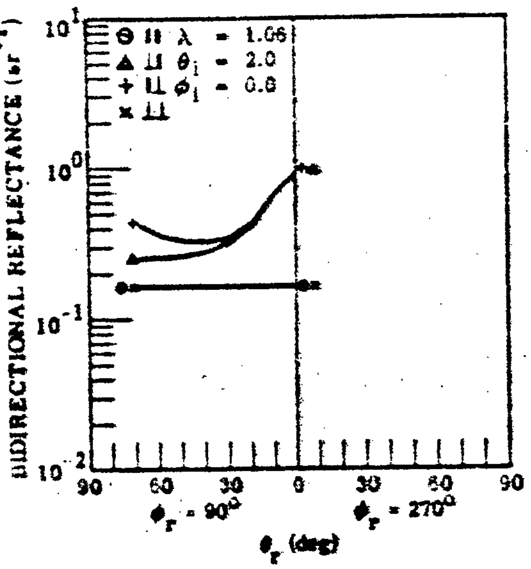

FIGURE 92. ρ' FOR MATERIAL NO. 4.
θ_i = 2°; ϕ_r = 90°, 270°.

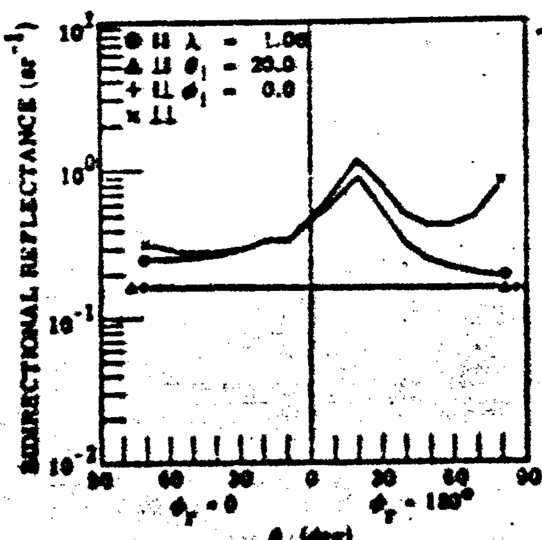

FIGURE 93. ρ' FOR MATERIAL NO. 4.
θ_i = 20°; ϕ_r = 0°, 180°.

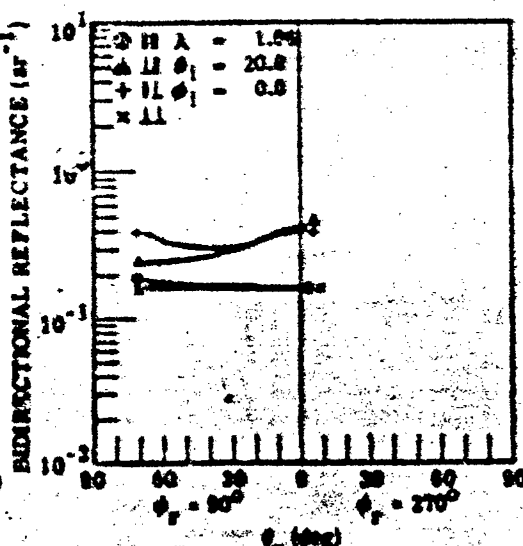

FIGURE 94. ρ' FOR MATERIAL NO. 4.
θ_i = 20°; ϕ_r = 90°, 270°.

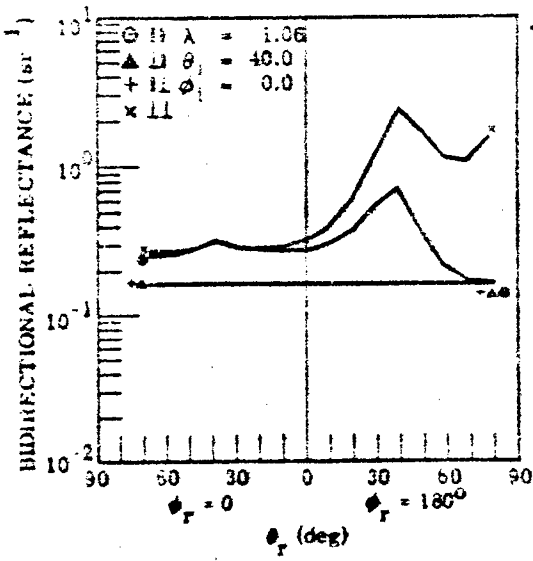

FIGURE 95. ρ' FOR MATERIAL NO. 4.
$\theta_i = 40^\circ$; $\phi_r = 0^\circ, 180^\circ$.

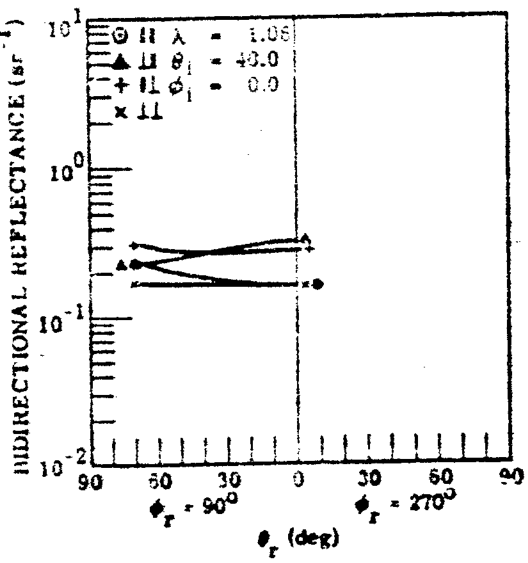

FIGURE 96. ρ' FOR MATERIAL NO. 4.
$\theta_i = 40^\circ$; $\phi_r = 90^\circ, 270^\circ$.

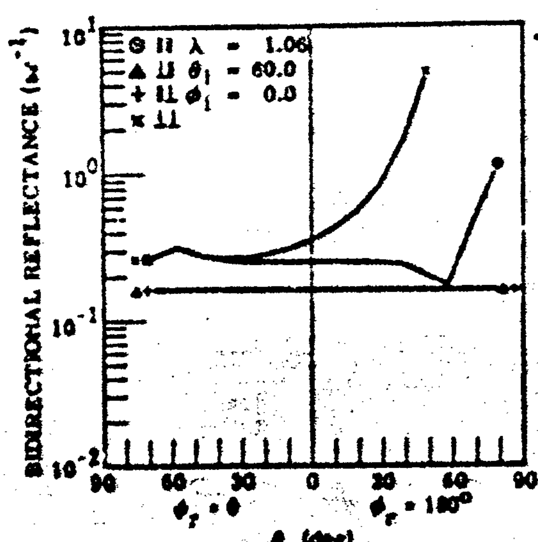

FIGURE 97. ρ' FOR MATERIAL NO. 4.
$\theta_i = 60^\circ$; $\phi_r = 0^\circ, 180^\circ$.

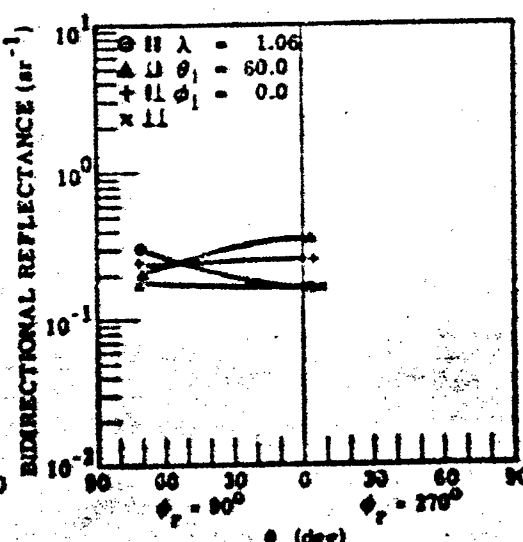

FIGURE 98. ρ' FOR MATERIAL NO. 4.
$\theta_i = 60^\circ$; $\phi_r = 90^\circ, 270^\circ$.

Appendix III
DOCUMENTATION OF BIDIRECTIONAL REFLECTANCE PROGRAM (RHOPRIME)

Program RHOPRIME is the main calling program for subroutines to read and store materials data, perform geometrical calculations, compute bidirectional reflectances for any source/receiver position and polarization, and prepare the output in a convenient format. The calling sequence, purpose, and calculations performed by each subroutine are given below, followed by details on the input data formats.

III.1. DESCRIPTIONS OF SUBROUTINES

SUBROUTINE INDATA. This is the first subroutine called. Material parameters needed for the calculation of bidirectional reflectance are read and stored. Material parameters are

MAT = material specifier

N = n = real part of refractive index

K = k = imaginary part of refractive index

RX1 = $\rho_{\chi 1}$ = diffuse reflectance for ⊥ polarized source

RX2 = $\rho_{\chi 2}$ = diffuse reflectance for ∥ polarized source

RHOV = ρ_v = volume reflectance

SIGMA, RPO } parameters available to calculate $\rho'\left(\theta_{\hat{n}}, \phi_{\hat{n}}; \theta_{\hat{n}}, \phi_{\hat{s}}\right)$ in subroutine FUNC

TAU = τ(deg)

OMEGA = Ω (deg), Q1, Q2 } parameters to calculate a shadowing and obscuration factor to be applied to ρ' (cos βNP) in subroutine FUNC

RCOSBNP = $\rho'\left(\theta_{\hat{n}}, \phi_{\hat{n}}; \theta_{\hat{n}}, \phi_{\hat{s}}\right) \cos^2 \theta_{\hat{s}}$, BNP = $\theta_{\hat{s}}$ (deg) } table of zero-degree bistatic bidirectional reflectance data

TITLE. A title card (optional) is read and used to identify on the printed output the calculations to be performed.

FACET. The source and receiver are located in an earth-fixed, right-handed XYZ coordinate system. The XYZ components of the unit normal vector of the reflecting surface are read (optional). If the facet definition card is not supplied, the facet unit normal vector defaults to (0, 0, 1).

COMPUTATION REQUEST. The specification of source and receiver positions and source polarization for computation of the bidirectional reflectance is read.

ISW = model selector

TS = zenith angle of source (deg)

PS = azimuth angle of source (deg)

TD = zenith angle of receiver (deg)

PD = azimuth angle of receiver (deg)

A = intensity of major axis of polarization ellipse

B = intensity of minor axis of polarization ellipse

PSI = angle of major axis of polarization ellipse from the normal to the plane of incidence measured CCW looking into the source, $0 \le PSI \le 180$ (deg)

P = polarization of source ($0 \le P \le 1.0$)

H = handedness of polarization ellipse (±1.0 or 0.0)

MI = material specifier

SUBROUTINE SCAN. This subroutine defines a sequence of detector positions for a specified source position and polarization.

ISW = model selector

TS = zenith angle of source (deg)

PS = azimuth angle of source (deg)

TDS = start zenith angle of receiver (deg)

TDE = end zenith angle of receiver (deg)

TSTEP = zenith angle scan increment (deg)

PDS = start azimuth angle of receiver (deg)

PDE = end azimuth angle of receiver (deg)

PSTEP = azimuth angle scan increment (deg)

A = intensity of major axis of polarization ellipse

B = intensity of minor axis of polarization ellipse

PSI = angle of major axis of polarization ellipse from the normal to the plane of incidence measured CCW looking into the source, $0 \le PSI \le 180$ (deg)

P = polarization of source ($0 \le P \le 1.0$)

H = handedness of polarization ellipse (±1.0 or 0.0)

MI = material specifier

SUBROUTINE GEOM. This subroutine does the necessary geometrical calculations of angles needed for the bidirectional reflectance calculations (see Fig. 89).

OR = (0, 0, 1) is a unit vector along the earth-fixed Z axis

PSI = the angle of the major axis of polarization ellipse from the normal vector of the OR, E plane measured CCW looking into the source, $0 \le PSI \le 180$ (deg)

$$X = \frac{D + E}{|D + E|}$$

$$Y = \frac{OR \times E}{|OR \times E|}$$

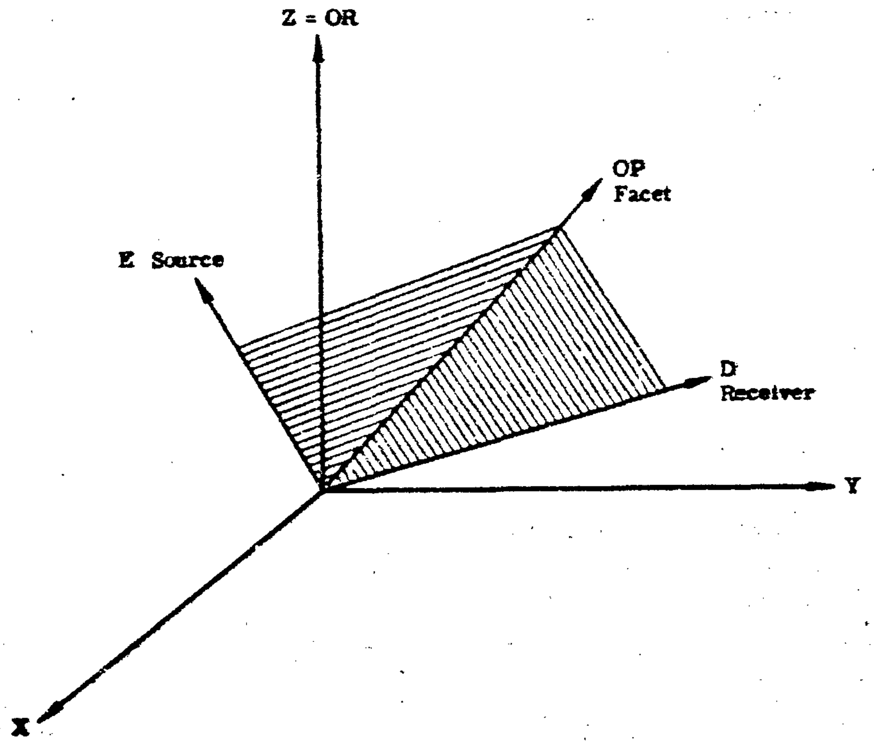

FIGURE 99. BIDIRECTIONAL REFLECTANCE GEOMETRY

$$YA = \frac{OR \times D}{|OR \times D|}$$

$$XA = \frac{E \times D}{|E \times D|}$$

$$U = \frac{D \times E}{|D \times E|}.$$

$$XAP = \frac{OP \times E}{|OP \times E|}.$$

$$YAP = \frac{OP \times D}{|OP \times D|}$$

COSB = X · D

COSBDP = OP · D

COSBEP = OP · E

COSBNP = OP · X

PSIPE = PSI - SIGN(-XAP · OR)ARCOS(XAP · Y)

= angle of major axis of polarization ellipse from the normal vector of the OP, E plane

PSIDE = PSI - SIGN(Y · D)ARCOS(U · Y)

= angle of major axis of polarization ellipse from the normal vector of the D, E plane

WADE = -SIGN(-YA · E)ARCOS(XA · YA)

= angle for transforming the output angle of polarization from E, D plane to OR, D plane

EDPHI = ARCOS(XAP · YAP) = the relative azimuth angle between E and D in the facet coordinate system

DC = (-SINBEP, 0, COSBEP) = direction of specular ray in the facet coordinate system

D1 = (SINBDP COS EDPHI, SINBDP SIN EDPHI, COSBDP) = direction of reflected ray in the facet coordinate system

NZ1 = DC × OP

NZ = NZ1 × DC

DN = D1 · NZ

$$\left.\begin{aligned} \text{PHIEN} &= 0 \text{ IF DN} > 0 \\ &= \pi/2 - \text{ARCOS}(-\text{DN}) \text{ IF DN} < 0 \end{aligned}\right\} \quad \text{parameter required in FUNCTION FUNC for shadowing and obscuration}$$

<u>SUBROUTINE GFRM.</u> GFRM does all of the bidirectional reflectance calculations. The surbroutine requires:

F = series of switches which can be set (optional) to reduce the number of redundant computations when GFRM is used as part of a multifaceted target model

COSB = defined in SUBROUTINE GEOM

COSBDP = defined in SUBROUTINE GEOM

COSBEP = defined in SUBROUTINE GEOM

COSBNP = defined in SUBROUTINE GEOM

PSIPE = defined in SUBROUTINE GEOM

PSIDE = defined in SUBROUTINE GEOM

WADE = defined in SUBROUTINE GEOM

AP = area of facet (if AP = zero, GFRM returns a bidirectional reflectance Stokes vector; if AP ≠ 0, GFRM returns a Stokes vector for the reflected radiant intensity for unity irradiance in the incident beam)

MI = material specifier (available in COMMON)

ISW = model selector (available in COMMON)

W = wavelength specifier (available in COMMON), not used

TABLE = array containing all of the materials properties data read in SUBROUTINE INDATA

GFRM returns the bidirectional reflectance Stokes vector (AP = 0) or radiant intensity Stokes vector (AP ≠ 0).

I11 = Stokes vector for surface plus Lambertian model with polarized source

I21 = Stokes vector for surface plus Lambertian model with unpolarized source

I13 = Stokes vector for non-Lambertian volume model with polarized source

I23 = Stokes vector for non-Lambertian volume model with unpolarized source

I14 = Stokes vector for combined model with polarized source

I24 = Stokes vector for combined model with unpolarized source

FUNCTION GETDAT returns the appropriate material parameters for bidirectional reflectance calculations, namely N, K, RX1, RX2, RHOV, RCOSBNP, DP0, DP90, F, G.

FUNCTION FUNC provides the optional capability for deriving RCOSBNP analytically (if SIGMA ≠ 0) and for deriving a shadowing and obscuration correction factor (optional) to the RCOSBNP used in the specular model. In addition, the depolarization factors DP0(B) and DP90(B), as well as F(B) and G(BNP) needed in the volume model, are defined analytically. FUNCTION FUNC currently yields

DP0(B) = 1.0

DP90(B) = 1.0

F(B) = 1.0

G(BNP) = 1.0

$$\text{RCOSBNP} = (\text{COSBNP})^2\,\text{RPO}\left[\text{Q1}e^{-1/2}e^{-\frac{1}{2}\left(\frac{\text{BNP}^2}{\text{SIGMA}^2}\right)} + \text{Q2 RHOV}\right]$$

for BNP < SIGMA

$$= (\text{COSBNP})^2\,\text{RPO}\left(\text{Q1}e^{-\frac{\text{BNP}}{\text{SIGMA}}} + \text{Q2 RHOV}\right)$$

for BNP > SIGMA

The shadowing and obscuration factor applied to RCOSBNP (measured values read during the input phase of RHOPRIME or defined analytically in FUNC) is

$$\frac{1 + \frac{BNP}{OMEGA} e^{\frac{-2B}{TAU}}}{1 + \frac{BNP}{OMEGA}} \cdot \frac{1}{1 + \frac{PHIEN}{OMEGA} \cdot \frac{BEP}{OMEGA}}$$

(a) <u>SURFACE-PLUS-LAMBERTIAN MODEL CALCULATION</u>

$$RO = \frac{(N+1)^2 + K^2}{(N-1)^2 + K^2} \cdot \frac{(V2 - COSB)^2 + V3}{(V2 + COSB)^2 + V3}$$

= normalized reflectance for $\perp$ polarized incidence

$$R90 = \frac{(V2COSB + COS^2 B - 1)^2 + V3COS^2 B}{(V2COSB - COS^2 B + 1)^2 + V3COS^2 B} \cdot RO$$

= normalized reflectance for $\parallel$ polarized incidence

where

$$V2 = \sqrt{\frac{\sqrt{4N^2K^2 + (N^2 - K^2 - 1 + COS^2 B)^2} + (N^2 - K^2 - 1 + COS^2 B)}{2}}$$

$$V3 = \frac{\sqrt{4N^2K^2 + (N^2 - K^2 - 1 + COS^2 B)^2} - (N^2 - K^2 - 1 + COS^2 B)}{2}$$

<u>If H = 0</u> the calculation is made for a plane polarized source (polarization angle PSI). The calculation ignores the induced elliptical polarization for $K \neq 0$.

$$PSIED = ATAN \left[\sqrt{\frac{R90}{R0}} \cdot TAN\ PSIDE \cdot SIGN\ (COSATAN(N) - COSB) \right]$$

= polarization angle with respect to D, E reference plane, after reflection

C = 1 if AP = 0, then a bidirectional reflectance Stokes vector is computed

C = AP · COSBEP · COSBDP if AP ≠ 0, then a reflected radiant intensity Stokes vector is computed

$$I11(1) = C \left[\frac{RCOSBNP}{COSBEP\ COSBDP} (R0 \cdot COS^2 PSIDE + R90 \cdot SIN^2 PSIDE + (RX1 \cdot COS^2 PSIPE + RX2 \cdot SIN^2 PSIPE) \right]$$

$$I11(2) = C \left[\frac{RCOSBNP}{COSBEP\ COSBDP} (R0 \cdot COS^2 PSIDE + R90 \cdot SIN^2 PSIDE) COS2\ (PSIED-WADE) \right]$$

$$I11(3) = C \left[\frac{RCOSBNP}{COSBEP\ COSBDP} (R0 \cdot COS^2 PSIDE + R90 \cdot SIN^2 PSIDE) SIN2\ (PSIED-WADE) \right]$$

$$I21(1) = C\left[\frac{RCOSBNP}{COSBEP\ COSBDP}\frac{1}{2}(R0 + R90) - \frac{1}{2}(RX1 + RX2)\right]$$

$$I21(2) = C\left[\frac{RCOSBNP}{COSBEP\ COSBDP}\frac{1}{2}(R0 - R90)\ COS2\ (-WADE)\right]$$

$$I21(3) = C\left[\frac{RCOSBNP}{COSBEP\ COSBDP}\frac{1}{2}(R0 - R90)\ SIN2\ (-WADE)\right]$$

If $H = \pm 1$ the calculation includes the phase difference and ellipticity induced by reflection for $K \neq 0$ and is an exact treatment of the Fresnel equations.

SUBROUTINE ELIPS1 (AA, AB, PSIDE, H; AA1, AA2, D) defines the following input elliptical polarization parameters: the amplitudes perpendicular (AA1) and parallel (AA2) to the D, E plane and the relative phase $D = \phi_\parallel - \phi_\perp$ of the amplitudes of the major (AA) and minor (AB) axes of polarization ellipse; the orientation of the ellipse with respect to the D, E plane; PSIDE; and the handedness, H.

$DR = \phi_\parallel - \phi_\perp$ induced by reflection

FOR $K = 0$, $DR = 0$ if $COSB < COS\ ARTAN(N)$

$= -\pi$ if $COSB > COS\ ARTAN(N)$

$$\text{FOR } K \neq 0,\ DR = -\pi + ATAN\left(-\frac{2\sqrt{V3}(1 - COS^2B)COSB}{(1 - COS^2B)^2 - COS^2B(V2^2 + V3)}\right)$$

if ( ) < 0

$$DR = -\ ATAN\left(-\frac{2\sqrt{V3}(1 - COS^2B)COSB}{(1 - COS^2B)^2 - COS^2B(V2^2 + V3)}\right)$$

if ( ) > 0

The intensities A1R and A2R and the relative phase of the parallel and perpendicular components of the reflected radiance induced by the reflections, are

$A1R = A1 \cdot R0$

$A2R = A2 \cdot R0$

$DR = DR + D$

SUBROUTINE ELIPS2 (AA1, AA2, DR, AAR, ABR, PSIED, HR) defines the elliptically polarized reflected radiance as amplitudes AAR and ABR of the major and minor axes, the angle of the ellipse relative to the D, E plane, PSIED, and the handedness, HR. PSIDR = PSIED-WADE is the angle that the polarization ellipse of the reflected radiance makes with the normal vector to the OR, D plane.

CHI = HR · ATAN(ABR/AAR) is the parameter used to define the ellipticity of the reflected radiance.

C = 1 if AP = 0

$C = AP \cdot COSBEP \cdot COSBDP$ if $AP \neq 0$

$$I11(1) = C\left[\frac{AR + BR}{A + B}\ \frac{RCOSBNP}{COSBEP\ COSBDP} + (RX1\ COS^2(PSIPE) + RX2\ SIN^2(PSIPE))\right]$$

$$I11(2) = C\left[\frac{AR + BR}{A + B}\ \frac{RCOSBNP}{COSBEP\ COSBDP}\ COS(2PSIDE)COS(2CHI)\right]$$

$$I11(3) = C\left[\frac{AR - BR}{A + B}\ \frac{RCOSBNP}{COSBEP\ COSBDP}\ SIN(2PSIDE)COS(2CHI)\right]$$

$$I11(4) = C\left[\frac{AR + BR}{A + B}\ \frac{RCOSBNP}{COSBEP\ COSBDP}\ SIN(2CHI)\right]$$

$$I21(1) = C\left[\frac{RCOSBNP}{COSBEP\ COSBDP}\ \frac{1}{2}(R0 + R90) + \frac{1}{2}(RX1 + RX2)\right]$$

$$I21(2) = C\left[\frac{RCOSBNP}{COSBEP\ COSBDP}\ \frac{1}{2}(R0 - R90)\ COS(-2WADE)\right]$$

$$I21(3) = C\left[\frac{RCOSBNP}{COSBEP\ COSBDP}\ \frac{1}{2}(R0 - R90)\ SIN(-2WADE)\right]$$

$$I21(4) = 0$$

(b) VOLUME MODEL CALCULATION

The angular-dependent, volume reflectance model, Stokes vector is given by

$$I13(1) = C\frac{1}{DP90(1+DP0)}\ \frac{2RHOV \cdot F \cdot G}{COSBEP+COSBDP}[COS^2\ PSIDE \cdot DP90(1+DP0) + SIN^2 PSIDE \cdot DP90(1+DP90)]$$

$$I13(2) = C\ \frac{1}{DP90(1+DP0)}\ \frac{2RHOV \cdot F \cdot G}{COSBEP+COSBDP}[COS^2\ PSIDE \cdot DP90(1-DP0) + SIN^2 PSIDE \cdot DP0(1-DP90)]\ COS^2\ 2AD$$

$$I13(3) = C\ \frac{1}{DP90(1+DP0)}\ \frac{2RHOV \cdot F \cdot G}{COSBEP+COSBDP}[COS^2\ PSIDE \cdot DP90(1-DP90) + SIN^2 PSIDE \cdot DP0(1-DP90)]\ SIN^2\ 2AD$$

$$I23(1) = C\ \frac{1}{DP90(1+DP0)}\ \frac{2RHOV \cdot F \cdot G}{COSBEP+COSBDP}\ \frac{1}{2}[DP90(1+DP0) + DP0(1+DP90)]$$

$$I23(2) = C\ \frac{1}{DP90(1+DP0)}\ \frac{2RHOV \cdot F \cdot G}{COSBEP+COSBDP}\ \frac{1}{2}[DP90 - DP0]\ COS(-2WADE)$$

$$I23(3) = C\ \frac{1}{DP90(1+DP0)}\ \frac{2RHOV \cdot F \cdot G}{COSBEP+COSBDP}\ \frac{1}{2}[DP90 - DP0]\ SIN(-2WADE)$$

where

$C = 1$ for $AP = 0$

$C = AP \cdot COSBEP \cdot COSBDP$ for $AP \neq 0$

The angle of polarization of the reflected radiance, AED, from the normal vector of the D, E plane is

$$\text{AED} = \text{ATAN}\left[\sqrt{\frac{\text{DP0}(1 - \text{DP90})}{\text{DP90}(1 - \text{DP0})}}\ \text{TAN(PSIDE)} \cdot \text{SIGN(COS ATAN(N) - COSB)}\right]$$

and the angle of polarization referred to the OR, D plane is

$$\text{AD} = \text{AED} - \text{WADE}$$

SUBROUTINE OUTPUT. This subroutine prints the Stokes vectors for the bidirectional reflectance (AP = 0) or reflected radiant intensity for unit incident irradiance (AP $\neq$ 0) for the surface model, the volume models, and for the combined specular and volume model. Stokes vectors are printed for a completely polarized source, for a completely unpolarized beam, and also for a partially polarized beam (polarization defined by the input parameter P).

In addition, several calculations are made with the Stokes vectors. For a bidirectional reflectance (or radiant intensity) Stokes vector, the bidirectional reflectance (or radiant intensity) for a receiver polarized $\perp$ or $\parallel$ to the OR, D plane is

$$\text{receiver}_{\perp} = \frac{A + B}{2}$$

$$\text{receiver}_{\parallel} = \frac{A - B}{2}$$

where the Stokes vector is of the form: $\begin{bmatrix} A \\ B \\ C \\ D \end{bmatrix}$

The angle of the major axis of the reflected radiance and the percent polarization of the reflected radiance are also given; they are

$$\text{AL} = \pm\frac{1}{2}\ \text{ATAN}\left|\frac{C}{B}\right| \quad -90 \le \text{AL} \le 90$$ (looking into the source, AL > 0 is a CCW angle; AL < 0 is a CW angle)

$$\%P = \frac{\sqrt{B^2 + C^2 + D^2}}{A} \times 100\%$$

The output includes TS, PS, TD, PD, P, as well as the input and output values of A, B, PSI, H from the surface model calculation (if the input H = 0, the input and output values of A, B, H default to 1, 0, and 0).

SUBROUTINE ELIPS1 (A, B, PSI, H; A1, A2, DELTA). The basic equations which relate two specifications of an elliptically polarized beam (A, B, PSI, H) and (A1, B1, DELTA) are

$$\tan\alpha = A1/A2 \quad 0 \le \alpha \le \pi/2$$

$$\tan\chi = \pm B/A \text{ for } {rt \atop lt} \quad -\pi/4 \le \chi \le \pi/4$$

$$\tan 2\psi = \tan 2\alpha \cos \delta$$

$$\sin 2\chi = \sin 2\alpha \sin \delta$$

from which we obtain

$$\sin^2 2\alpha = \frac{\sin^2 2\chi + \tan^2 2\psi}{1 + \tan^2 2\psi}$$

or equivalently

$$\cos 2\alpha = \cos 2\chi \cos 2\psi$$

Subroutine ELIPS1 determines A1, A2, DELTA from A, B, PSI, H

LAMBDA = $\sqrt{A^2 + B^2}$

If B = 0, A1 = LAMBDA COS PSI
A2 = LAMBDA SIN PSI
DELTA = 0 when 0 ≤ PSI ≤ π/2
DELTA = π when π/2 ≤ PSI ≤ π

Otherwise:

CHI = H · ATAN(B/A)
TI = |COS 2CHI COS 2PSI|
ALPHA = 1/2 ARCOS(-TI) if π/4 ≤ PSI ≤ 3π/4
= 1/2 ARCOS(TI) if PSI < π/4 or > 3π/4
If ALPHA = 0, A1 = LAMBDA, A2 = 0, DELTA = 0
If ALPHA = π/4, A1 = A2 = LAMBDA/√2, DELTA = 2CHI if PSI = π/4,
= H·π - 2 CHI if PSI = 3π/4,

If ALPHA = π/2, A1 = 0, A2 = LAMBDA, DELTA = 0

Otherwise

TI = |SIN 2CHI/SIN2ALPHA|
MU = ARSIN TI
A1 = LAMBDA COS ALPHA
A2 = LAMBDA SIN ALPHA
COSD = TAN 2PSI/TAN 2ALPHA
If COSD > 0 DELTA = H·MU
If COSD < 0 DELTA = H·(π - MU)

SUBROUTINE ELIPS2 (A1, A2, DELTA; A, B, PSI, H). **Subroutine ELIPS2 determines A, B, PSI, H from A1, A2, DELTA.**

$$\text{LAMBDA} = \sqrt{A1^2 + A2^2}$$

If A1 = 0 or A2 = 0, then A = LAMBDA, B = 0, H = 1, and

PSI = 0 if A2 = 0

PSI = $\pi/2$ if A1 = 0

If A1 = A2, then CHI = 1/2|DELTA|, A = LAMBDA COS CHI, B = LAMBDA SIN CHI, and

H = 1 if DELTA > 0

= -1 if DELTA < 0

PSI = $\pi/4$ if CHI < $\pi/4$

= $3\pi/4$ if CHI > $\pi/4$

If DELTA = $\pm\pi$, A = LAMBDA, B = 0, H = 1, PSI = π - ATAN $\frac{A2}{A1}$

If DELTA = 0, A = LAMBDA, B = 0, H = 1, PSI = ATAN $\frac{A2}{A1}$

If DELTA = $\pm\pi/2$, H = +1 if DELTA > 0

-1 if DELTA < 0

If A1 > A2, A = A1, B = A2, PSI = 0

If A1 < A2, A = A2, B = A1, PSI = $\pi/2$

Otherwise

If A1 > A2, ALPHA = ATAN A2/A1

CHI = 1/2 ARSIN|SIN2ALPHA SINDELTA|

LAMBDA = |TAN2ALPHA COSDELTA|

A = LAMBDA COS CHI

B = LAMBDA SIN CHI

H = ± if DELTA $\gtrless$ 0

Part 1: 0 < |DELTA| < $\pi/2$; PSI = 1/2 ATANLAMDA

Part 2: $\pi/2$ < |DELTA| < π; PSI = π - 1/2 ATANLAMDA

and

If A1 < A2, 0 < |DELTA| < $\pi/2$ PSI = $\pi/2$ - 1/2 ATANLAMDA

$\pi/2$ < |DELTA| < π PSI = $\pi/2$ + 1/2 ATANLAMDA

III.2. INPUT DATA FORMATS

The input to the RHOPRIME program is segmented into logical blocks. Each block is initiated by a block header and terminated by an end card. Blocks may be in any order, but a data block is assumed to precede any computation request blocks or scan request blocks. If a block header specifies an invalid block types, all input up to and including the next end card is ignored.

DATA TABLES BLOCK. The data tables block specifies all physical characteristics of the materials to be studied. The block header is one card with the following format:

Columns	Description
1-4	'TABL'
5-19	ignored
20-25	maximum material index to be expected
26-80	ignored

The data tables block is itself segmented into material blocks each characterizing one material to be studied. Each material block is initiated by a material header and terminated by an end card. The material header is two cards with the following format:

Card 1

Columns	Description
1-4	'MATR'
5-8	ignored
9-10	material index
11-20	n
21-30	k
31-40	$\rho_{\chi 1}$
41-50	$\rho_{\chi 2}$
51-60	ρ_v
61-70	SIGMA [if SIGMA $\neq$ 0, RCOSBNP is computed]
71-80	RP0

Card 2

Columns	Description
1-10	ignored
11-20	τ
21-30	Ω
31-40	Q1
41-50	Q2
51-80	blank

Following a material header, there may be a set of ρ' data. If present, the ρ' is a function of $\theta_{\hat{n}}$ and the $\theta_{\hat{n}}$'s must be in ascending order. The format is

Columns	Description
1-4	blank or 'ANGL'
5-10	ignored
11-20	$\theta_{\hat{n}}$ (deg)
21-30	$\rho'\left(\theta_{\hat{n}},\phi_{\hat{n}};\ \theta_{\hat{n}},\phi_{\hat{n}}\right)\cos^2\theta_{\hat{n}}$
31-80	ignored

WARNING: Each material block must be terminated by an end card. The entire data tables block must also be terminated by an end card.

COMPUTATION REQUEST BLOCK. The computation requests block contains all information needed to perform desired computations. The block header is one card with the following format:

Columns	Description
1-4	'COMP'
5-19	ignored
20-25	model selector
26-80	ignored

The model selector, ISW, is:

1—if specular and diffuse models are desired

3—if volume model is desired

7—if combined model is desired

Following the block header, computation requests are processed sequentially until an end card is encountered. The format of a computation request is:

Columns	Description
1-4	blank
5-9	ignored
10-16	source zenith (deg)
17	ignored
18-24	source azimuth (deg)
25	ignored
26-32	detector zenith (deg)
33	ignored
34-40	detector azimuth (deg)
41	ignored
42-48	polarization major axis length
49	ignored
50-56	polarization minor axis length
57	ignored
58-64	angle of source polarization (deg)
65	ignored
66-72	source percent polarization ÷ 100
73	ignored
74-76	handedness of polarization (if ≠ 0, elliptical polarization is assumed)
77	ignored
78-80	material index

SCAN REQUEST BLOCK. If a scan of the detector zenith and/or azimuth is desired, a scan request block may be used. The block header is one card with the following format:

Columns	Description
1-4	'SCAN'
5-19	ignored
20-25	model selector
26-80	ignored

One card follows the block header giving all required parameters. The format of this card is:

Columns	Description
1-6	source zenith (deg)
7-12	source azimuth (deg)
13-18	initial detector zenith (deg)
19-24	final detector zenith (deg)
25-30	zenith increment (deg)
31-36	initial detector azimuth (deg)
37-42	final detector azimuth (deg)
43-48	azimuth increment (deg)
49-54	polarization major axis length
55-60	polarization minor axis length
61-66	angle of source polarization (deg)
67-72	source percent polarization + 100
73-76	handedness of polarization
77-80	material index

TITLE SPECIFICATION BLOCK. A title may be printed at the top of each page of long form output using the title specification block. The block header is one card in the following format:

Columns	Description
1-4	'TITL'
5-19	ignored
20-25	blank
26-80	ignored

One card following the block header specifies the title. The format of this card is:

Columns	Description
1-60	title
61-80	ignored

FACET DEFINITION BLOCK. If default facet definition is not desired, the facet may be redefined using the facet definition block. The block header is one card in the following format:

Columns	Description
1-4	'FACE'
5-19	ignored
20-25	blank
26-80	ignored

One card following the block header defines the facet. The format of this card is:

Columns	Description
1-4	blank
5-9	ignored
10-16	facet area (default = 0)
17	ignored
18-24	facet normal - x (default = 0)
25	ignored
26-32	facet normal - y (default = 0)
33	ignored
34-40	facet normal - z (default = 1)
41-80	blank

END BLOCK. The end block terminates the program. The format of the block header is the same as that of the end card.

Columns	Description
1-4	'END'
5-80	blank

This block does not need an end card.

Appendix IV
INSTRUCTIONS FOR USE OF PROGRAM WITH SAMPLE COMPUTER OUTPUT

The program documentation in Appendix III, together with the sample computations included in this appendix should enable the user to (1) modify this program to accommodate the requirements of his own computer and (2) verify output from his modified program by comparison with the samples given herein.

Note that the input parameter values shown in Table III are the ones with which the program has been run.

Sample outputs presented in this appendix include

(1) a listing of the input information (Table III)

(2) the computed output of the program (long form) (Table IV)

(3) a short form of the computed output, containing only that information necessary to feed into a computer program for the purpose of obtaining plots of the data (Table V)

The three tables mentioned above appear at the end of this appendix. All of the sample information is keyed and labelled so that elements may be identified easily. However, the further descriptive detail below may be helpful in studying the samples given.

RHOPRIME Input Listing

The following items appear across the top of Table III. On line 2:

n = real part of index of refraction

k = imaginary part of index of refraction

$\left.\begin{array}{l}\rho_{\chi 1} = \text{cross component } (2\rho_{\parallel\perp}) \\ \rho_{\chi 2} = \text{cross component } (2\rho_{\perp\parallel})\end{array}\right\}$ used for surface model

ρ_V = volume component used for volume model

SIGMA = generating function parameter

RPO = generating function parameter

And on line 3:

τ = shadowing and obscuration parameter

Ω = shadowing and obscuration parameter

Q1 = generating function parameter

Q2 = generating function parameter

Following these items in Table III is the $\rho'\left(\theta_{\hat{n}}, \phi_{\hat{n}}; \theta_{\hat{n}}, \phi_{\hat{n}}\right)\cos^2\theta_{\hat{c}}$ tabulation which, in this case, was extracted from measured data and determined from the zero bistatic scan. Alternatively, such a tabulation can be generated by use of a generating function specified in the SUBROUTINE FUNC.

Note in the sample input information of Table III that values are provided for $\rho_{\chi 1}$, and $\rho_{\chi 2}$ and also for ρ_V. In practice, $\rho_{\chi 1}$, and $\rho_{\chi 2}$ will be used or ρ_V will be used; all three values will never be nonzero simultaneously.

If the table is supplied as part of the input, the parameters SIGMA and RPO are set to 0 and Q1 = Q2 = 1.

The $\rho'\left(\theta_{\hat{n}}, \phi_{\hat{n}}; \theta_{\hat{n}}, \phi_{\hat{n}}\right)\cos^2 \theta_{\hat{n}}$ tabulation is followed by scan request information telling the computer what source-receiver combinations are to be computed and what model is to be selected:

θ_i = θ for source
ϕ_i = ϕ for source
θ_{r1} = initial θ for receiver
θ_{r2} = maximum θ for receiver
θ_{r3} = size of angular step for θ_r scan
ϕ_{r1} = ϕ for receiver
ϕ_{r2} = ϕ for receiver (value for second scan)
ϕ_{r3} = size of angular step for ϕ_r
A = semi-major axis of polarization ellipse (normalized to 1.0)
B = semi-minor axis of polarization ellipse (B = 0 implies linear polarization)
PSI = angle of source polarization
P = percent polarization (1.0 = 100%)
MI = material index
ISW = 7 for combined model. (When volume model is used, set $\rho_{\chi 1} = \rho_{\chi 2} = 0$.)

Note that in addition to these input parameters, others must be added in the SUBROUTINE FUNC:

DP0, DP90 = depolarizations for perpendicular and parallel components of incident beam
f, g = volume model parameters.

For the materials in the sample listing, values for DP0, DP90, f, and g have been set equal to 1.0.

Computer Output (Long Form)

As exemplified by Table IV, each page of the computed output corresponds to one source-receiver configuration. Items at the upper left are self-explanatory. However it should be borne in mind that MAJOR refers to the semi-major elliptical axis (a), which is taken to be 1.0. Since MINOR, which refers to the semi-minor axis (b), is 0, the MAJOR-MINOR combination implies linear polarization with polarization angle PSI for the incident beam. HANDED = 0 whenever the polarization is linear only.

The entries in the three main columns are reflectances. From the top, the first four entries in each column are the surface model elements of the Stokes vector which describes the polarization state of the beam as it leaves the target:

A = total reflectance

B = reflectance with receiver polarization angle = 0 (perpendicular polarization)

C = reflectance with receiver polarization angle = 45°

D = reflectance with receiver circularly polarized

The second four entries, still in the surface model block, are

$\frac{A+B}{2}$ = reflectance recorded from receiver with analyzer set for perpendicular polarization

$\frac{A-B}{2}$ = reflectance recorded from receiver with analyzer set for parallel polarization

AL = angle of polarization for reflected beam

P = percent polarization of reflected beam

Thus far the first two blocks of four entries have been discussed. The foregoing, as previously stated, apply to the surface plus Lambertian volume model.

The third and fourth blocks apply to the non-Lambertian volume model and are to be interpreted in exactly the same manner as above.

The fifth and sixth blocks consist of the sum of the surface + volume models and are printed out for convenience.

Note that in the volume model output and in the summed output, item D (circularly-polarized component) is not present.

Computer Output (Short Form)

The short form of the computer output consists of the information in the last four entries of the summed output (surface + volume), $\frac{A+B}{2}$, $\frac{A-B}{2}$, AL, P (see Table V). Moreover, the data are compressed so that, whereas the long form has only one source-receiver configuration per page, the short form contains a complete scan in one block.

One scan consists of four item numbers. Preceding each of the first two item numbers in each scan are

Wavelength (1.06 μm)

θ_i (0°)

ϕ_i (180°)

ϕ_r (0° or 180°)

The first item number in each scan contains $\frac{A+B}{2}$. Each output entry is preceded by the θ_r scan angle—i.e., 0.0, 0.0288 means that the reflectance at $\theta_r = 0$ is 0.0288. The second item number contains $\frac{A-B}{2}$. The third item number contains the polarization angle, AL, at each receiver angle. The fourth item number contains the percent polarization.

The scans are in the same overall order as those in the long form of the output

TABLE III. RHOPRIME INPUT LISTING

```
SC -T TO APUNCHO
T80,37 0200
SL -DATA
      TABLES
      MATP      2      1.05     6     0.5     0.0     0.0     0.08     0.0     0.0
                       15.0          40.0     1.0     1.0
                1.15      .02497
                3.15      .02520
                5.15      .02368
                7.15      .01975
                9.15      .02135
               11.15      .02177
               13.15      .02335
               15.15      .02353
               17.15      .02300
               19.15      .02243
               21.15      .02338
               23.15      .02022
               25.15      .02656
               27.15      .01726
               29.15      .01805
               31.15      .01966
               33.15      .01875
               35.15      .02605
               37.15      .01882
               39.15      .01709
               41.15      .01785
               43.15      .01604
               45.15      .01545
               47.15      .01295
               49.15      .01319
               51.15      .01434
               53.15      .01188
               55.15      .01385
               57.15      .01190
               59.15      .00922
               61.15      .01149
               63.15      .00869
               65.15      .00954
               67.15      .00808
               69.15      .01349
      END
      END
      TITLE
      A02109001
      END
      SCAN
      0.0  180.0  0.0   85.0  170.0  0.0   185.0  180.0  1.0  0.0  5.0  1.0     2
      END
      SCAN
```

Labels on the MATP lines: T, n, 6, k, ρ_{x1}, ρ_{x2}, ρ_V, SIGMA, RPO; Ω, Q1, Q2

Labels on the first SCAN line: θ_i, ϕ_i, θ_{r1}, θ_{r2}, θ_{r3}, ϕ_{r1}, ϕ_{r2}, ϕ_{r3}, A, B, PSI, P, MI

Label below the SCAN values: 7 NW

Scan Angle Where $(\theta_i, \phi_i) = (\theta_r, \phi_r)$

Reflectances for Zero Bistatic Scan:

$$\rho'\left(\theta_{\hat{n}},\phi_{\hat{n}};\theta_{\hat{n}},\phi_{\hat{n}}\right)\cos^2\theta_{\hat{n}}$$

$$= \left[\rho'_{\perp\perp}\left(\theta_{\hat{n}},\phi_{\hat{n}};\theta_{\hat{n}},\phi_{\hat{n}}\right) - \rho'_{\perp\parallel}\left(\theta_{\hat{n}},\phi_{\hat{n}};\theta_{\hat{n}},\phi_{\hat{n}}\right)\right]\cos^2\theta_{\hat{n}}$$

TABLE IV. LONG FORM OUTPUT

REFLECTANCE TTTT A02100901

	THETA	PHI
SOURCE	40.00	180.00
DETECTOR	40.00	180.00
PERCENT POLAR.		1.00

	IN	OUT
MAJOR	1.00	0.0
MINOR	0.0	0.0
PSI	5.00	0.0
HANDED	0.	0.

Model	POLARIZED		UNPOLARIZED	PARTIAL POLARIZED
Surface Plus Lambertian Volume Model	0.29667E-01	A	0.29667E-01	0.29667E-01
	0.29216E-01	B	0.0	0.29216E-01
	-0.51516E-02	C	0.0	-0.51516E-02
	0.0	D	0.0	0.0
	0.29441E-01	$\left(\frac{A+B}{2}\right)$	0.14833E-01	0.29441E-01
	0.22535E-03	$\left(\frac{A-B}{2}\right)$	0.14833E-01	0.22535E-03
	-0.50001E 01	AL	0.99999E 09	-0.50001E 01
	0.10000E 03	P	0.0	0.10000E 03
Non-Lambertian Volume Model	0.10443E 00	A	0.10443E 00	0.10443E 00
	0.0	B	0.0	0.0
	0.0	C	0.0	0.0
	0.52216E-01	$\left(\frac{A+B}{2}\right)$	0.52216E-01	0.52216E-01
	0.52216E-01	$\left(\frac{A-B}{2}\right)$	0.52216E-01	0.52216E-01
	0.99999E 09	AL	0.99999E 09	0.99999E 09
	0.0	P	0.0	0.0
Surface Plus Volume Models	0.13410E 00	A	0.13410E 00	0.13410E 00
	0.29216E-01	B	0.0	0.29216E-01
	-0.51516E-02	C	0.0	-0.51516E-02
	0.81658E-01	$\left(\frac{A+B}{2}\right)$	0.67050E-01	0.81658E-01
	0.52442E-01	$\left(\frac{A-B}{2}\right)$	0.67050E-01	0.52442E-01
	-0.50001E 01	AL	0.99999E 09	-0.50001E 01
	0.22123E 02	P	0.0	0.22123E 02

TABLE V. SHORT FORM OUTPUT

SL -T			Item No.		λ	θ_i	ϕ_i		ϕ_r
1		A021009015001	$\left(\frac{A+B}{2}\right)$ 010						
2	First Set of 4-Item Numbers	9001	1	9	1.06	0.0	180.00		0.0
3			$\left(\frac{A-B}{2}\right)$	0.0 0.0647 10.000.0620	20.000.0601	30.000.0642		40.000.0661	
4				50.000.0733 60.000.0837	70.000.1101	80.000.1580			
5		9001	2	9	1.06	0.0	180.00		0.0
6				0.0 0.0402 10.000.0405	20.000.0414	30.000.0430		40.000.0454	
7				50.000.0485 60.000.0534	70.000.0597	80.000.0683			
8		9001	3(AL)	9					
9				0.0 -5.0 10.00 -5.0	20.00 -4.8	30.00	-4.6	40.00	-4.3
10				50.00 -3.9 60.00 -3.5	70.00 -2.9	80.00	-2.4		
11		9001	4(P)	9					
12				0.0 23.76 10.00 21.33	20.00 18.72	30.00	20.00	40.00	20.23
13				50.00 20.23 60.00 22.22	70.00 29.79	80.00	39.78		
14	Second Set of 4-Item Numbers	9001	5	9	1.06	0.0	180.00		180.0
15				0.0 0.0647 10.000.0620	20.000.0601	30.000.0642		40.000.0681	
16				50.000.0733 60.000.0837	70.000.1101	80.000.1550			
17		9001	6	9	1.06	0.0	180.00		180.0
18				0.0 0.0402 10.000.0405	20.000.0414	30.000.0430		40.000.0454	
19				50.000.0488 60.000.0534	70.000.0597	80.000.0683			
20		9001	7	9					
21				0.0 -5.0 10.00 -5.0	20.00 -4.8	30.00	-4.6	40.00	-4.3
22				50.00 -3.9 60.00 -3.5	70.00 -2.9	80.00	-2.4		
23		9001	8	9					
24				0.0 23.76 10.00 21.33	20.00 18.72	30.00	20.00	40.00	20.23
25				50.00 20.23 60.00 22.22	70.00 29.79	80.00	39.78		
26		9001	9	9	1.06	20.00	180.00		0.0
27				0.0 0.0601 10.000.0664	20.000.0751	30.000.0734		40.000.0734	
28				50.000.0827 60.000.0943	70.000.1132	80.000.1677			
29		9001	10	9	1.06	20.00	180.00		0.0
30				0.0 0.0414 10.000.0417	20.000.0427	30.000.0444		40.000.0470	
31				50.000.0506 60.000.0556	70.000.0625	80.000.0719			
32		9001	11	9					
33				0.0 -4.8 10.00 -4.6	20.00 -4.3	30.00	-3.9	40.00	-3.5
34				50.00 -2.9 60.00 -2.4	70.00 -1.8	80.00	-1.2		
35		9001	12	9					
36				0.0 18.72 10.00 23.13	20.00 27.73	30.00	24.83	40.00	22.08
37				50.00 24.17 60.00 25.87	70.00 28.92	80.00	40.02		
38		9001	13	9	1.06	20.00	180.00		180.0
39				0.0 0.0601 10.000.0601	20.000.0678	30.000.0599		40.000.0626	
40				50.000.0703 60.000.0769	70.000.0908	80.00[illegible]			
		9001							

Appendix V
RHOPRIME PROGRAM LISTING

```
RHOPRIME  AS OF 02.20.73
          DIMENSION K(500),OP(3),E(3),D(3),OR(3),LABEL(15),TABLE(500)
          EQUIVALENCE (TABLE,K)
          INTEGER CODE,TABLES/'TABL'/,COMP/'COMP'/,END/'END '/,SCANT/'SCAN'/
          INTEGER TITLE/'TITL'/,FACET/'FACE'/
          REAL I21(4),I11(4),I23(3),I13(3),I24(3),I14(3)
          COMMON MI,ISW,W,TABLE,I21,I11,I23,I13,I24,I14
          COMMON /CMPT/PS1,PD1,BETA,BETAB,RPO,COSINE,SIGMA,PHIEN,REP,TS
          DATA OP/0.0,0.0,1.0/,AP/0.0/,OR/0.0,0.0,1.0/
C*****************************************************************
C
C         FORMATS
C
C*****************************************************************
  100     FORMAT(A4,15X,I6)
  110     FORMAT(A4,5X,8(E7.2,1X),F3.0,1X,I3)
  120     FORMAT('1NORMAL TERMINATION')
  140     FORMAT('1','***** END-OF-FILE ENCOUNTERED')
  150     FORMAT('1','***** TABLE READ ERROR -- CONDITION CODE =',F3.0)
  170     FORMAT('1','***** WARNING EOF IN COMPUTATION REQUESTS')
  180     FORMAT('1','***** INVALID CARD TYPE')
  190     FORMAT('1','***** EOF IN SCAN DATA.')
  200     FORMAT(15A4)
C*****************************************************************
C
C         DATA BLOCK READ-IN PHASE
C
C*****************************************************************
 1000     READ(2,100,END=8000)CODE,NMAT
C*****
C         MATERIAL TABLES
C*****
 1010     IF(CODE .NE. TABLES)GO TO 1020
          CALL INDATA(NMAT,CC)
          IF(CC .GT. 0.0)GO TO 8010
          GO TO 1000
C*****
C         COMPUTATION REQUEST
C*****
 1020     IF(CODE .NE. COMP)GO TO 1040
          ASSIGN 1030 TO MODE
          ISW = NMAT
 1030     READ(2,110,END=8030)CODE,TS,PS,TD,PD,A,B,PSI,P,H,MI
          IF(CODE .EQ. END)GO TO 5000
          IF(H .GT. 0.0)H = 1.0
          IF(H .LT. 0.0)H = -1.0
          IF(H .EQ. 0.0)A = 1.0
          IF(H .EQ. 0.0)B = 0.0
          GO TO 2000
C*****
C         DETECTOR SCAN REQUEST
C*****
 1040     IF(CODE .NE. SCANT)GO TO 1060
          ISW = NMAT
          ASSIGN 1050 TO MODE
 1050     CALL SCAN(CC,TS,PS,TD,PD,P,A,B,PSI,H)
          IF(CC .GT. 0.0)GO TO 9000
          GO TO 2000
C*****
C         TITLE SPECIFICATION
```

```
C*****
1060  IF(CODE .NE. TITLE)GO TO 1070
      READ(2,200)LABEL
      CALL AUXIO(LABEL,0.0,0.0,0.0,0.0,0.0,1)
      IF(DP(3) .EQ. 1.0)GO TO 1090
      UP(1) = 0.0
      UP(2) = 0.0
      UP(3) = 1.0
      GO TO 1090
C*****
C     FACET DEFINITION
C*****
1070  IF(CODE .NE. FACET)GO TO 1080
      READ(2,110)CODE,AP,DP
      GO TO 1090
C*****
C     PROGRAM TERMINATION
C*****
1080  IF(CODE .NE. END)GO TO 8040
      WRITE(3,120)
      CALL SYSTEM
C*****
C     READ END CARD
C*****
1090  READ(2,100,END=8000)CODE
      IF(CODE .NE. END)GO TO 1090
      GO TO 1000
C**********************************************************************
C
C     COMPUTATION PHASE
C
C**********************************************************************
2000  PSI1 = PSI/57.29577
      TS1 = TS/57.29577
      PS1 = PS/57.29577
      TD1 = TD/57.29577
      PD1 = PD/57.29577
      E(1) = SIN(TS1)*COS(PS1)
      E(2) = SIN(TS1)*SIN(PS1)
      E(3) = COS(TS1)
      D(1) = SIN(TD1)*COS(PD1)
      D(2) = SIN(TD1)*SIN(PD1)
      D(3) = COS(TD1)
      CALL GEOM(D,E,UP,DP,PSI1,PSIDF,PSIPF,COSB,COSBDP,COSBEP,
     1          COSB2,RADF)
      CALL GPRM(COSB,COSBDP,COSBEP,COSHNP,COSB2,PSIPE,PSIDE,RADF,AP,
     1          A,AB,B,BH,H,HB,PSID)
      PSID = PSID*57.29577
C**********************************************************************
C
C     OUTPUT PHASE
C
C**********************************************************************
C*****
C     LONG FORM
C*****
      CALL OUTPUT(TS,PS,TD,PD,P,A,AB,B,BH,PSI,PSID,H,HB,LABEL,AP)
      GO TO MODE,(1030,1050)
C*****
C     SHORT FORM
```

```
C*****
 5000 IF(CC .GT. 2.0)GO TO 8050
      CALL AUXIO(LABEL,0.0,0.0,0.0,0.0,0.0,3)
      IF(CC .EQ. 1.0)GO TO 2000
      CC = 0.0
      GO TO 1000
C***********************************************************************
C
C     ERROR HANDLING PHASE
C
C***********************************************************************
 8000 WRITE(0,140)
      STOP 8000
 8010 WRITE(0,150)CC
      STOP 8010
 8030 WRITE(0,170)
      STOP 8030
 8040 WRITE(0,180)
      GO TO 1090
 8050 WRITE(0,190)
      STOP 8050
      END
      SUBROUTINE INDATA(NMAT,CC)
      DIMENSION TABLE(500),KTAB(500)
      EQUIVALENCE (TABLE,KTAB)
      REAL N,K
      INTEGER WPS,CODE,END/'END '/,ANGLE/'ANGL'/,BLANK/'    '/
      DATA MATR/'MATR'/
      COMMON MI,ISW,W,TABLE,I21,I11,I23,I13,I24,I14
C*****
C     FORMATS
C*****
  100 FORMAT(A4,4X,I2,7E10.3)
  110 FORMAT(A4,6X,2E10.3)
  120 FORMAT(/' ***** WARNING -- ANGLES OUT OF ORDER.'/)
  130 FORMAT(10X,7E10.3)
      CC = 0.0
      WPS = NMAT+2
C*****
C     READ MATERIAL HEADER
C*****
 1000 READ(2,100,END=8000)CODE,MAT,N,K,RX1,RX2,RHOV,SIGMA,RPO
      IF(CODE .EQ. END)RETURN
      IF(CODE .NE. MATR)GO TO 8010
      READ(2,130,END=8000)TAU,OMEGA,Q1,Q2
      IF(MAT .GT. NMAT)GO TO 8020
      BETA0 = -5.0
C*****
C     STORE MATERIAL CONSTANTS
C*****
      KTAB(MAT)    = WPS
      TABLE(WPS+1) = N
      TABLE(WPS+2) = K
      TABLE(WPS+3) = RX1
      TABLE(WPS+4) = RX2
      TABLE(WPS+5) = RHOV
      TABLE(WPS+6) = SIGMA*0.0174533
      TABLE(WPS+7) = RPO
      TABLE(WPS+8) = TAU*0.0174533
      TABLE(WPS+9) = OMEGA*0.0174533
```

```
      TABLE(NPS+10) = U1
      TABLE(NPS+11) = U2
C*****
C     READ AND STORE RCS/BNP TABLE IF GIVEN
C*****
      K1 = NPS+12
      NA = 0
1010  READ(2,110,END=8000)CODE,BETA,RCUS
      IF(CODE .EQ. END)GO TO 1020
      IF(CODE .NE. ANGLE .AND. CODE .NE. BLANK)GO TO 8030
      IF(BETA .LE. BETA0)WRITE(6,120)MAT
      BETA0 = BETA
      BETA = BETA*0.0174533
      TABLE(K1)   = COS(BETA)
      TABLE(K1+1) = RCUS
      K1 = K1+2
      NA = NA+1
      GO TO 1010
C*****
C     SET NUMBER OF BETAS
C*****
1020  KTAB(NRS) = NA
      NPS = NPS+NA+NA+12
      GO TO 1000
C*****
C     ERROR HANDLING
C*****
8000  CC = 1.0
      RETURN
8010  CC = 2.0
      RETURN
8020  CC = 3.0
      RETURN
8030  CC = 4.0
      RETURN
      END
      SUBROUTINE SCAN(CC,TS,PS,TD,PD,P,A,B,PSI,H)
      COMMON M1,ISW,W,TABLE,I21,I11,I23,I13,I24,I14
      DIMENSION TABLE(500)
      REAL I21(4),I11(4),I23(3),I13(3),I24(3),I14(3)
      INTEGER CODE,END/'END '/
      DATA ENTER/0.0/
C*****
C     FORMATS
C*****
100   FORMAT(12F6.2,F4.0,T4)
110   FORMAT(A4)
C*****
C     READ SCAN PARAMETERS
C*****
      CC = 0.0
      IF(ENTER .GT. 0.0)GO TO 2000
      ENTER = 1.0
      READ(2,100,END=9000)TS,PS,TDS,TDE,TSTEP,PDS-PDE,PSTEP,A,B,PSI,P,H,
     1                         HT
      IF(TDE - TDS)1000,1000,1010
1000  TDS = 0.0
      TDE = 89.0
1010  TD = TDS-TSTEP
      IF(PDE-PDS)1020,1020,1030
```

```
1020  PDS = 0.0
      PDE = 180.0
      PSTEP = 180.0
1030  IF(PSTEP .LT. 5.0)PSTEP = 5.0
      IF(TSTEP .LT. 2.0)TSTEP = 2.0
      IF(H .GT. 0.0)H = 1.0
      IF(H .LT. 0.0)H = -1.0
      IF(H .EQ. 0.0)A = 1.0
      IF(H .EQ. 0.0)B = 0.0
      PD = PDS
1040  READ(2,110,END=9000)CODE
      IF(CODE .NE. END)GO TO 1040
C*****
C     INCREMENT THETA
C*****
2000  TD = TD+TSTEP
      IF(TD .LE. TDF)RETURN
C*****
C     INCREMENT PHI
C*****
      PD = PD+PSTEP
      IF(PD .GE. PDF)GO TO 3000
      TD = TDS
      CC = 1.0
      RETURN
C*****
C     SCAN COMPLETE
C*****
3000  CC = 2.0
      ENTER = 0.0
      RETURN
C*****
C     ERROR HANDLING
C*****
9000  CC = 3.0
      ENTER = 0.0
      RETURN
      END
      SUBROUTINE SETDAT(R,COSB)
      DIMENSION TABLE(500),KTAB(500),R(10)
      EQUIVALENCE (TABLE,KTAB)
      INTEGER NPS
      COMMON NI,ISW,M,TABLE,I21,I11,I23,I13,I24,I14
      COMMON /CMPY/PS,PD,BETA,BETAB,NPO,COSINE,SIGMA,PHIEN,REP,TS
C*************************************************************************
C
C     THIS SUBROUTINE RETRIEVES DATA FROM TABLE
C     INPUT:
C        COSB   - COS(BETA)
C        COSINE - COS(BETA-H,P)
C
C      OUTPUT:
C          R(1)  - N
C          R(2)  - K
C          R(3)  - RHO-CHI,1
C          R(4)  - RHO-CHI,2
C          R(5)  - RHO-V
C          R(6)  - RHO(BETA-H,P)
C          R(7)  - DP-PERP
C          R(8)  - DP-PAR
```

```
C          R(9)   = F
C          R(10)  = G
C
C***********************************************************************
C*****
C     RETRIEVE MATERIAL CONSTANTS
C*****
1000  IF(MI .LT. 1 .OR. MI .GT. 500)STOP 8000
      NRS    = KTAB(MI)
      NA     = KTAB(NRS)
      R(1)   = TABLE(NRS+1)
      R(2)   = TABLE(NRS+2)
      R(3)   = TABLE(NRS+3)
      R(4)   = TABLE(NRS+4)
      R(5)   = TABLE(NRS+5)
      SIGMA  = TABLE(NRS+6)
      RPO    = TABLE(NRS+7)
      R(10)  = TABLE(NRS+8)
      R(7)   = TABLE(NRS+9)
      R(8)   = TABLE(NRS+10)
      R(9)   = TABLE(NRS+11)
C*****
      R(6)   = 0.0
C     TABLE LOOK-UP FOR RCOSBNP)
C*****
      IF(NA .LE. 0)GO TO 3000
      K1 = NRS+12
      IF(NA .EQ. 1)GO TO 2020
      K2 = K1+NA+NA
2010  IF(ABS(COSINE-TABLE(K1)) .LE. 0.0001)GO TO 2020
      K3 = K1+2
      IF(K3 .GE. K2)GO TO 2030
      IF(TABLE(K3) .LT. COSINE)GO TO 2030
      K1 = K3
      GO TO 2010
C*****
C     COSINE FOUND, RETRIEVE RCOSBNP
C*****
2020  R(6) = TABLE(K1+1)
      GO TO 3000
C*****
C     INTERPOLATE RCOSBNP
C*****
2030  FACT = (COSINE-TABLE(K1))/(TABLE(K3)-TABLE(K1))
      R(6) = FACT*(TABLE(K3+1)-TABLE(K1+1))+TABLE(K1+1)
      GO TO 3000
C*****
C     COMPUTE DPO, DPPO, F, G (,RCOSBNP - IF SIGMA NE 0)
C*****
3000  BETA   = ARCOS(COSB)
      BETAB  = ATAN(R(1))
      CALL FUNC(R)
      RETURN
      END
      SUBROUTINE GEOM(D,E,DP,DP,PSI,PSIPE,PSIPE,COSB,COSBDP,COSBEP,
     1                 COSB2,RADF)
      DIMENSION D(3),E(3),DP(3),DP(3),X(3),Y(3),XA(3),YA(3),U(3),
     1          XAP(3),YAP(3),U1(3),UP(3),NZ(3),NZ1(3),YAM(3)
      REAL NZ,NZ1
      EXTERNAL SIGN
      COMMON /CMPT/PS,PO,BETA,BETAB,RPO,COSBNP,SIGMA,PHIEN,REP,TS
```

```
C*****
C     FORMATS
C*****
100   FORMAT(' ***** FACET NOT VISIBLE.')
C
      IF(PSI .GE. 1.5707963)PSI = PSI-3.1415927
      IT = 0
C*****
C
C*****
      X(1) = O(1)+E(1)
      X(2) = O(2)+E(2)
      X(3) = O(3)+E(3)
      TT = VNORM(X,X)
C*****
C
C*****
      IF(ABS(F(3)-1.0) .GT. 0.0001)GO TO 1000
      Y(1) = COS(PS+1.570796)
      Y(2) = SIN(PS+1.570796)
      Y(3) = 0.0
      GO TO 1010
1000  CALL CROSS(ON,E,Y)
      TT = VNORM(Y,Y)
C*****
C
C*****
1010  IF(ABS(O(3)-1.0) .GT. 0.0001)GO TO 1020
      YA(1) = COS(PO+1.570796)
      YA(2) = SIN(PO+1.570796)
      YA(3) = 0.0
      GO TO 1030
1020  CALL CROSS(OR,D,YA)
      TT = VNORM(YA,YA)
C*****
C
C*****
1030  IF(ABS(F(1)-D(1)) .GT. 0.0001 .OR. ABS(F(2)-D(2)) .GT. 0.0001)
     1   GO TO 1040
      U(1) = Y(1)
      U(2) = Y(2)
      U(3) = Y(3)
      XA(1) = YA(1)
      XA(2) = YA(2)
      XA(3) = YA(3)
      IT = 1
      GO TO 1050
1040  CALL CROSS(F,O,XA)
      TT = VNORM(XA,XA)
      U(1) = -XA(1)
      U(2) = -XA(2)
      U(3) = -XA(3)
C*****
C
C*****
1050  IF(ABS(OP(1)-F(1)) .GT. 0.0001 .OR. ABS(UP(2)-E(2)) .GT. 0.0001)
     1   GO TO 1060
      XAP(1) = Y(1)
      XAP(2) = Y(2)
      XAP(3) = Y(3)
```

```
      GO TO 1070
1060  CALL CROSS(OP,E,XAP)
      T1 = VNORM(YAP,YAP)
C*****
C
C*****
1070  IF(ABS(OP(1)-D(1)) .GT. 0.0001 .OR. ABS(OP(2)-D(2)) .GT. 0.0001)
     1   GO TO 1080
      YAP(1) = YA(1)
      YAP(2) = YA(2)
      YAP(3) = YA(3)
      GO TO 1090
1080  CALL CROSS(OP,D,YAP)
      T1 = VNORM(YAP,YAP)
C*****
C
C*****
1090  COSR   = DOT(X,D)
      COSRDP = DOT(OP,D)
      COSREP = DOT(OP,E)
      COSRNP = DOT(OP,X)
      COSR2  = COSB*COSR
      PSIPE = PSI-ARCOS(DOT(XAP,Y))*SIGN(-DOT(XAP,UR))
      PSIPE = PSI-ARCOS(DOT(U,Y))*SIGN(DOT(Y,D))
      IF(TI .LT. 1)GO TO 1100
      IF(ABS(F(1)-DP(1)) .GT. 0.0001 .OR. ABS(E(2)-DN(2))
     1   .GT. 0.0001)GO TO 1100
      WADE = PD-PS
      IF(WADE .GE. 3.14159)WADE = WADE-3.14159
      IF(WADE .LT. 0.0)WADE = WADE+3.14159
      GO TO 1110
1100  YAM(1) = -YA(1)
      YAM(2) = -YA(2)
      YAM(3) = -YA(3)
      WADE = -ARCOS(DOT(XA,YA))*SIGN(DOT(YAM,F))
C*****
C
C*****
1110  BDP = ARCOS(COSRDP)
      BEP = ARCOS(COSREP)
      IF(BEP .GT. 1.57079 .OR. BDP .GT. 1.57079)WRITE(6,100)
      EDPHI = ARCOS(DOT(XAP,YAP))
      PHIEN = 0.0
      IF(ABS(Y(1)-DP(1)) .LT. 0.0001 .AND. ABS(Y(2)-UP(2)) .LT. 0.0001)
     1   RETURN
      IF(ABS(D(1)-UP(1)) .LT. 0.0001 .AND. ABS(D(2)-UP(2)) .LT. 0.0001)
     1   RETURN
      IF(ABS(F(1)-UP(1)) .LT. 0.0001 .AND. ABS(F(2)-UP(2)) .LT. 0.0001)
     1   RETURN
C
      DC(1) = -SIN(BEP)
      DC(2) = 0.0
      DC(3) = COSREP
C
      D1(1) = SIN(BDP)*COS(EDPHI)
      D1(2) = SIN(BDP)*SIN(EDPHI)
      D1(3) = COSRDP
C
      CALL CROSS(DC,UR,NZ1)
      T1 = VNORM(NZ1,NZ1)
```

```
      CALL CROSS(HZ1,DC,HZ)
      T1 = VNORM(HZ,HZ)
      DM = DOT(D1,HZ)
      IF(DM .LT. 0.0)PHIEN = 1.57079-ARCOS(-DM)
      RETURN
      END
      SUBROUTINE SPEN(COSR,COSBMP,COSREM,COSBMP,COSR2,PRIME,PRIME,
     1               MAOF,AP,A,AP,R,RP,H,HP,PSTO)
      DIMENSION TABLE(500),KTAB(500),R(10),ST(5)
      LOGICAL MOD1,MOD2,MOD3,MOD4
      EQUIVALENCE (MOD1,MOD2,T1),(MOD3,T3),(MOD4,T4),(R(1),N),(R(2),K),
     1            (R(3),NV1),(R(4),RA2),(R(5),HMUV),(R(6),HMO),
     2            (R(7),DPO),(R(8),DP00),(R(9),FF),(R(10),G)
      INTEGER SHFTR
      REAL I21(3),I11(3),I23(3),I13(3),I24(3),I14(3),I12,I22,N,K
      COMMON M1,ISW,M,TABLE,I21,I11,I23,I13,I24,I14
      DATA MASK/Z0000000F/
      EXTERNAL SIGN
C*********************************************************************
C
C     CHOOSE MODEL AND RETRIEVE DATA
C
C*********************************************************************
      I1 = LAND(MASK,ISW)
      I3 = LAND(MASK,SHFTR(ISW,1))
      I4 = LAND(MASK,SHFTR(ISW,2))
      CALL GETDAT(N,COSR)
      DO 1000 I = 1,3
      I21(I) = 0.0
      I11(I) = 0.0
      I23(I) = 0.0
      I13(I) = 0.0
      I24(I) = 0.0
 1000 I14(I) = 0.0
C*********************************************************************
C
C      SPECULAR AND DIFFUSE MODEL (MOD1 & MOD2)
C
C*********************************************************************
      IF(.NOT. MOD1 .AND. .NOT. MOD2)GO TO 3000
C*****
C     COMPUTE FRESNEL COEFFICIENTS
C*****
      V1 = DIVIDE(((N+1.0)*(N+1.0)+K*K),((N-1.0)*(N-1.0)+K*K))
      G = N*N-K*K-1.0+COSR2
      P = SQRT(4.0*N*N*K*K+G*G)
      V2 = SQRT(ABS((P+G)*0.5))
      V3 = ABS((P-G)*0.5)
C
      R0 = V1*(((V2-COSR)*(V2-COSR)+V3)/((V2+COSR)*(V2+COSR)+V3))
C
      V4 = V2*COSR
      R0P = R0*(((V4+COSR2-1.0)**2+V3*COSR2)/((V4-COSR2+1.0)**2+
     1      V3*COSR2))
      I21(4) = 0.0
      I11(4) = 0.0
      IF(N .NE. 0)GO TO 2000
      AP = 0.0
      RP = 0.0
      PRIN = 0.0
```

```
      HP = 0.0
C*****
C     PLANE POLARIZED MODEL
C*****
      T1 = ABS(ABS(PSTOF)-1.570796)
      T2 = ABS(ABS(PSTOF)-4.712389)
      IF(T1 .GT. 0.001 .AND. T2 .GT. 0.001)PSTEP = ATAN(SQRT(DIVIDE
     1  (P0R,R0)))*TAN(PRIME)*SIGN(COS(ATAN(H))*CUSP))
      IF(T1 .LE. 0.001 .OR.  T2 .LE. 0.001)PSTEP = PSTOF*SIGN(COS(ATAN
     1  (H))*CUSP)
      API1 = PSTEP-WANE
      T1 = API1+API1
      ST(1) = COS(T1)
      ST(2) = SIN(T1)
      T1     = -WANE-WAUF
      V1     = (P0-RP0)*0.5
      ST(3) = (P0+RP0)*0.5
      ST(4) = V1*COS(T1)
      ST(5) = V1*SIN(T1)
C
      IF(AP .GT. 0.0)GO TO 1010
      V1 = RHO/(COSNE*P*CUSHOP)
      V4 = 1.0
      GO TO 1020
C
1010  V1 = RHO*AP
      V4 = (USHFP*COSR)P*AP
C*****
C     COMPUTE STOKES VECTOR
C*****
C
C     UNPOLARIZED SOURCE
C
1020  I22 = (RX1*RX2)*V4*0.5
      I21(1) = V1*ST(3)+I22
      I21(2) = V1*ST(4)
      I21(3) = V1*ST(5)
C
C     POLARIZED SOURCE
C
      I12 = (RX1*COS(PSTOF)**2+RX2*SIN(PSTOF)**2)*V4
C
      V1     = (COS(PRIME)**2*R1+SIN(PSTOF)**2*RVN)*V1
      I11(1) = V1+I12
      I11(2) = V1*ST(1)
      I11(3) = V1*ST(2)
      GO TO 3000
C*****
C     ELLIPTICAL MODEL
C*****
2000  IF(PSTOF .GT. 3.141593)PSTOF = PSTOF-3.141593
      IF(PSTOF .LT. 0.0)PRIME = PRIME+3.141593
      IF(PSTOF .LT. 0.0)PRIME = PRIME+3.141593
      A6 = RWO(A)
      A8 = RWO(B)
      CALL ELTPS(A6,A8,PRIME,H,AA1,AA2,D)
      A1 = AA1*AA1
      A2 = AA2*AA2
C
      IF(ABS(PORG-1.0) .LT. 0.0)PSTOF = -3.141593
```

```
      IF(ABS(COSB) .LT. 0.001)DR = 0.0
C
      IF(R .NE. 0.0)GO TO 2040
      BETAB = COS(ATAN(R))
      IF(COSB-BETAB)2010,2020,2030
2010  DR =0.0
      GO TO 2060
2020  DR = -1.570796
      GO TO 2060
2030  DR = -3.141593
      GO TO 2060
C
2040  T3 = 2.0*SQRT(V3)*(1.0-COSB2)*COSB
      T4 = (1.0-COSB2)**2-COSB2*(V2*V2+V3)
      IF(ABS(T4) .LT. 0.000001)GO TO 2050
      DR = -1.570796
      GO TO 2060
C
2050  T1 = T3/T4
      IF(T1 .LT. 0.0)DR = -3.141593+ATAN(-T1)
      IF(T1 .GE. 0.0)DR = -ATAN(T1)
C
2060  DT = DR+D
      A1R = A1*R2
      A2R = A2*R2
      AA1R = SQRT(A1R)
      AA2R = SQRT(A2R)
      CALL FLYPR2(AA1R,AA2R,DT,AAR,AAM,PSTEP,[illegible])
C
      AR = [illegible]
      AM = [illegible]
      IF(PSTEP .GE. [illegible])PSTEP = [illegible]
      PSID = PSTEP[illegible]
      IF(PSID .GE. [illegible])PSID = [illegible]
      IF(PSID .LE. [illegible])PSID = [illegible]
      [illegible]
      [illegible]
      IF([illegible])[illegible]
      [illegible]
C
      IF([illegible])[illegible]
      [illegible]
      [illegible]
      GO TO [illegible]
C
      [illegible]
      [illegible]
C
C*****
C     COMPUTE STOKES VECTOR
C*****
C
C     [illegible] SOURCE
C
2[illegible] [illegible]
      [illegible]
      [illegible]
      [illegible]
C
C     [illegible] SOURCE
```

```
C
      I12    = (RY1*COS(PSIPE)**2+RY2*SIN(PSIPE)**2)*V2
C
      V3     = V1*(AP+BR)
      I11(1) = V3+I12
      I11(2) = V3*COS(T1)*COS(T2)
      I11(3) = V3*SIN(T1)*COS(T2)
      I11(4) = V3*SIN(T2)
C**************************************************************
C
C     VOLUME MODEL (MOD3)
C
C**************************************************************
3000  IF(.NOT. MOD3)GO TO 4000
      V1 = 1.0
      IF(AP .GT. 0.0)V1 = COSBEP*COSBOP*AP
      V1 = 2.0*V1*RHOV*FF*G/(COSBEP+COSBOP)
      AFD = 0.0
      T1 = ABS(ABS(PSIDE)-1.570796)
      T2 = ABS(ABS(PSIDE)-4.712389)
      IF(T1 .GE. 0.001 .AND. T2 .GE. 0.001)GO TO 3010
      AFD = PSIDE
      GO TO 3030
C
3010  IF(DP90 .GT. 0.001 .AND. DP0 .LT. 0.999)GO TO 3020
      AFD = 1.57079
      GO TO 3030
3020  V2 = SQRT(DP0 *(1.0-DP90)/(DP90*(1.0-DP0)))*TAN(PSIDE)*SIGN
     1      (COS(ATAN(N))-COSB)
      AFD = ATAN(V2)
C
3030  AD = AFD-WADE
      C1 = COS(PSIDE)
      C1 = C1*C1*DP90
      S1 = SIN(PSIDE)
      S1 = S1*S1*DP0
      V1 = V1/((1.0+DP0)*DP90)
C*****
C     COMPUTE STOKES VECTOR
C*****
C
C     POLARIZED SOURCE
C
      I13(1) = V1*(C1*(1.0+DP0)+S1*(1.0+DP90))
      I13(2) = V1*(C1*(1.0-DP0)+S1*(1.0-DP90))*COS(AD+AD)
      I13(3) = V1*(C1*(1.0-DP0)+S1*(1.0-DP90))*SIN(AD+AD)
C
C     UNPOLARIZED SOURCE
C
      V1     = V1*0.5
      I23(1) = V1*(DP90*(1.0+DP0)+DP0*(1.0+DP90))
      I23(2) = V1*(DP90-DP0)*COS(-WADE-WADE)
      I23(3) = V1*(DP90-DP0)*SIN(-WADE-WADE)
C**************************************************************
C
C      INTERFACE MODEL (MOD4)
C
C**************************************************************
4000  IF(.NOT. MOD4)RETURN
      RETURN
```

```
      END
      SUBROUTINE OUTPUT(TS,PS,TD,PD,P,AA,AB,BA,BB,PSI,PSID,H,HH,LABEL,
     1                  AP)
      DIMENSION A(3),B(3),C(3),AES(3,3),AEP(3,3),AL(3,3),PP(3,3)
      DIMENSION LABEL(15),D(1),TABLE(500)
      LOGICAL MOD1,MOD2,MOD3,MOD4
      REAL I21(4),I11(4),I23(3),I13(3),I24(3),I14(3)
      INTEGER SHFTR
      COMMON MI,ISW,W,TABLE,I21,I11,I23,I13,I24,I14
      EQUIVALENCE (MOD1,MOD2,I1),(MOD3,I3),(MOD4,I4)
      DATA MASK/Z00000001/,ZERO/0.0/,ONE/1.0/
C*****
C     FORMATS
C*****
100   FORMAT(T1,10X,'REFLECTANCE',2X,4L1,2X,15A4//21X,'THETA',6X,'PHI',
     1     13X,'POLARIZED',13X,'UNPOLARIZED',12X,'PARTIAL POL.')
110   FORMAT(T1,10X,'INTENSITY'  ,2X,4L1,2X,15A4//21X,'THETA',6X,'PHI',
     1     13X,'POLARIZED',13X,'UNPOLARIZED',12X,'PARTIAL POL.')
120   FORMAT(11X,'SOURCE',2(4X,F6.2),3(10X,F13.5)/11X,'DETECTOR',2X,
     1     F6.2,4X,F6.2,3(10X,F13.5)/11X,'PERCENT POLAR.',6X,F6.2,3(10X,
     2     E13.5)/37X,3(10X,F13.5))
130   FORMAT(23X,'IN',8X,'OUT'/11X,'MAJOR',1X,2(4X,F6.2),3(10X,F13.5)/
     1     11X,'MINOR',1X,2(4X,F6.2),3(10X,E13.5)/11X,'PSI',3X,2(4X,F6.2)
     2     ,3(10X,F13.5)/11X,'HANDED',2(4X,F5.0),2X,3(10X,F13.5)//)
140   FORMAT(3(37X,3(10X,F13.5)/)/4(37X,3(10X,E13.5)/)//)
      PA = ABS(P)
      IT = 1
      I1 = LAND(MASK,ISW)
      I3 = LAND(MASK,SHFTR(ISW,1))
      I4 = LAND(MASK,SHFTR(ISW,2))
      IF(.NOT. MOD1 .AND. .NOT. MOD2)GO TO 2000
      A(1)     = PA*I11(1)+(1.0-PA)*I21(1)
      B(1)     = PA*I11(2)+(1.0-PA)*I21(2)
      C(1)     = PA*I11(3)+(1.0-PA)*I21(3)
      D(1)     = PA*I11(4)+(1.0-PA)*I21(4)
      AES(1,1) = (I11(1)+I11(2))/2.0
      AES(2,1) = (I21(1)+I21(2))/2.0
      AES(3,1) = (A(1)+B(1))/2.0
      AEP(1,1) = (I11(1)-I11(2))/2.0
      AEP(2,1) = (I21(1)-I21(2))/2.0
      AEP(3,1) = (A(1)-B(1))/2.0
      AL(1,1)  = 0.99999E9
      IF(I11(2) .NE. 0.0 .OR. I11(3) .NE. 0.0)
     1 AL(1,1) = ATAN2(I11(3),I11(2))*28.6478
      AL(2,1)  = 0.99999E9
      IF(I21(2) .NE. 0.0 .OR. I21(3) .NE. 0.0)
     1 AL(2,1) = ATAN2(I21(3),I21(2))*28.6478
      AL(3,1)  = 0.99999E9
      IF(B(1) .NE. 0.0 .OR. C(1) .NE. 0.0)
     1 AL(3,1) = ATAN2(C(1),B(1))*28.6478
      PP(1,1)  = SQRT(I11(2)*I11(2)+I11(3)*I11(3)+I11(4)*I11(4))/
     1            I11(1)*100.0
      PP(2,1)  = SQRT(I21(2)*I21(2)+I21(3)*I21(3)+I21(4)*I21(4))/
     1            I21(1)*100.0
      PP(3,1)  = SQRT(B(1)*B(1)+C(1)*C(1)+D(1)*D(1))/A(1)*100.0
2000  IF(.NOT. MOD3)GO TO 3000
      A(2)     = PA*I13(1)+(1.0-PA)*I23(1)
      B(2)     = PA*I13(2)+(1.0-PA)*I23(2)
      C(2)     = PA*I13(3)+(1.0-PA)*I23(3)
      AES(1,2) = (I13(1)+I13(2))/2.0
```

```
      AFS(2,2) = (I23(1)+I23(2))/2.0
      AFS(3,2) = (A(2)+B(2))/2.0
      AFP(1,2) = (I13(1)-I13(2))/2.0
      AFP(2,2) = (I23(1)-I23(2))/2.0
      AFP(3,2) = (A(2)-B(2))/2.0
      AL(1,2)  = 0.99999E9
      IF(I13(2) .NE. 0.0 .OR. I13(3) .NE. 0.0)
     1 AL(1,2) = ATAN2(I13(3),I13(2))*28.6488
      AL(2,2)  = 0.99999E9
      IF(I23(2) .NE. 0.0 .OR. I23(3) .NE. 0.0)
     1 AL(2,2) = ATAN2(I23(3),I23(2))*28.6488
      AL(3,2)  = 0.99999E9
      IF(B(2) .NE. 0.0 .OR. C(2) .NE. 0.0)
     1 AL(3,2) = ATAN2(C(2),B(2))*28.6488
      PP(1,2)=SQRT(I13(2)*I13(2)+I13(3)*I13(3))/I13(1)*100.0
      PP(2,2)=SQRT(I23(2)*I23(2)+I23(3)*I23(3))/I23(1)*100.0
      PP(3,2)=SQRT(B(2)*B(2)+C(2)*C(2))/A(2)*100.0
 5000 IF(.NOT. MOD4)GO TO 4000
      I14(1) = I11(1)+I13(1)
      I24(1) = I21(1)+I23(1)
      I14(2) = I11(2)+I13(2)
      I24(2) = I21(2)+I23(2)
      I14(3) = I11(3)+I13(3)
      I24(3) = I21(3)+I23(3)
      A(3)       = PA*I14(1)+(1.0-PA)*I24(1)
      B(3)       = PA*I14(2)+(1.0-PA)*I24(2)
      C(3)       = PA*I14(3)+(1.0-PA)*I24(3)
      AFS(1,3)= (I14(1)+I14(2))/2.0
      AFS(2,3)= (I24(1)+I24(2))/2.0
      AFS(3,3) = (A(3)+B(3))/2.0
      AFP(1,3) = (I14(1)-I14(2))/2.0
      AFP(2,3) = (I24(1)-I24(2))/2.0
      AFP(3,3) = (A(3)-B(3))/2.0
      AL(1,3) = 0.99999E9
      IF(I14(2) .NE. 0.0 .OR. I14(3) .NE. 0.0)
     1 AL(1,3) = ATAN2(I14(3),I14(2))*28.6488
      AL(2,3) = 0.99999E9
      IF(I24(2) .NE. 0.0 .OR. I24(3) .NE. 0.0)
     1 AL(2,3) = ATAN2(I24(3),I24(2))*28.6488
      AL(3,3) = 0.99999E9
      IF(B(3) .NE. 0.0 .OR. C(3) .NE. 0.0)
     1 AL(3,3)= ATAN2(C(3),B(3))*28.6488
      PP(1,3)=SQRT(I14(2)*I14(2)+I14(3)*I14(3))/I14(1)*100.0
      PP(2,3)=SQRT(I24(2)*I24(2)+I24(3)*I24(3))/I24(1)*100.0
      PP(3,3)=SQRT(B(3)*B(3)+C(3)*C(3))/A(3)*100.0
      CALL AUXIO(LABEL,TD,AFS(1,3),AFP(1,3),AL(1,3),PP(1,3),2)
 4000 IF(AP .LE. 0.0)WRITE(3,100)II,MOD1,MOD2,MOD3,MOD4,LABEL
      IF(AP .GT. 0.0)WRITE(3,110)II,MOD1,MOD2,MOD3,MOD4,LABEL
      IF(.NOT. MOD1 .AND. .NOT. MOD2)GO TO 4020
      WRITE(3,120)TS,PS,I11(1),I21(1),A(1),TD,PD,I11(2),I21(2),B(1),PA,
     1      I11(3),I21(3),C(1),I11(4),I21(4),D(1)
      WRITE(3,130)AA,AR,(AFS(I,1),I=1,3),BB,BR,(AFP(I,1),I=1,3),PSI,
     1      PSID,(AL(I,1),I=1,3),H,HR,(PP(I,1),I=1,3)
      IF(.NOT. MOD3)GO TO 4010
      WRITE(3,140)I13(1),I23(1),A(2),I13(2),I23(2),B(2),I13(3),I23(3),
     1      C(2),(AFS(I,2),I=1,3),(AFP(I,2),I=1,3),(AL(I,2),I=1,3),
     2      (PP(I,2),I=1,3)
 4010 IF(.NOT. MOD4)RETURN
      WRITE(3,140)I14(1),I24(1),A(3),I14(2),I24(2),B(3),I14(3),I24(3),
     1      C(3),(AFS(I,3),I=1,3),(AFP(I,3),I=1,3),(AL(I,3),I=1,3),
```

```
     2      (PP(I,3),I=1,3)
      RETURN
 4020 IF(.NOT. MJ03)GO TO 4030
      WRITE(3,120)TS,PS,I13(1),T23(1),A(2),TD,PO,T13(2),I23(2),R(2),PA,
     1      T13(3),I23(3),C(2)
      WRITE(3,130)ONE,ZERO,(AES(I,2),I=1,3),ZERO,ZERO,(AEP(I,2),I=1,3),
     1      PST,ZERO,(AL(I,2),I=1,3),ZERO,ZERO,(PP(I,2),I=1,3)
      IF(.NOT. MJ04)RETURN
      WRITE(3,140)I14(1),T24(1),A(3),T14(2),I24(2),R(3),I14(3),T24(3),
     1      C(3),(AES(I,3),I=1,3),(AEP(I,3),I=1,3),(AL(I,3),I=1,3),
     2      (PP(I,3),I=1,3)
      RETURN
 4030 IF(.NOT. MJ04)RETURN
      WRITE(3,120)TS,PS,I14(1),T24(1),A(3),TD,PO,T14(2),I24(2),R(3),PA,
     1      T14(3),I24(3),C(3)
      WRITE(3,130)ONE,ZERO,(AES(I,3),I=1,3),ZERO,ZERO,(AEP(I,3),I=1,3),
     1PSI,ZERO,(AL(I,3),I=1,3),ZERO,ZERO,(PP(I,3),I=1,3)
      RETURN
      END
      SUBROUTINE AUXIO(TITLE,X1,Y1,Y2,Y3,Y4,ICODE)
      COMMON /CMPT/PSI,PO1,BETA,BETAB,RPO,COSINF,SIGMA,PHIEM,REP,TS
      DIMENSION TITLE(3),X(5,46)
      DATA WL/1.06/
C***********************************************************************
C
C      FORMATS
C
C***********************************************************************
 100  FORMAT(A4,A4,A1,'5001',17X,'010')
 110  FORMAT(9X,'9001',I5,27X,I3,2X,3F6.2,6X,F6.1)
 120  FORMAT(20X,5(F6.2,F6.4)/(20X,5(F6.2,F6.4)))
 130  FORMAT(20X,5(F6.2,F6.1)/(20X,5(F6.2,F6.1)))
 140  FORMAT(20X,5(F6.2,F6.2)/(20X,5(F6.2,F6.2)))
C***********************************************************************
C
C      SUBROUTINE CONTROL
C
C***********************************************************************
      GO TO(1000,2000,3000),ICODE
      STOP 1111
C***********************************************************************
C
C      HEADER
C
C***********************************************************************
 1000 IS = 0
      IP = 0
      WRITE(4,100)TITLE
      RETURN
C***********************************************************************
C
C      STORE
C
C***********************************************************************
 2000 IP = IP+1
      X(1,IP) = X1
      X(2,IP) = Y1
      X(3,IP) = Y2
      X(4,IP) = Y3
      X(5,IP) = Y4
```

```
      IF(IP .GE. 45)GO TO 3000
      RETURN
C***********************************************************************
C
C     WRITE OUT
C
C***********************************************************************
 3000 CONTINUE
C*****
C     REFLECTANCES
C*****
      RP = PU*57.29577
      RS = PS*57.29577
      DO 3010 I=2,3
      IS = TS+1
      WRITE(4,110)IS,IP,RL,TS,PS,PU
      WRITE(4,120)(X(1,J),X(I,J),J=1,IP)
 3010 CONTINUE
C*****
C     ANGLE OF POLARIZATION
C*****
      IS = TS+1
      WRITE(4,110)IS,IP
      WRITE(4,130)(X(1,J),X(4,J),J=1,IP)
C*****
C     PERCENT POLARIZATION
C*****
      IS = TS+1
      WRITE(4,110)IS,IP
      WRITE(4,140)(X(1,J),X(5,J),J=1,IP)
      IP = 0
      RETURN
      END
      SUBROUTINE ELIPSI(A,B,PSI,H,A1,A2,DELTA)
      REAL LAMBDA,MU
      IF(PSI .LT. 0.0 .OR. PSI .GT. 3.141593)GO TO 8000
      LAMBDA = SQRT(A*A+B*B)
C*****
C     DEGENERATE CASE
C*****
      IF(B .GT. 0.0)GO TO 1000
      A1 = ABS(COS(PSI))*LAMBDA
      A2 = ABS(SIN(PSI))*LAMBDA
      DELTA = 0.0
      IF(PSI .GT. 1.570796)DELTA = 3.141593
      RETURN
C*****
C     ELLIPTICAL CASE
C*****
 1000 CHI = H*ATAN(B/A)
      T1 = ABS(COS(2.0*CHI)*COS(2.0*PSI))
      IF(PSI .GT. 0.785398 .AND. PSI .LT. 2.356195)ALPHA = .5*ARCOS(-T1)
      IF(PSI .LE. 0.785398 .OR.  PSI .GE. 2.356195)ALPHA = .5*ARCOS( T1)
      IF(ALPHA .NE. 0.0)GO TO 1010
      A1 = LAMBDA
      A2 = 0.0
      DELTA = 0.0
      RETURN
 1010 IF(ABS(ALPHA-0.785398) .GT. 0.0001)GO TO 1020
      A1 = LAMBDA/1.414214
```

```
      A2 = A1
      DELTA = 2.0*CHI
      IF(ABS(PSI-2.356195).LT.0.0001) DELTA = H*3.141593 - 2.0*CHI
      RETURN
C
1020  IF(ABS(ALPHA-1.570796) .GT. 0.0001)GO TO 1030
      A1 = 0.0
      A2 = LAMBDA
      DELTA = 0.0
      RETURN
C
1030  T1 = ABS(SIN(2.0*CHI)/SIN(2.0*ALPHA))
      IF(T1 .GT. 1.0)T1 = 1.0
      MU = ARSIN(T1)
      A1 = LAMBDA*COS(ALPHA)
      A2 = LAMBDA*SIN(ALPHA)
      COSD = TAN(2.0*PSI)/TAN(2.0*ALPHA)
      IF(COSD .GT. 0.0)DELTA = H*MU
      IF(COSD .LE. 0.0)DELTA = H*(3.141593-MU)
      RETURN
C*****
C     ERROR HANDLING
C*****
8000  WRITE(3,100)PSI
100   FORMAT(///' *****PSI ANGLE OUT OF RANGE --',F10.3)
      STOP
      END
      SUBROUTINE ELIPS2(A1,A2,DELTA,A,B,PSI,H)
      REAL LAMBDA,LAMDA
      IF(DELTA .LT. -3.141593)DELTA = DELTA+6.283185
      IF(DELTA .GT.  3.141593)DELTA = DELTA-6.283185
      LAMBDA = SQRT(A1*A1+A2*A2)
C*****
C     CASE 1 (A1 = 0  OR  A2 = 0)
C*****
      IF(A1 .NE. 0.0 .AND. A2 .NE. 0.0)GO TO 1010
      A = LAMBDA
      B = 0.0
      H = 1.0
      IF(A1 .EQ. 0.0)PSI = 1.570796
      IF(A2 .EQ. 0.0)PSI = 0.0
      RETURN
C*****
C     CASE 2 (A1 = A2)
C*****
1010  IF(A1 .NE. A2)GO TO 1020
      CHI = 0.5*ABS(DELTA)
      A = LAMBDA*COS(CHI)
      B = LAMBDA*SIN(CHI)
      H = 1.0
      IF(DELTA .LT. 0.0)H = -1.0
      PSI = 0.785398
      IF(CHI .GT. 0.785398)PSI = 2.356195
      RETURN
C*****
C     CASE 3 (DELTA = PI OR -PI)
C*****
1020  IF(ABS(ABS(DELTA)-3.141593) .GT. 0.0001)GO TO 1030
      A = LAMBDA
      B = 0.0
```

```
      H = 1.0
      PSI = 3.141593-ATAN(A2/A1)
      RETURN
C*****
C     CASE 4 (DELTA = 0)
C*****
1030  IF(ABS(DELTA) .GT. 0.0001)GO TO 1040
      A = LAMBDA
      B = 0.0
      H = 1.0
      PSI = ATAN(A2/A1)
      RETURN
C*****
C     CASE 5 (DELTA = PI HALVES OR -PI HALVES)
C*****
1040  IF(ABS(ABS(DELTA)-1.570796) .GT. 0.0001)GO TO 1060
      H = 1.0
      IF(DELTA .LT. 0.0)H = -1.0
C
C     PART 1 (A1 > A2)
C
      IF(A1 .LT. A2)GO TO 1050
      A = A1
      B = A2
      PSI = 0.0
      RETURN
C
C     PART 2 (A1 < A2)
C
1050  A = A2
      B = A1
      PSI = 1.570796
      RETURN
C*****
C     CASE 6 (A1 > A2)
C*****
1060  ALPHA = ATAN(A2/A1)
      CHI = 0.5*ARSIN(ABS(SIN(2.0*ALPHA)*SIN(DELTA)))
      LAMDA = ABS(TAN(2.0*ALPHA)*COS(DELTA))
      A = LAMBDA*COS(CHI)
      B = LAMBDA*SIN(CHI)
      H = 1.0
      IF(DELTA .LT. 0.0)H = -1.0
      IF(A1 .LT. A2)GO TO 1080
C
C     PART 1 (0 < DELTA < PI HALVES)
C
      IF(ABS(DELTA) .GT. 1.570796)GO TO 1070
      PSI = 0.5*ATAN(LAMDA)
      RETURN
C
C     PART 2 (DELTA > PI HALVES)
C
1070  PSI = 3.141593-0.5*ATAN(LAMDA)
      RETURN
C*****
C     CASE 7 (A1 < A2)
C*****
C
C     PART 1 (0 < DELTA < PI HALVES)
```

```
C
1080  IF(ABS(DELTA) .GT. 1.570796)GO TO 1090
      PSI = 1.570796-0.5*ATAN(LAMDA)
      RETURN
C
C     PART 2(DELTA > PI HALVES)
C
1090  PSI = 1.570796+0.5*ATAN(LAMDA)
      RETURN
      END
      FUNCTION DOT(A,B)
          DIMENSION A(3), B(3)
C*****
C     THIS FUNCTION RETURNS THE DOT PRODUCT OF A AND B
C*****
          DOT = A(1)*B(1) + A(2)*B(2) + A(3)*B(3)
         RETURN
         END
      SUBROUTINE CROSS(A,B,X)
          DIMENSION A(3), B(3), X(3)
C*****
C     THIS FUNCTION RETURNS THE CROSS PRODUCT OF A AND B IN X
C*****
          X(1) = A(2)*B(3) - A(3)*B(2)
          X(2) = A(3)*B(1) - A(1)*B(3)
          X(3) = A(1)*B(2) - A(2)*B(1)
         RETURN
         END
      FUNCTION VNORM(A,X)
          DIMENSION A(3),X(3)
C*****
C     THIS FUNCTION RETURNS THE NORM OF A AND THE NORMALIZED VECTOR IN X
C*****
         VNORM = SQRT ( A(1)*A(1) + A(2)*A(2) + A(3)*A(3) )
         X(1) = A(1) / VNORM
         X(2) = A(2) / VNORM
         X(3) = A(3) / VNORM
         RETURN
         END
      FUNCTION SIGN(A)
C*****
C     THIS FUNCTION RETURNS THE ALGEBRAIC SIGN OF THE ARGUMENT
C*****
      SIGN = 1.0
      IF(A .LT. 0.0)SIGN = -1.0
         RETURN
         END
      FUNCTION DIVIDE(A,B)
      DIVIDE = 0.0
      IF(ABS(B) .GE. 1.0E-20)DIVIDE=A/B
         RETURN
         END
END OF FILE
```

FUNCTION AS OF 02.20.73

```
      SUBROUTINE FUNC(R)
      COMMON /CMPT/PS,PD,BETA,BETAB,RPO,COSINE,SIGMA,PHIEM,REP,TS
      DIMENSION R(10)
      TAU   = R(10)
      OMEGA = R(7)
      Q1    = R(8)
      Q2    = R(9)
      BNP   = ARCOS(COSINE)
      IF(ABS(SIGMA) .LE. 0.001)GO TO 1000
      IF(BNP .GE. SIGMA)
     1      R(6) = RPO*COSINE*COSINE*(Q1*EXP(-BNP/SIGMA)+Q2*R(5))
      IF(BNP .LT. SIGMA)
     1      R(6) = RPO*COSINE*COSINE*(Q1*EXP(-0.5-0.5*BNP*BNP/(SIGMA*
     2             SIGMA))+Q2*R(5))
 1000 R(6) = R(6)
      R(7) = 1.0
      R(8) = R(7)
      R(9) = 1.0
      R(10) = 1.0
      RETURN
      END
      SUBROUTINE FUNC(R)
      COMMON /CMPT/PS,PD,BETA,BETAB,RPO,COSINE,SIGMA,PHIEM,REP,TS
      DIMENSION R(10)
      TAU   = R(10)
      OMEGA = R(7)
      Q1    = R(8)
      Q2    = R(9)
      BNP   = ARCOS(COSINE)
      IF(ABS(SIGMA) .LE. 0.001)GO TO 1000
      IF(BNP .GE. SIGMA)
     1      R(6) = RPO*COSINE*COSINE*(Q1*EXP(-BNP/SIGMA)+Q2*R(5))
      IF(BNP .LT. SIGMA)
     1      R(6) = RPO*COSINE*COSINE*(Q1*EXP(-0.5-0.5*BNP*BNP/(SIGMA*
     2             SIGMA))+Q2*R(5))
 1000 R(6) = R(6)
      R(7) = 1.0
      R(8) = R(7)
      R(9) = 1.0
      R(10) = 1.0+EXP(-131.31221*BNP*BNP)
      RETURN
      END
      SUBROUTINE FUNC(R)
      COMMON /CMPT/PS,PD,BETA,BETAB,RPO,COSINE,SIGMA,PHIEM,REP,TS
      DIMENSION R(10)
C**********************************************************************
C
C     THIS IS A REPLACEABLE SUBROUTINE USED TO COMPUTE RPO,DRPO,F,AND G.
C      OUTPUT:
C       R(6)  - RCOSBNP
C       R(7)  - DPO
C       R(8)  - DPRO
C       R(9)  - F
C       R(10) - G
C
C**********************************************************************
      TAU   = R(10)
      OMEGA = R(7)
      Q1    = R(8)
```

```
      Q2    = R(9)
      BNP   = ARCOS(COSINE)
C
C     RCOSBNP
C
      IF(ABS(SIGMA) .LE. 0.001)GO TO 1000
      IF(BNP .GE. SIGMA)
     1      R(6) = RP0*COSINE*COSINE*(Q1*EXP(-BNP/SIGMA)+Q2*R(5))
      IF(BNP .LT. SIGMA)
     1      R(6) = RP0*COSINE*COSINE*(Q1*EXP(-0.5-0.5*BNP*BNP/(SIGMA*
     2             SIGMA))+Q2*R(5))
 1000 R(6) = R(6)*((1.0+BNP/OMEGA*EXP(-2.0*BETA/TAU))/(1.0+BNP/OMEGA))
     1         /(1.0+PHIEN*REP/(OMEGA*OMEGA))
C
C     DPP
C
      R(7) = 1.0
C
C     DPP0
C
      R(8) = R(7)
C
C     F
C
      R(9) = 1.0
C
C     F
C
      R(10) = 1.0
      RETURN
      END
      SUBROUTINE FUNC(R)
      COMMON /CMPT/PS,P0,BETA,BETA0,RP0,COSINE,SIGMA,PHIEN,REP,TS
      DIMENSION R(10)
      TAU   = R(10)
      OMEGA = R(7)
      Q1    = R(8)
      Q2    = R(9)
      BNP   = ARCOS(COSINE)
      IF(ABS(SIGMA) .LE. 0.001)GO TO 1000
      IF(BNP .GE. SIGMA)
     1      R(6) = RP0*COSINE*COSINE*(Q1*EXP(-BNP/SIGMA)+Q2*R(5))
      IF(BNP .LT. SIGMA)
     1      R(6) = RP0*COSINE*COSINE*(Q1*EXP(-0.5-0.5*BNP*BNP/(SIGMA*
     2             SIGMA))+Q2*R(5))
 1000 R(6) = R(6)*((1.0+BNP/OMEGA*EXP(-2.0*BETA/TAU))/(1.0+BNP/OMEGA))
     1         /(1.0+PHIEN*REP/(OMEGA*OMEGA))
      R(7) = 1.0
      R(8) = R(7)
      R(9) = 1.0
      R(10) = 1.0*EXP(-131.3122*BNP*BNP)
      RETURN
      END
END OF FILE
```

REFERENCES

1. Target Signature Analysis Center: Data Compilation, Eleventh Supplement, Vol. I, Report No. 32210-41-B, Willow Run Laboratories of the Institute of Science and Technology, The University of Michigan, Ann Arbor, AFAL-TR-72-226, October 1972.

2. Target Signature Analysis Center: Data Compilation, Eleventh Supplement, Vol. II, Report No. 32210-41-B, Willow Run Laboratories of the Institute of Science and Technology, The University of Michigan, Ann Arbor, AFAL-TR-72-226, October 1972.

3. M. Born and E. Wolf, Principles of Optics, Pergamon Press, London, 1964.

4. K. E. Torrance and E. M. Sparrow, "Theory for Off-Specular Reflection from Roughened Surfaces," J. Opt. Soc. Amer., Vol. 57, No. 9, September 1967, pp. 1105-1114.

5. W. A. Shurcliff, Polarized Light, Harvard University Press, Cambridge, 1962.

6. H. B. Holl, Reflection of Electromagnetic Radiation, Vol. I, Report RF-TR-63-4, U.S. Army Missile Command, Redstone Arsenal, Huntsville, Alabama, 15 March 1963.

UNCLASSIFIED

Security Classification

DOCUMENT CONTROL DATA - R & D

(Security classification of title, body of abstract and indexing annotation must be entered when the overall report is classified)

1. ORIGINATING ACTIVITY (Corporate author) Infrared and Optics Division Environmental Research Institute of Michigan P.O. Box 618	2a. REPORT SECURITY CLASSIFICATION Unclassified 2b. GROUP

3. REPORT TITLE

BIDIRECTIONAL REFLECTANCE MODEL VALIDATION AND UTILIZATION

4. DESCRIPTIVE NOTES (Type of report and inclusive dates)

Final Report, 1 November 1969 through 31 December 1972

5. AUTHOR(S) (First name, middle initial, last name)

J. R. Maxwell   S. Weiner   S. Ladd
J. Beard   D. Ladd

6. REPORT DATE	7a. TOTAL NO. OF PAGES	7b. NO. OF REFS
October 1973	124	6

8a. CONTRACT OR GRANT NO. F33615-70-C-1123 b. PROJECT NO. 6103 c. Task 610304 d.	9a. ORIGINATOR'S REPORT NUMBER(S) 196400-1-T 9b. OTHER REPORT NO(S) (Any other numbers that may be assigned this report) AFAL-TR-73-303

10. DISTRIBUTION STATEMENT

Distribution limited to U.S. Government agencies only; Test and Evaluation: 6 October 1973. Other requests for this document must be submittedto AFAL/RSP, Wright-Patterson Air Force Base, Ohio 45433

11. SUPPLEMENTARY NOTES	12. SPONSORING MILITARY ACTIVITY
	Air Force Avionics Laboratory Air Force Systems Command Wright-Patterson Air Force Base, Ohio 45433

13. ABSTRACT

This report describes a method for using bidirectional reflectance information previously reported in the Eleventh Supplement to the Target Signature Analysis Center: Data Compilation and further validates the bidirectional reflectance model originated and extended under recent contracts. It includes bidirectional reflectance model parameters for a variety of paints. Parameters were extracted from measurement data reported in the Eleventh Supplement. Reduced reflectance data are also provided; these data may be used with the computer model or, optionally, in an interpolation procedure for estimating reflectances without the aid of a computer.

The computer model makes it possible to calculate bidirectional reflectance data from a very small amount of measured data. Accuracy demonstrated in the Model Validation section indicates that the model is very effective, although improvement can still be obtained at large receiver zenith angles. The interpolation procedure also shows excellent agreement with measurement.

DD FORM 1473

UNCLASSIFIED

Security Classification

UNCLASSIFIED
Security Classification

14 KEY WORDS	LINK A		LINK B		LINK C	
	ROLE	WT	ROLE	WT	ROLE	WT
Bidirectional reflectance						
Shadowing						
Obscuration						
Lambertian reflectance						
Non-Lambertian reflectance						
Surface model						
Polarization parameters						
Source receiver						
Fixed-bistatic data						

UNCLASSIFIED
Security Classification